INSIGHTS INTO KEY BARRIERS IN THE IMPLEMENTATION OF RENEWABLE BIOFUEL TECHNOLOGIES

by

Jesse Beau Therien

A dissertation submitted in partial fulfillment
of the requirements for the degree

of

Doctor of Philosophy

in

Biochemistry

MONTANA STATE UNIVERSITY
Bozeman, Montana

July, 2013

APPROVAL

of a dissertation submitted by

Jesse Beau Therien

This dissertation has been read by each member of the dissertation committee and has been found to be satisfactory regarding content, English usage, format, citation, bibliographic style, and consistency and is ready for submission to The Graduate School.

Prof. John W. Peters

Approved for the Department of Chemistry and Biochemistry

Prof. Mary Cloninger

Approved for The Graduate School

Dr. Ronald W. Larsen

STATEMENT OF PERMISSION TO USE

In presenting this dissertation in partial fulfillment of the requirements for a doctoral degree at Montana State University, I agree that the Library shall make it available to borrowers under rules of the Library. I further agree that copying of this dissertation is allowable only for scholarly purposes, consistent with "fair use" as prescribed in the U.S. Copyright Law. Requests for extensive copying or reproduction of this dissertation should be referred to ProQuest Information and Learning, 300 North Zeeb Road, Ann Arbor, Michigan 48106, to whom I have granted "the right to reproduce and distribute my dissertation in and from microform along with the non-exclusive right to reproduce and distribute my abstract in any format in whole or in part."

Jesse Beau Therien

July 2013

TABLE OF CONTENTS

TABLE OF CONTENTS – CONTINUED

TABLE OF CONTENTS – CONTINUED

LIST OF TABLES

LIST OF FIGURES

LIST OF FIGURES – CONTINUED

ABSTRACT

Bioenergy can be defined as renewable energy derived from biological sources. As world energy consumption increases and fossil fuel supplies are depleted, national and international energy requirements will become more diverse and more complicated. Clearly, the niche that alternative and renewable energy sources occupy in the energy portfolio will continue to increase over time. Currently, bioenergy in the form of biofuel production including alcohols, lipids, and hydrogen represent working technologies that are in large part only economically limited where large scale production is currently too costly to compete with fossil fuels. As a result, there has been a significant investment in basic science research to make these technologies more robust and more amenable to scale up. This includes large scale cultures of model biofuel producing organisms, consortia of organisms, and even mimetic systems in which components derived from biological sources are incorporated into materials. The success of future biofuel technologies is dependent on advancing these technologies by overcoming some of the key barriers that decrease the practicality of wide scale implementation. A key to the large scale production of biofuels in the form of alcohols, lipids, or hydrogen is to develop mechanisms to limit the costs associated with culturing organisms and harvesting fuels. A technique used to facilitate the production of bio-hydrogen from eukaryotic algae is described and shows promise as a way to reduce costs associated with handling microorganisms used in bioreactors. Immobilization the hydrogen producing alga *Chlamydomonas reinhardtii* in calcium alginate facilitates manipulation of culture conditions during biofuel production and their subsequent harvest. The design of tailored microbial consortia or co-culturing multiple organisms provides a means of simplifying and reducing costs of media components required for biofuel production by providing key media components metabolically. Finally, genomic and gene expression studies have provided clues into structural determinants responsible for superior hydrogen production by certain enzymes that can be incorporated into model hydrogen producing organisms or merged into biomaterials. Together, these studies have contributed to the progression and knowledge of bioenergy promoting an increasing and long lasting presence of renewable fuels in the global energy portfolio. /

CHAPTER 1

INTRODUCTION

World Energy

Energy can be categorized as either renewable or nonrenewable. The majority of world energy comes from nonrenewable sources. Non-renewable resources can be defined as resources that are depleted faster than they can be reformed naturally. Fossil fuels, including oil, natural gas and coal are prime examples of non-renewable resources. Renewable energy sources, on the other hand, include solar, wind, geothermal, biomass, and hydropower and are not a finite resource. Presently however, fossil fuels account for greater than 80% of the energy produced globally (1). Liquid fuels are the most consumed form of energy and fuel around half the transportation sector (2). Emissions of carbon dioxide (CO_2) are primarily anthropogenic and stem from the combustion of fossil fuels, chiefly coal. Nevertheless, as fossil fuel reserves decline and world population rises, renewable energy will account for an ever increasing portion of the energy produced and consumed. Also, due to environmental concerns with the use of conventional fossil fuels, such as greenhouse gas emissions, use of renewable energies will likely increase since their net CO_2 emissions are very low.

Domestic Renewable Energy

In the U.S., the number one consumed energy form is petroleum derived from crude oil. Annually, over the last ten years, imports of crude oil have been between 4-5 billion barrels, currently more than half of the total crude oil consumed in the U.S. (3).

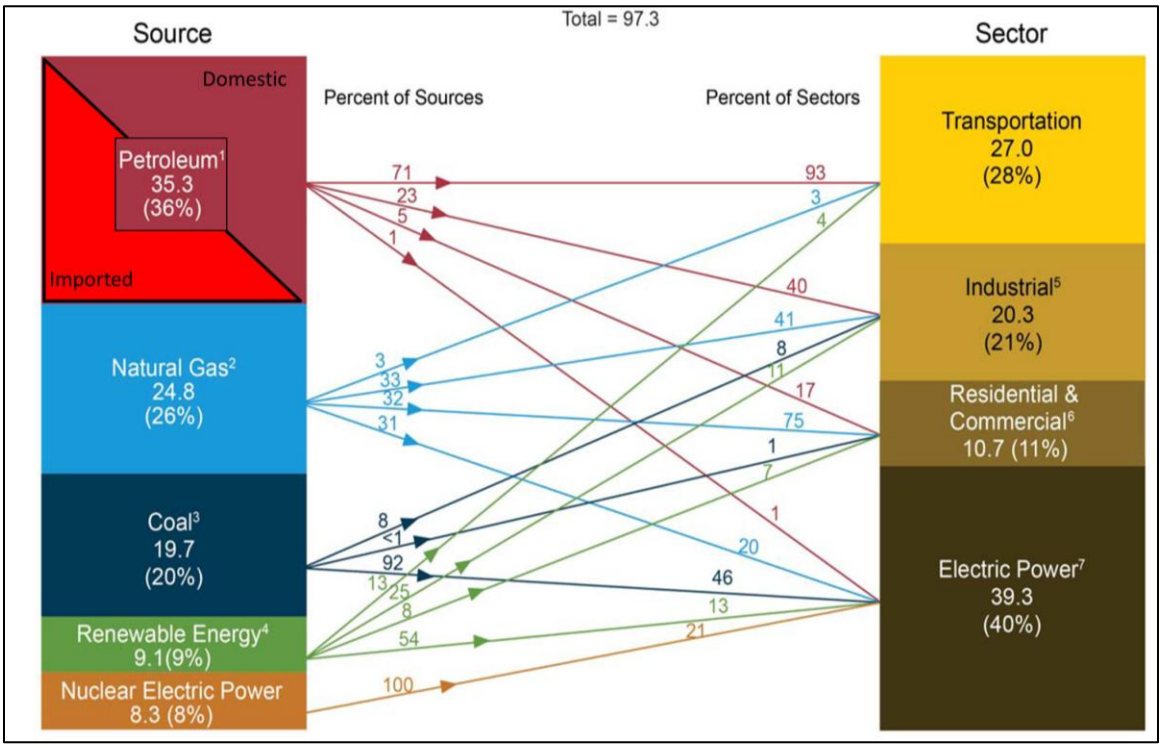

Figure 1.1. U.S. Energy Consumption in 2011 by Source and Sector. Modified from (4).

Dependence on imported oil, its rising cost, and the negative environmental effects of fossil fuel use have recently prompted many renewable energy initiatives. In order to strengthen national security, the U.S. Department of Energy's (DOE) Office of Energy Efficiency and Renewable Energy (EERE) have set goals to advance domestic energy resources, diversify energy supplies, while reducing greenhouse emissions. An ever

growing portion of the energy portfolio has been renewable energies. Renewable energies are comprised of solar, geothermal, waste, wind, biofuels, wood and hydroelectric and now account for about 9% of total energy consumption in the U.S.

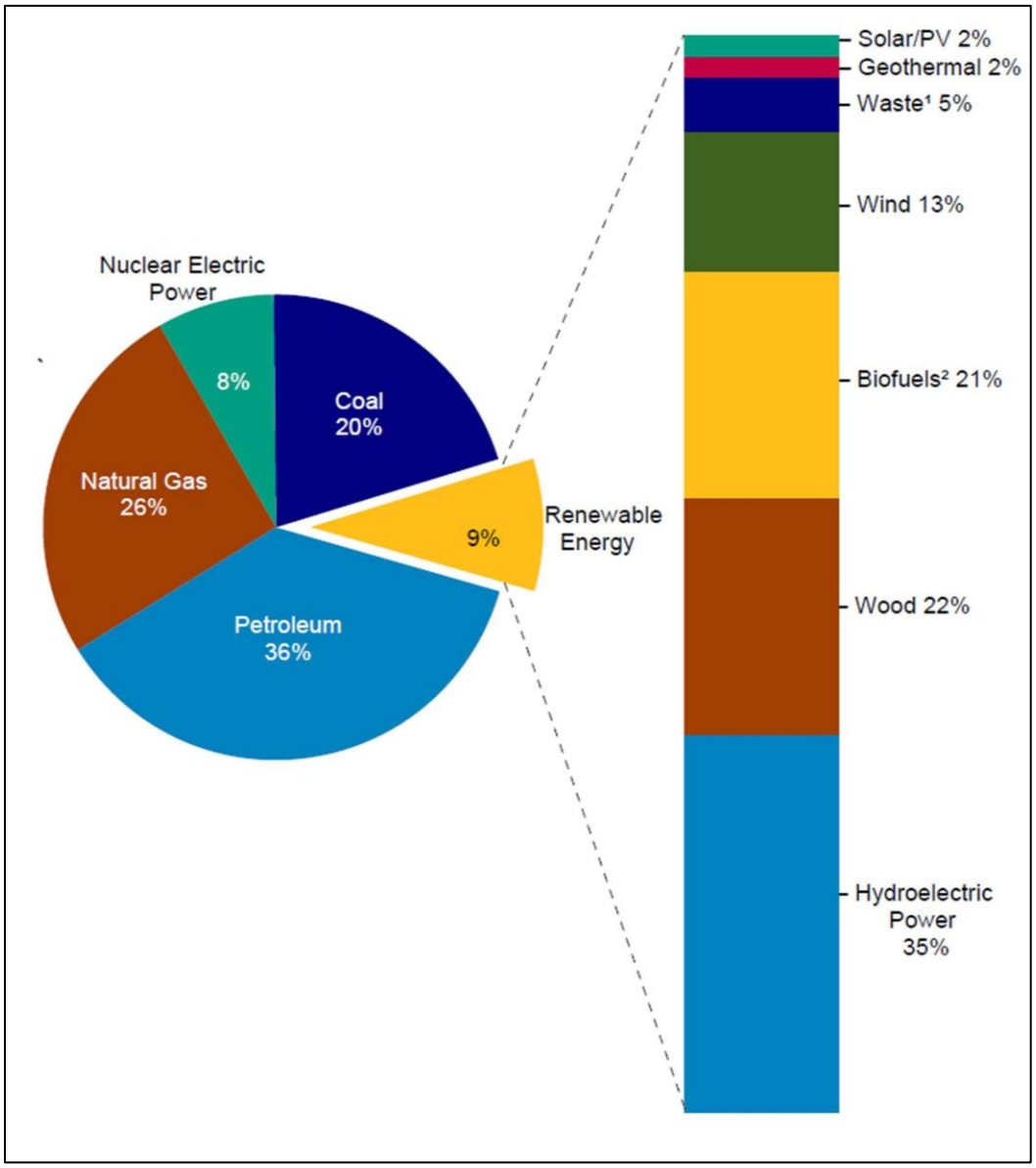

Figure 1.2. U.S. Renewable Energy as a Share of Total Energy Consumption, 2011. [1]Includes landfill biogas and agricultural byproducts. [2]Includes ethanol and biodiesel, plus losses and co-products from their production. Modified from (4).

The U.S. congress and some federal agencies have committed considerable funds towards research of renewable energy and technologies including solar, wind, geothermal, hydrogen and fuel cells, and biomass. Funding for EERE has nearly doubled in the last decade going from $1.2 billion in 2003 to a requested $3.2 billion for 2013. The predominant types of renewable energies consumed are hydroelectric power (35%), wood (22%), and biofuels (21%) (4). Hydroelectric power has been around since the late 1800's, while wood has been used for millennia. Biofuels are not new, but the expanding type of feedstocks used, called biomass, and type of biofuels produced is unprecedented. Funding for biomass research in the U.S. has risen since 2012 by about 72% to $65 million (requested) in 2013 (5).

Biofuels

As the term infers, biofuels are derived from biological materials/processes and as such, are renewable. At the heart of biofuel production are microorganisms that transform a carbon source into a fuel or feedstock for further refinement. These organisms are as diverse as the carbon sources used to produce biofuels and range from anaerobic bacteria to photosynthetic eukaryotes. Some of the microbially produced fuels are biomethanol, bioethanol, biobutanol, biomethane, biohydrogen and biodiesel. Although biodiesel is a biofuel, it typically requires further processing (transesterification) before it can be used as a fuel.

Alcohols

By far the largest scale biofuel currently produced is bioethanol (6). Ethanol can be used in conventional gasoline engines by mixing it with gasoline up to 10% and can be used up to 85% in newer E85 vehicles (7). Mixing ethanol with gasoline adds oxygen to the fuel which helps reduce emissions of CO and non-combusted hydrocarbons. Brazil is currently one of the world leaders in ethanol production and predominantly uses what is called first generation processes (8). In this case, sugarcane or molasses, both from crops grown on arable land, are fermented by yeast, yielding ethanol. First generation biofuel production is not ideal because feedstocks compete for land with the production of food crops. Second generation production, however, involves the fermentation of crop waste or biomass and therefore doesn't compete with food crops. After the initial breakdown of the biomass, usually enzymatically, ethanol production can proceed as in first generation production. Recently, the world's largest ethanol producer announced it plans to build eight second generation plants starting in 2014 (9).

Methane/Biogas

Using mixed organic wastes such as animal manures, sewage sludge and effluents from biomass-based industries (10), mixed bacteria, typically containing fermenting bacteria, syntrophic bacteria and methanogens, produce methane and CO_2 along with smaller amounts of hydrogen, alcohol, and fatty acids (11). This mixture of gases make up what is called biogas and can be compressed and used like natural gas. As with natural gas, biogas can be used commercially for heat and electricity. Systems designed to ferment wastes for the production of biogas are called anaerobic digesters and, in the

U.S., are most often found at wastewater treatment plants, landfills and on large dairy farms. In the U.S. in 2012, there were an estimated 1,200 wastewater treatment plants (12), 594 landfill (13), and 192 dairy farms (14, 15) with anaerobic digester systems in operation, most of which consume the biogas they produce. Biogas can be burned to provide heat and electricity (16) in addition to diminishing released greenhouse gases that would otherwise be emitted (17). Biogas can also be treated/cleaned and compressed to power conventional vehicles like cars, truck, and buses with slight modification to their engines (18).

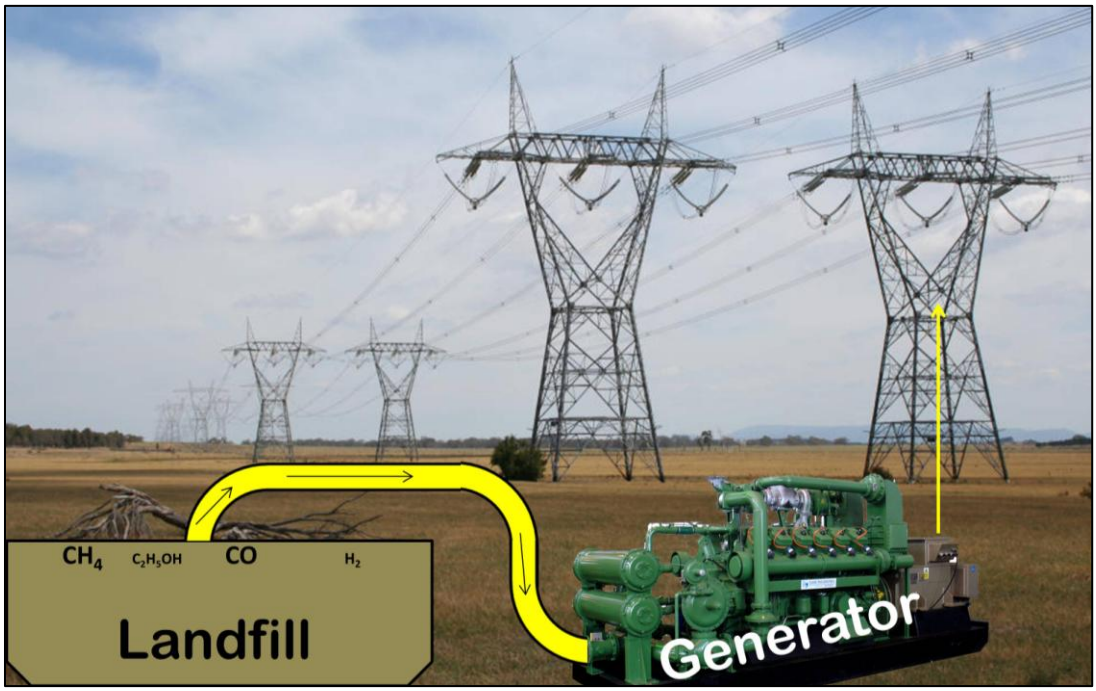

Figure 1.3. Representation of landfill biogas conversion to electricity.

Biodiesel

Biodiesel is produced by the transesterification of fat, lard, tallow and vegetable/plant oils with an alcohol yielding fatty acid methyl esters (biodiesel). These fatty acids can be used as a 100% substitute for petro diesel or blended with petro diesel, usually to 2%, 5%, and 20%. With the higher freezing point of biodiesel, low percentage blends are used in colder climates to prevent gelling. Biodiesel is mostly used in the transportation sector, powering cars, trucks, trains, and even jet aircraft (19). As with bioethanol, the majority of biodiesel feedstocks currently come from crops grown on arable land. For this reason, and others such as superior photosynthetic efficiency, second generation biodiesel has focused on microalgae as a source for oil (20).

Hydrogen

Microbially, hydrogen can be produced by algal and cyanobacterial bio-photolysis of water or by microbes performing anaerobic fermentation of carbohydrates. The former method invokes photosystem II (PSII) to split water using the energy of absorbed photons and eventually, through photosystem I (PSI), reduces ferredoxin which can in turn reduce protons to H_2 via the enzyme hydrogenase (21). Alternatively, the latter method can evolve H_2 from virtually any source of biodegradable organic matter including human, animal and food-processing waste (22). This process is often coupled to the evolution of organic acids and alcohols, such as ethanol, acetate, butanol, and butyrate (21, 23). As hydrogen is not a primary source of energy, but rather used to carry energy like electricity, it can be referred to as an ideal energy carrier rather than an energy source (24). Hydrogen is easily converted to electricity via a hydrogen fuel cell,

producing only water and heat as a byproduct, and is easily produced abiotically by electrolysis of water. By applying a current through electrodes, water can be split into H_2 and O_2. Although not biotic, this can be another renewable source of H_2 if the electricity is produced with wind, solar, or hydroelectricity. Currently, the vast majority of hydrogen used in fuel cells is derived from fossil fuels and natural gas. Superior mechanisms of hydrogen production, both abiotic and biotic, are currently being researched. New material technologies that incorporate simple and abundant non-rare metals are geared toward improving abiotic hydrogen production while improvements in biohydrogen production via the aforementioned photoproduction and fermentation are also being made. Microbially however, regardless of the metabolism yielding H_2, the enzyme responsible for its production is hydrogenase.

Hydrogenase

As eluded to previously, organisms housing hydrogenases are diverse both metabolically and taxonomically. They can be found in all domains of life, bacteria, archaea and eukaryotes, however, the majority of organisms able to metabolize H_2 are prokaryotes (25). They include fermenters, photosynthesizers, aerobes, anaerobes, autotrophs and heterotrophs (25). Even though hydrogenases catalyze a reversible reaction, that is production or consumption of molecular hydrogen, they are usually devoted to catalyzing the reaction in one direction or the other (26); [FeFe]-hydrogenases generally catalyze the production of H2 while [NiFe]-hydrogenases are typically used for

H_2 uptake (25). This is likely why many hydrogen-metabolizing organisms contain multiple copies of hydrogenase (27).

Classification

[FeFe]-hydrogenase. [FeFe]-hydrogenases are frequently monomeric and often contain accessory clusters that function to transfer electrons to the active site called the H-cluster (25). It has been proposed that the first characterized [FeFe]-hydrogenase (CpI) functions in central metabolism in recycling reduced electron carriers that accumulate during fermentation under non nitrogen-fixing conditions via proton reduction (28). Although cases exist where an [FeFe]-hydrogenase preferentially oxidizes H_2 (29-31), structural or sequence based characteristics have yet been revealed that allow their functional classification. They have thus been grouped by their modular structures, not function (32). Simplified, the groupings are separated into "M" for monomeric, "D" for dimeric, "TR" for trimeric, and "TE" for tetrameric.

[NiFe]-hydrogenase. [NiFe]-hydrogenases are more easily categorized by function and two signature sequences have been shown for each category and will be explained later (25). The four main groups of [NiFe]-hydrogenases are: group 1, uptake; group 2, cyanobacterial uptake/sensing; group 3, bidirectional; and group 4, H_2-evolving/energy conserving (25). Uptake [NiFe]-hydrogenases are membrane-bound and are typically linked to the oxidation of H_2 energy conserving reactions, like respiration, NAD(P)H formation and methanogenesis (27). Cyanobacterial uptake hydrogenases of group 2 have been linked to the occurrence of nitrogenase and shown to be induced under

N_2-fixing conditions (33, 34) minimizing the loss of energy during nitrogenase catalysis by recycling H_2 produced as a byproduct (35). The sensing hydrogenases of group 2 control the transcription of other hydrogenases using multiple component signal transduction chain consisting of a histidine protein kinase and a response regulator (36). Group 3, bidirectional hydrogenases are associated with other subunits that are able to bind cofactors like NAD and NADP. The oxidation of H_2 is linked to the reduction of these cofactors and, as their name implies, can re-oxidize these substrates by reducing protons (25). Finally, enzymes of the fourth group are made up of six or more subunits and reduce protons to dispose of excess reducing equivalents, much like some of the [FeFe]-hydrogenases (25).

Hmd-hydrogenase. A third type of hydrogenase, called H_2-forming methylene-H_4MPT dehydrogenase (Hmd), catalyzes the reduction of N^5,N^{10}-methenyl-5,6,7,8-tetrahydromethanopterin ($CH{\equiv}H_4MPT^+$) with H_2 to N^5,N^{10}-methylene-5,6,7,8-tetrahydromethanopterin ($CH_2{=}H_4MPT$) and a proton (37). This third type of hydrogenase is different from the [FeFe]- and [NiFe]-hydrogenases in that it does not contain iron or nickel (37). A structure of Hmd hydrogenase from *Methanocaldococcus jannaschii* has been published (38) but due to the mechanistic and structural differences when compared to [FeFe]- and [NiFe]-hydrogenases, no further discussion of Hmd hydrogenase will follow.

Structure and Function

[FeFe]-hydrogenase. Structures of two [FeFe]-hydrogenases have been solved using X-ray crystallography, namely those of *Clostridium pasteurianum* (CpI) (39) and *Desulfovibrio desulfuricans* (DdH) (40). As such, these structures have been the models for many theoretical studies.

CpI is a monomeric enzyme, 60 kDa in size, used to dissipate reducing equivalents accumulated during the fermentation process. It possesses four domains that each contains an (41) cluster. As with all [FeFe]-hydrogenases, CpI contains a [4Fe4S] cluster connected to a 2Fe center via a bridging cysteine thiolate. This cluster is referred to as the H-cluster and resides in the H-domain (28). It is here that catalysis takes place. Interestingly, this biologically unique cluster contains CO and CN^- ligands found only in hydrogenases (38-40). The other (41) clusters, found in the majority of [FeFe]-hydrogenases, are dubbed accessory clusters and function to mediate electron transfer between the active site and electron donors/acceptors. In CpI, these clusters have been labeled FS4A, FS4B, FS4C (all [4Fe4S] clusters) and FS2 (a [2Fe2S] cluster) (39). Starting at the N-terminus of the 574 amino acid sequence of CpI, there are conserved cysteine residues for each cluster sequentially binding clusters FS2, FS4C, FS4B and FS4A.

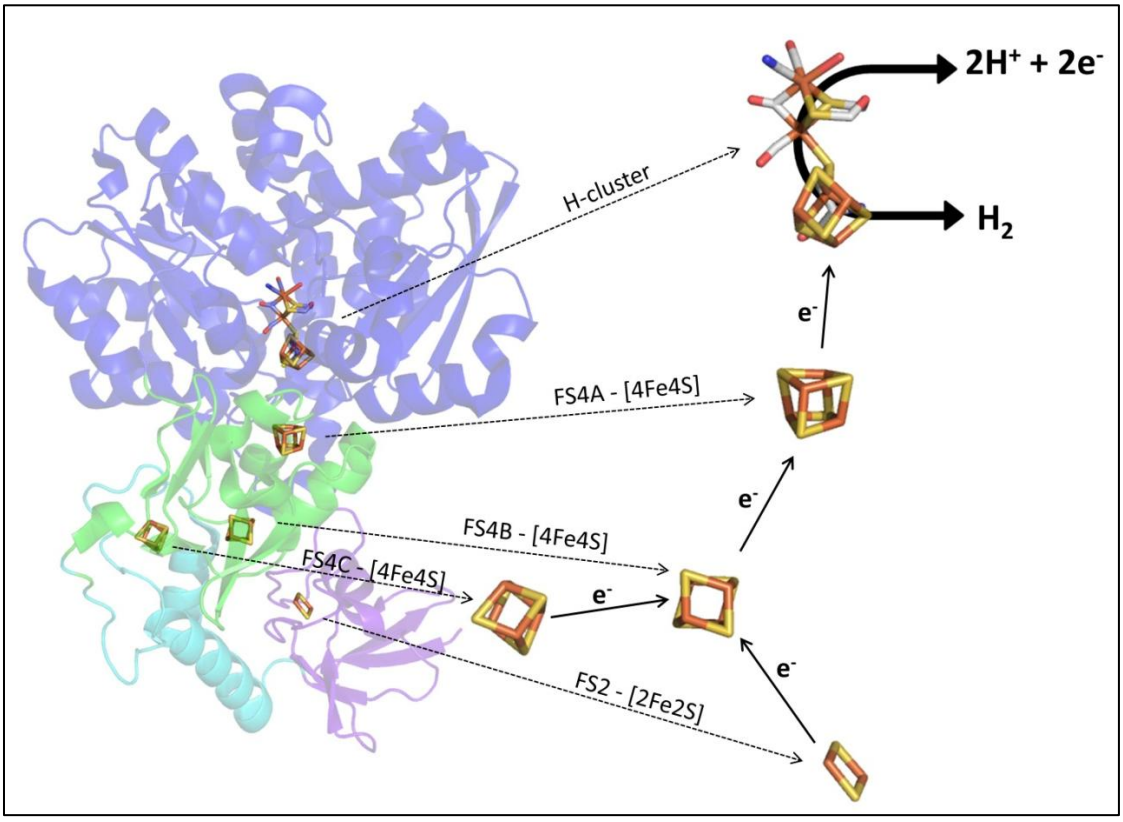

Figure 1.4. Ribbon representation of the x-ray crystal structure of [FeFe]-hydrogenases from *Clostridium pasteurianum* (39) and hypothesized electron transfer pathway through accessory iron-sulfur clusters to the active site. The catalytic domain (H-cluster domain) is colored in blue, while accessory domains are colored green (FS4A), violet (FS4B), and magenta (FS4C/FS2).

Unlike CpI, DdH from *Desulfovibrio desulfuricans,* is a heterodimeric enzyme with subunit sizes of 42 kDa and 11 kDa and is said to be involved in H_2 uptake (29). In addition to the H-cluster, DdH has two accessory [4Fe4S] clusters bound by characteristic cysteine residues.

The simplest [FeFe]-hydrogenases contain only the required H-domain and no accessory clusters. Examples can be found in eukaryotic algae such as *C. reinhardtii*, *Chlorella fusca*, and *Scenedesmus obliquus*. For this reason, these types of hydrogenases,

mainly that of *Chlamydomonas reinhardtii*, are often used for biochemical characterization of the active site.

A notable feature of [FeFe]-hydrogenases is that they all share characteristic sequence signatures within the active site domain encompassing cysteine ligands that bind the H-cluster. These motifs have been dubbed P1 (TSCCPxW), P2 (MPCxxKxxE), and P3 (ExMACxxGCxxGGGxP) (25). Each of the three patterns can be found by itself in non-hydrogenase proteins, but when found all together, indicates an [FeFe]-hydrogenase.

[NiFe]-hydrogenase. The most numerous and best studied hydrogenases have been the [NiFe]-hydrogenases (25). As a result, it is not surprising that x-ray crystal structures of [NiFe]-hydrogenase are more numerous than that of the [FeFe] version. Structures of the *Desulfovibrio gigas* (42), *Desulfovibrio vulgaris* (43), *Desulfovibrio fructosovorans* (44), and *Desulfovibrio desulfuricans* (29), *Allochromatium vinosum* (45) and *Hydrogenovibrio marinus* (46) have been solved. Unlike most of the [FeFe]-hydrogenases, the nickel-containing type is made up of a two subunit core (25). This core contains a large (~60 kDa) and a small (~30 kDa) subunit. The small subunit can contain up to three [4Fe4S] clusters, one of which is essential for activity (25).

The structure of the [NiFe]-hydrogenase of *Desulfovibrio gigas*, shown in figure 1.5, includes three iron-sulfur centers found in the small (28 kDa) subunit, presumed to facilitate electron transport to and from the active site. The heterobimetalic active site is located in the large (60 kDa) subunit and is comprised of a Ni atom and an Fe atom bridged by two cysteine thiolate ligands. Again, as with the [FeFe]-hydrogenases,

signature motifs for [NiFe]-hydrogenases have been revealed, however these motifs are specific for each type of hydrogenase within the four main groups previously mentioned (25).

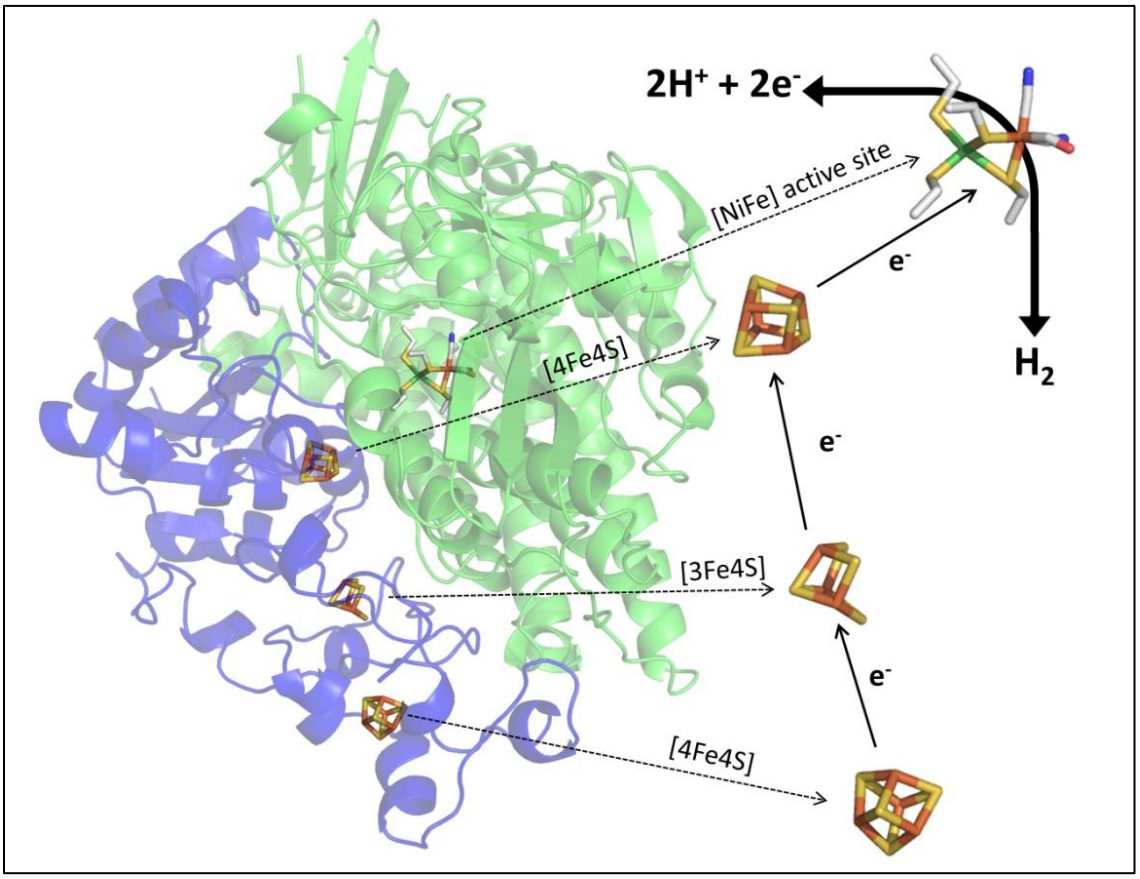

Figure 1.5. Ribbon representation of the x-ray crystal structure of [NiFe]-hydrogenases from *Desulfovibrio gigas* and hypothesized electron transfer pathway through accessory iron-sulfur clusters to the active site. The large subunit is colored green and the small subunit is colored blue (42).

Genes and Biosynthesis

As with other complex metal clusters, like FeMo-co found in nitrogenase, the biosynthetic machinery essential for the maturation of an active hydrogenase requires

multiple components called maturases. Although [FeFe]- and [NiFe]-hydrogenases have completely unrelated amino acid sequences, both versions contain CO and CN^- ligands bound to iron atoms in their active sites. CO and CN^- are biologically toxic molecules, shown to inhibit both forms of hydrogenase (47, 48), and therefore they must be inserted carefully through the action of maturases.

[FeFe]-hydrogenase. For the [FeFe]-hydrogenases, a set of three maturases named HydE, HydF, and HydG perform the maturation process. Genes encoding the [FeFe]-hydrogenase and its maturases can be found together as a cluster (*hydAEFG*), in sets (ex. *hydAFG*, *hydE* or *hydA*, *hydEFG*), or alone (25). Both HydE and HydG belong to the radical S-adenosylmethionine superfamily of proteins while HydF is a GTPase. It has been proposed that HydE and HydG act on HydF assembling an active site 2-Fe subcluster precursor which can then be inserted into HydA making it active (49, 50).

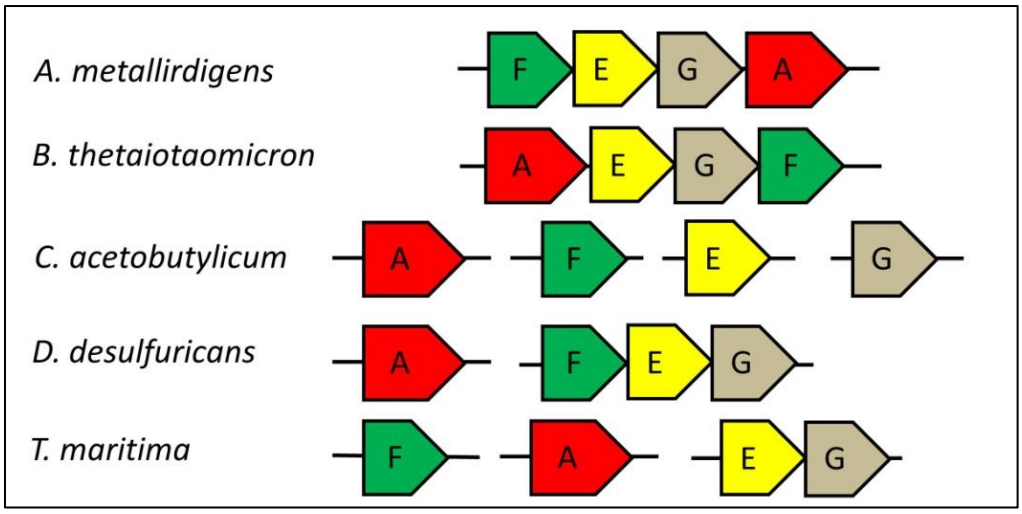

Figure 1.6. [FeFe]-hydrogenase genes showing variation in cluster composition. Genes encoding maturases (HydE, HydF and HydG) and the structural protein (HydA) are shown as E, F, G and A respectively.

[NiFe]-hydrogenase. In addition to the small and large subunits, [NiFe]-hydrogenases require at least seven auxiliary proteins (HypA, HypB, HypC, HypD, HypE HypF, and an endopeptidase) whose genes are often clustered as is the case in all *Proteobacteria* (25). The structural genes are usually present at the beginning of the gene cluster and can have prefixes *hya*, *hyb*, *hyc* (as in *E. coli*), *hyp*, *hox* (for **h**ydrogen **ox**idation) or *hup* (for **h**ydrogen **up**take) (51).

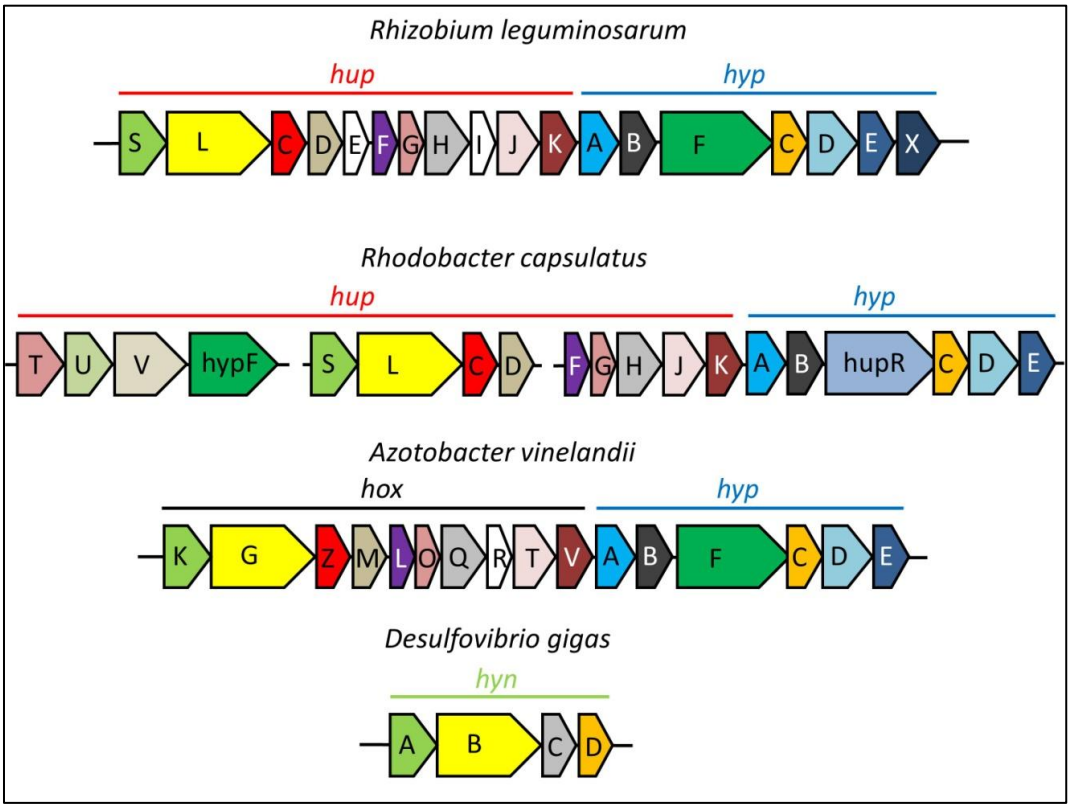

Figure 1.7. Examples of [NiFe]-hydrogenase gene clusters. Functionally homologous genes are the same color. Modified from (51).

The maturation process has been divided in to four steps (52). The first step is the synthesis of the structural apoenzyme; the enzyme without its cofactor. The second step

consists of the delivery of the active site metals. The third and fourth steps consist of synthesizing the active site ligands and assembling/inserting the active site into the apoenzyme (52).

HypA and HypB appear to be responsible for the transport or insertion of nickel into the active site (51, 52). HypC, a small ~10 kDa protein, and HypD, a larger ~41 kDa protein, interact with one another while the former also interacts with the large subunit of the hydrogenase (51, 52). HypE and HypF act together in the process of CN^- synthesis (53, 54). Finally, the endopeptidase is responsible for the proteolytic cleavage of a portion of the C-terminus of the large hydrogenase subunit (51).

Chlamydomonas reinhardtii

Metabolism

Chlamydomonas reinhartdii (*C. reinhartdii)* is a unicellular eukaryotic alga able to grow photosynthetically, chemotrophically on acetate or mixotrophically, a combination of the two (55, 56). As such, it can operate aerobically and anaerobically. When grown on a diurnal cycle, *C. reinhartdii* undergoes oxygenic photosynthesis during the day, fixing CO_2 and storing energy in the form of starch and lipids (Figure 1.8) (57, 58). At night, *C. reinhartdii* switches its metabolism to degrade the stored starch into acetate (59) which can then be used either aerobically or anaerobically through the ATP-dependent production of acetyl CoA (60). Aerobically, under saturating light and CO_2, photosynthesis is reduced in the presence of acetate, however, growth rates are not negatively affected (60). In fact, *C. reinhartdii* grows more quickly using acetate

mixotrophically, than it does when growing photosynthetically (61). Simultaneous detailed description of all carbohydrate metabolism has been difficult due to the compartmentalization of many pathways (62). Prolonged exposure to natural anaerobic conditions (in the dark) leads to the expression of hydrogenase and subsequent evolution of H_2 (63). In other words, hydrogen production requires temporal separation of oxygenic photosynthesis. By manipulating culture media this can be overcome as will be explained shortly.

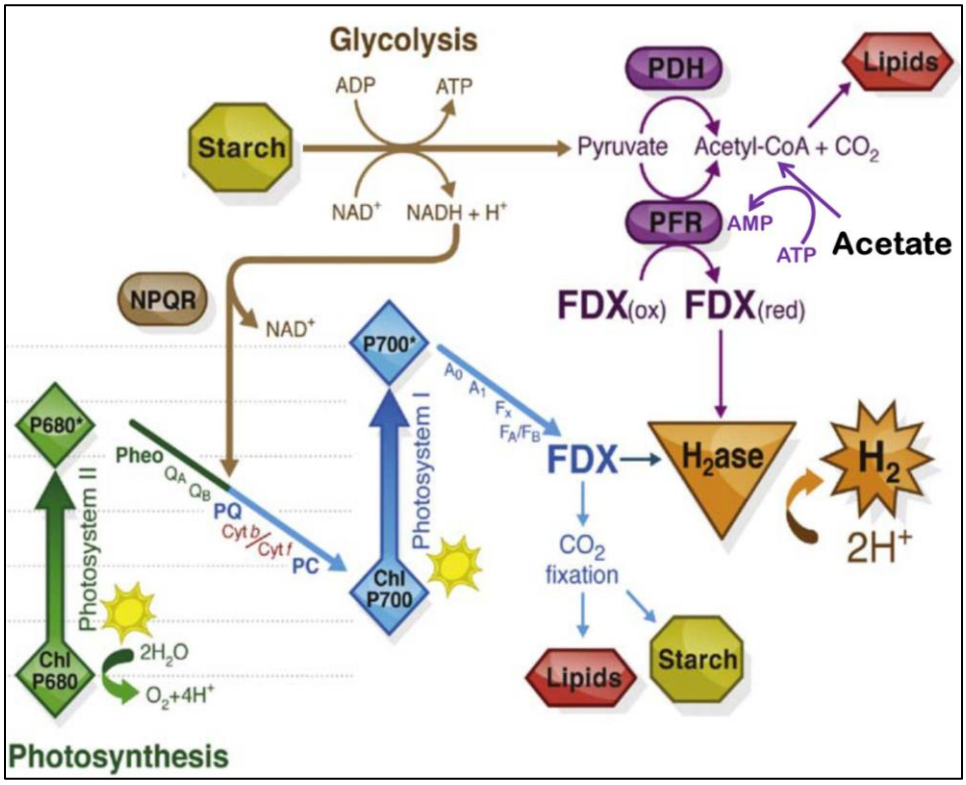

Figure 1.8. Simplified photosynthetic and glycolytic pathways of *C. reinhardtii*. Reducing potential for hydrogen production, mediated by ferredoxin (FDX), can come from PSII, starch degradation, or oxidation of pyruvate. Pyruvate dehydrogenase (PDH) is used under aerobic conditions while pyruvate-ferredoxin oxidoreductase (PFR) is used under anaerobic conditions. Lipid accumulation can occur via CO_2 fixation or acetate uptake. Modified from Beer *et al*. (57).

Hydrogen Production

For continuous H_2 production by *C. reinhartdii*, either an endless supply of starch would be required while dark fermentation took place or both photosynthesis and hydrogen production would need to occur simultaneously. However, the irreversible oxygen inactivation of hydrogenase prevents the two metabolisms from taking place at the same time. This problem has been overcome by depriving cultures of sulfur (63, 64). When cultures are deprived of sulfur, rates O_2 evolution by PSII decreases significantly, allowing for H_2 production in the daytime (65-67). More specifically, sulfur deprivation prevents the synthesis of amino acids required to repair PSII centers thereby preventing oxygenic water splitting (68). What little oxygen remains, is consumed by cellular respiration. With the inability to build sulfur containing amino acids, cells slowly decay and would eventually die without the re-addition of sulfur to rejuvenate cellular components (68). To switch from media containing sulfur to media devoid of sulfur, centrifugation is employed (55). This step is energetically expensive and would decrease the financial feasibility of scaling up this process. One approach to overcome the energy intensive centrifugation step has been to immobilize cultures in a porous matrix (64). Using this method one is able to simply move the matrix from one media to another or use a bioreactor designed to allow easily changeable media to flow over the matrix (69). In such a system, a dedicated bioreactor to house the immobilized matrix must be built.

Another approach to overcome the inhibiting effects of O_2 on H_2 production has been to increase the oxygen tolerance of the hydrogenase. Mutational protein variant studies have been used to address this problem. After defined gas transport channels

within hydrogenase were theorized computationally (70), they were investigated biochemically via random mutagenesis studies (71). Random mutagenesis of residues within the gas channels of HydA from *C. reinhartdii* revealed no change in oxygen tolerance (72) however in CpI some mutations revealed decreased oxygen sensitivity (73). Further characterization of these channels and key gas channel amino acid substitutions are currently being explored by our lab in hopes of increasing the oxygen tolerance of [FeFe]-hydrogenase.

Lipid Production

Lipids accumulate in *C. reinhartdii* primarily for eventual conversion into membrane lipids which make up 5-20% of their dry cell weight (58). However, under conditions of stress, such as nitrogen limitation, many algae increase their accumulation of lipids, typically triacylglycerol (TAG), to 20-50% of their dry cell weight (58). TAGs perform no structural role, but serve as a carbon storage/energy reserve. This type of lipid is ideal for conversion into biodiesel and methods for their extraction directly from the cell have been shown (74, 75). Lipid accumulation was observed in nitrogen starved cells and was shown to be dependent on the carbon supply (76). Additionally, the amount of lipid has been shown to increase with increasing acetate concentration present in the growth media (76, 77). When compared to typical oil crops used for biodiesel production, such as oil palm, algae like *C. reinhartdii* are predicted to yield over fifteen times as much oil (20). With algae's ability to grow on non-arable land, algal lipid production shows great promise as the next bio-diesel feedstock.

Metabolic Manipulation for
Increased Metabolite Production

In addition to adjusting metabolic processes through manipulation of media composition, such as sulfur and nitrogen deprivation mentioned above, metabolic engineering has been used to increase lipid accumulation and H_2 production in *C. reinhartdii.* Starchless, mutants with deletions of ADP-glucose pyrophosphorylase (78) and isoamylase (79) have been isolated and cause a genetic blockage of starch synthesis, a competing pathway with lipid production. Starchless mutants therefore increase the accumulation of lipids, especially during nitrogen deprivation (76, 79, 80). For increased H_2 production, mutations of PSI have been made to increase electrons available to hydrogenase (81, 82). Interestingly, these mutants were also shown to have increased starch accumulation. Rapidly advancing genetic optimization of biofuel producing algae, including *C. reinhartdii,* is allowing us to tune these organisms for production of targeted biofuels (57).

Summary

With the ever increasing demand for energy and the finite supply of fossil fuels, accounting for 80 % of the energy produced worldwide, alternative energy sources are needed to supplement our current consumption. Environmentally, in addition to increasing energy efficiency, the fraction of energy provided by renewable sources must increase to reduce our impact on the earth and its non-renewable resources. For national security, alternative fuel sources provide a means to reduce or eliminate dependence on foreign energy.

Though biofuels appear to be a promising and important part of our future energy portfolio, from a financial perspective, there are numerous hurdles holding back their production and implementation. As technological and fundamental science advancements are made in the renewable energy sector, costs will decrease making biofuels more competitive with fossil fuels. Although cost is an overarching theme, each biofuel has its own set of impediments.

In Brazil and the U.S., ethanol is priced competitively with gasoline (20); however, competition of ethanol feedstocks with food production has been an issue (1, 20). Second generation bioethanol technology has allowed for the use of waste plant matter or even algae to be used as a feedstock (74, 83), thereby avoiding competition with food crops. However, costs associated with second generation technology are high and currently restrict its implementation.

Methane or biogas production usually takes place where an abundant source of waste is concentrated such as dairy farms and landfills. The application of this technology is in its infancy and there is great potential for expansion as many sources of biodegradable waste have yet to be tapped. Once cleaned and compressed, biogas has the ability to power cars and trucks that have been modified to run on natural gas.

Biodiesel, although currently viable, competes with food crops either directly or indirectly. Therefore, newer technologies using algae are currently being investigated. The increased accumulation of oils in algae and their increased photosynthetic efficiency, when compared to typical land crops, are salient benefits that can be had with this oil source.

For biohydrogen production, multiple microbial processes exist and have been used for decades. However, the numerous metabolisms that yield hydrogen all involve one enzyme, hydrogenase. Advancement in our knowledge of this enzyme continues and often centers on its oxygen sensitivity. Although [NiFe]-hydrogenases tend to be more oxygen tolerant than [FeFe]-hydrogenases, they are not nearly as efficient at producing hydrogen. Genetic manipulation has been shown to increase oxygen tolerance of [FeFe]-hydrogenases slightly, however the discovery of new hydrogenases continues to play a pivotal role in directing genetic manipulation experiments directed toward increased biohydrogen production.

Research Directions

Cell Immobilization for H_2 Production

Cell immobilization has been employed as a method to protect organisms from toxins (84), moderate light intensity (85), and increase production of metabolites (86-88) including H_2 (89). Alginate, as an immobilization matrix, is very inexpensive and can take on nearly any geometry. In the next chapter, the hypothesis that encapsulating *C. reinhartdii* in spherical beads might facilitate growth media exchange and allow for the production of H_2 will be investigated. The ability to change media in which an entire culture is growing typically requires cells be separated via centrifugation, an energy intensive procedure. As will be explained, with immobilization techniques, this step can be replaced by simply straining beads from their media.

Co-culturing for Simplified Phototrophic Biofuel Production

Lipid accumulation by algae is currently an attractive means of producing biodiesel sustainably while not competing with food production (20). Phototrophic algae have been exploited from many angles to optimize and maximize biofuel production and reduce costs associated with lipid extraction. Most current experimental growths of the model organism *C. reinhartdii* are grown mixotrophically using acetate as the organic carbon source. As a means of providing biofuel producing cultures with an inexpensive carbon source, co-culturing has provided acetate metabolically through photosynthesis of another organism. In chapter three, a study of co-culturing photosynthetic bacteria with eukaryotic algae as a means to produce acetate and lipids has been demonstrated. Employing alginate encapsulation techniques mentioned in chapter two, the two organisms in the co-culture are kept separate and growth stability is achieved. In summary, acetate provided by the cyanobacteria (*Synechococcus* PCC 7002) is able to sustain the co-cultured algae (*C. reinhartdii*) which in turn is able to accumulate lipids.

Physiological and Structural Characteristics of Hydrogen Producing and Hydrogen Oxidizing Hydrogenases from the Model Organism *Clostridium pasteurianum*

The enzyme responsible for biological production of H_2, hydrogenase, has been well studied over the years. Numerous examples of [NiFe]- and [FeFe]-hydrogenases exist and their preferential direction of catalysis has been investigate; hydrogen oxidation is typically catalyzed by the [NiFe]-hydrogenases while hydrogen production is predominantly catalyzed by the [FeFe]-hydrogenases. While [FeFe]-hydrogenases are

usually associated with production of H_2, some have been shown to favorably oxidize H_2. In chapter four, an investigation of active-site and accessory cluster environments of biochemically characterized representatives of H_2 oxidizing and H_2 producing hydrogenases, is undertaken. Additionally, we assign a biological function to a biochemically characterized "uptake" [FeFe]-hydrogenase. Results of this chapter also reveal additional hydrogenase enzymes in the well-studied model organism *C. pasteurianum*. Understanding how these enzymes are tuned to favor production or oxidation of hydrogen would be a large step toward optimizing bio-hydrogen production from a molecular level. From a metabolic perspective, the described associations of hydrogenases with nitrogen-fixation provide new insights into how a model nitrogen-fixer employs its numerous hydrogenases.

CHAPTER 2

EXTENDED HYDROGEN PRODUCTION BY ALGINATE-IMMOBILIZED, SULFUR-DEPRIVED *CHLAMYDOMONAS REINHARDTII*

Contribution of Authors and Co-Authors

Manuscript in Chapter 2

Author: Jesse B. Therien
Contributions: Conceived and implemented the study design. Collected and analyzed data. Prepared the manuscript for submission to a peer-reviewed journal.

Co-Author: Keith E. Cooksey
Contributions: Helped conceive and implement the study design. Discussed results and provided insight.

Co-Author: Matthew C. Posewitz
Contributions: Discussed results and provided insight.

Co-Author: John W. Peters
Contributions: Helped conceive and implement the study design, discussed results/implications, provided insight and edited the manuscript.

Manuscript Information Page

Jesse B. Therien, Keith E. Cooksey, Matthew C. Posewitz, John W. Peters
International Journal of Hydrogen Energy
Status of Manuscript:
_X_ Prepared for submission to a peer-reviewed journal
____ Officially submitted to a peer-review journal
____ Accepted by a peer-reviewed journal
____ Published in a peer-reviewed journal

Publisher: Elsevier Ltd

Abstract

As global energy consumption continues to increase, so do the demands for alternative and renewable energy solutions. Hydrogen is considered by many to be an attractive option given the multiple ways in which it can be produced and the efficacy of fuel cell technologies. One source of renewable H_2 is through the metabolism of a variety of microorganisms. Photosynthetic microorganisms are particularly attractive due to the potential to convert solar energy to H_2 directly; however this process does not occur naturally. The model green algae, *Chlamydomonas reinhardtii* has been studied extensively in an attempt to better couple the reducing power generated from sunlight during photosynthesis to biological H_2 production. It was revealed that under conditions of sulfur deprivation light driven H_2 production could be maintained for extended periods. Since cultures cannot be maintained under sulfur deprivation conditions, cultures need to be manipulated between growth media for maximal H_2 production. Immobilization of *C. reninhardii* allows for more facile changes in media composition and can be used to maximize solar H_2 production. Here, we demonstrate photoproduction of H_2 by *C. reinhardtii* immobilized in alginate beads in sulfur-depleted media. Immobilization was shown to increase the duration of the H_2 production phase compared to freely suspended cells. Bead size, cell density, and headspace gas composition were variable tested for optimal H_2 production. The alginate-immobilizing matrix was shown to afford protection from inhibiting O_2 in reactor headspace. The approach to immobilization shown here allows for flexible bioreactor geometries, easy culture handling, and a simplified immobilizing process.

Introduction

Hydrogen (H_2) is a simple energy carrier that has the potential to play a key role as clean fuel that can be utilized in combustion reactions and in well-developed fuel cell technologies (24). Although hydrogen is the most abundant element on Earth, it is associated with more complex molecules and it is rare to find the diatomic form in nature. Currently, the majority of the H_2 we use comes from reforming of crude oil and natural gas, both finite resources that can be expensive to extract from the Earth. Additionally, the process of reforming hydrocarbons releases large amounts of CO_2, a greenhouse gas. Extracting H_2 from the Earth's vast supply of water, on the other hand, requires no expensive drilling and releases no CO_2. Electrolysis uses an electrical current to split water into its two components, H_2 and O_2 following the reaction: $2\ H_2O(l) \rightarrow 2\ H_2(g) + O_2(g)$. However, this is an energy intensive operation and requires about 1.5 times the energy input than the energy available in the produced H_2. If the electric current used for this process comes from a hydrocarbon-burning power plant, the environmental benefits of using H_2 can be negated. Certain microorganisms produce H_2 naturally during metabolism as a mechanism to recycle reduced electron carriers produced during fermentation.

Many green algae naturally produce H_2 in the dark once their environment becomes anaerobic (90). In the absence of light, after photosynthesis and residual O_2 is consumed by cellular respiration, the culture becomes anaerobic. Algal cells maintain their metabolism and cell function through anaerobic metabolism fermenting starch stores accumulated during the daylight hours (65) and produce of H_2 as a means to recycle

electron carriers. H_2 production is catalyzed by [FeFe]-hydrogenases and continues until the cells are re-exposed to light (90) and oxygenic photosynthesis inactivates the oxygen sensitive hydrogenase diverting reducing equivalents to the production of ATP and carbon fixation.

In the model unicellular microalgae *C. reinhardtii*, it has been shown that O_2 production from photosynthesis can be inhibited by 75% through depriving the cell of sulfur (91). In the absence of sulfur, the reaction center of PSII cannot be re-manufactured and O_2 production slows below respiratory O_2 consumption levels (91-93). This allows the culture to become anaerobic while still converting the sunlight's energy to H_2 with the partially operational photosystem.

Sustained H_2 production by sulfur deprived *C. reinhardtii* has previously been shown by freely suspended cells (68, 93) and by immobilized cells (94). Under optimal conditions, freely suspended cells typically yield H_2 more quickly but lack the benefits provided by immobilizing matrices. In addition to facilitating culture handling, immobilization offers other advantages over freely suspended cells such as increased production of H_2 (95) and other metabolites (96-98) under less than ideal conditions, the ability to moderate light intensity (99), and protection from toxins (92). Benefits of alginate bead encapsulation over other types of immobilization of particular interest in this study are ease of replicate experimentation, flexible bioreactor geometries, facile fabrication, and their low cost. Alginate beads are superior to other stationary immobilization techniques since they can fill nearly any shape and can even circulate with media. To evaluate the efficacy of alginate bead encapsulation as a means to

immobilize *C. reinhardtii* for H_2 production, we performed the following studies. Firstly, we monitored rates of H_2 production of encapsulated cells deprived of sulfur in comparison to freely suspended cells deprived of sulfur. Once it was confirmed that alginate encapsulated cells were able to sustain production of H_2, other variables such as bead diameter, cell density within beads, and the influence of headspace volume and gas composition. Finally, H_2 and O_2 were added to the headspace in increasing concentrations to determine if the immobilization matrix provided any protection from their inhibiting effects. The experiments herein summarize some parameters and characteristics of alginate bead encapsulation as a method of immobilizing H_2-producing algae. In conjunction with the many other immobilization matrices and geometries, our study expands the possibilities of effective methods for bio-hydrogen production.

Methods

Strains and Media

For bulk cell stock, *C. reinhardtii* (CC124) was grown aerobically on TAP media at pH 7, 30ºC, shaken at 100 rpm and illuminated with a fluorescent light providing an intensity of 70 $\mu Em^{-2}s^{-1}$ in a water bath. For all experiments with sulfate-deprived cultures (grown on TAP-S), cells previously grown on TAP to a concentration of ~7.3 x 10^6 cells ml^{-1}, were harvested by centrifugation at 5000 rpm and the pellet was re-suspended in N_2-purged TAP-S in an anaerobic chamber. This wash step was repeated twice and the final re-suspension contained 2.9 x 10^6 – 4.0 x 10^6 cells ml^{-1}. To ensure consumption of any residual sulfur, cultures were sealed and incubated overnight under the same temperature, light intensity, and agitation speed. Optical densities were then re-

checked to ensure cultures were still within the desired range. Prior to harvest, cultures were purged with 0.2 µm filtered N_2 for 15 minutes. Sulfur-replete control cultures were spun and re-suspended in the same manner as sulfur-depleted controls and samples substituting TAP-S with TAP.

Immobilization Methods

Alginate beads were made by dissolving 3 g of sodium alginate in 100 ml of *C. reinhardtii* prepared as stated previously to densities between $2.9 \times 10^6 - 4.0 \times 10^6$ cells ml^{-1}. Alginate concentrations of 3% used in this work were previously shown to minimize substrate diffusion problems (100). The alginate-culture mixture was added drop-wise with a syringe and needle into a 1% solution of $CaCl_2$ in TAP-S at room temperature from a height of at least 30 cm in an anaerobic chamber with an atmosphere of N_2 containing < 2% H_2. Bead size was controlled by different dropper orifice sizes: 22G needles resulted in 2 mm beads, 18 G needles resulted in 3 mm beads, while 4 mm beads were made directly from a 10 ml syringe without a needle. Beads formed immediately and were allowed to harden further in the $CaCl_2$ solution for 15 minutes. After hardening, beads were removed from the $CaCl_2$ solution by straining, allowed to drip dry for 5 minutes and added to media in glass vials. Unless otherwise stated 4 mm beads were used in all experiments.

Reaction Vessel Setup and Operation

Experiments were carried out in 25, 70, or 120 ml glass serum vials (Wheaton, USA) sealed with black-butyl rubber stoppers (Geo-Microbial Technologies, Inc.

Ochelata, OK) and 20 mm crimped tops. Beads resulting from 9 ml of alginate-culture mixture were added to 6 ml of media leaving approximately 10, 55, and 105 ml headspaces respectively for gas accumulation. Twenty-five ml vials were used for all but the headspace volume experiments where 70 and 120 ml vials were introduced. Vials were then purged with N_2 for 15 minutes before being placed in a water bath at 160 rpm and 30 ºC illuminated with a 55 watt fluorescent light providing a light intensity of 70 $\mu Em^{-2}s^{-1}$.

H_2 Quantitation

Headspace gas samples were taken using a Hamilton 50 µl gas-tight syringe and were analyzed on a Shimadzu GC-8A/C-R8A gas chromatograph equipped with a Supelco 80/100 Porapak® N 6ft x 1/8 in or Restek® 80/100 molesieve 10 ft. x 1/8 in column and a TCD detector. After sampling headspaces (except for the headspace volume experiment in section 3.4), vials were purged for 15 minutes with 0.2 µM filtered (Fisherbrand Cat. No. 09-719C) N_2 from an in-house source to remove all other gases from the headspace. H_2 and O_2 were ≥99% pure and supplied by General Distributing (Great Falls, MT).

Chlorophyll Quantitation

Measurements of initial optical density correlated linearly with concentrations of total chlorophyll (R^2 = 0.92) and cell number (R^2 = 0.99) (data not shown) and were chosen as an efficient and accurate method to determine culture densities for comparison. Measurements were made spectrophotometrically at 750 nm.

Total chlorophyll was extracted with acetone following a published protocol (95, 101) and measured spectrophotometrically at 645 and 663 nm. For in situ determination of total chlorophyll in beads, the same procedure was performed with whole beads rather than cell pellets.

Results/Discussion

H_2 Production During Immobilization

To determine if alginate encapsulation of *C. reinhardtii* allowed for sustained production of H_2 in TAP-S media, we compared encapsulated cells to freely suspended cells during a period of just over 13 days, purging headspace gases with N_2 after each sampling event. It was observed that encapsulated *C. reinhardtii* in TAP-S exhibit an increased production of H_2 over freely suspended cells during the first 30 hours of incubation (Figure 2.1 and Table 2.1). Initially, the rate of H_2 production by encapsulated cells is over 2.6 times greater than that of freely suspended cells (Table 2.1). Increases in initial rates of H_2 production is a likely result of the respiratory capacity of the highly concentrated cells within the beads creating anaerobic microniches which allow a more rapid transition to H_2 production. Small bubbles are occasionally formed while the beads are being made and would initially contain an atmosphere of N_2. After 100 hours, freely suspended cells increased production of H_2 while the immobilized cells slowed H_2 production significantly to 8.5 times below that of free cells (Figure 2.1 and Table 2.1). This reduction in H_2 production by alginate encapsulated organisms has been observed in previous studies dating back to the 1980's (102, 103). Similarly, decreased rates of respiration by immobilized *Chlorella* have been attributed to mass transfer constraints by

alginate (104, 105). In a study of alginate as an immobilizing material, it was shown that for alginate concentrations above 1.9%, diffusivities are considerably lower in non-homogeneous beads (106). Our beads, of 3% alginate, are likely non-homogeneous as observed by the gaseous pockets formed during the fabrication process. The decrease in H_2 production rates in alginate immobilized *C. reinhardtii* may also be a consequence of the reduction in the ability of substrates and products to diffuse across the encapsulating matrix.

At maximum, freely suspended cells produce H_2 at a rate of 0.256 µmol of H_2 $hour^{-1,}$ while encapsulated cells generate H_2 at a steady rate of about 0.030 µmol of H_2 $hour^{-1}$ during this time under the conditions of this study. Although the rate of H_2 production by encapsulated cells is less than that of freely suspended cells during most of the first 200 hours, after the 268 hour time point, while H_2 evolution is no longer apparent in freely suspended cells, encapsulated cells continue to produce H_2. Growth of algae in alginate beads has been shown to be significantly less than that of freely suspended cells (104), thus increased duration of metabolite production could more simply be attributed to the slowed metabolism of immobilized cells or the slower diffusion of substrates to immobilized cells. The stability of encapsulated cells is finite and eventually algae start to grow in the suspension media. Migration of cells from the immobilizing matrix appears to have precedence when carrying out an encapsulation experiment for an extended time (92, 97, 104).

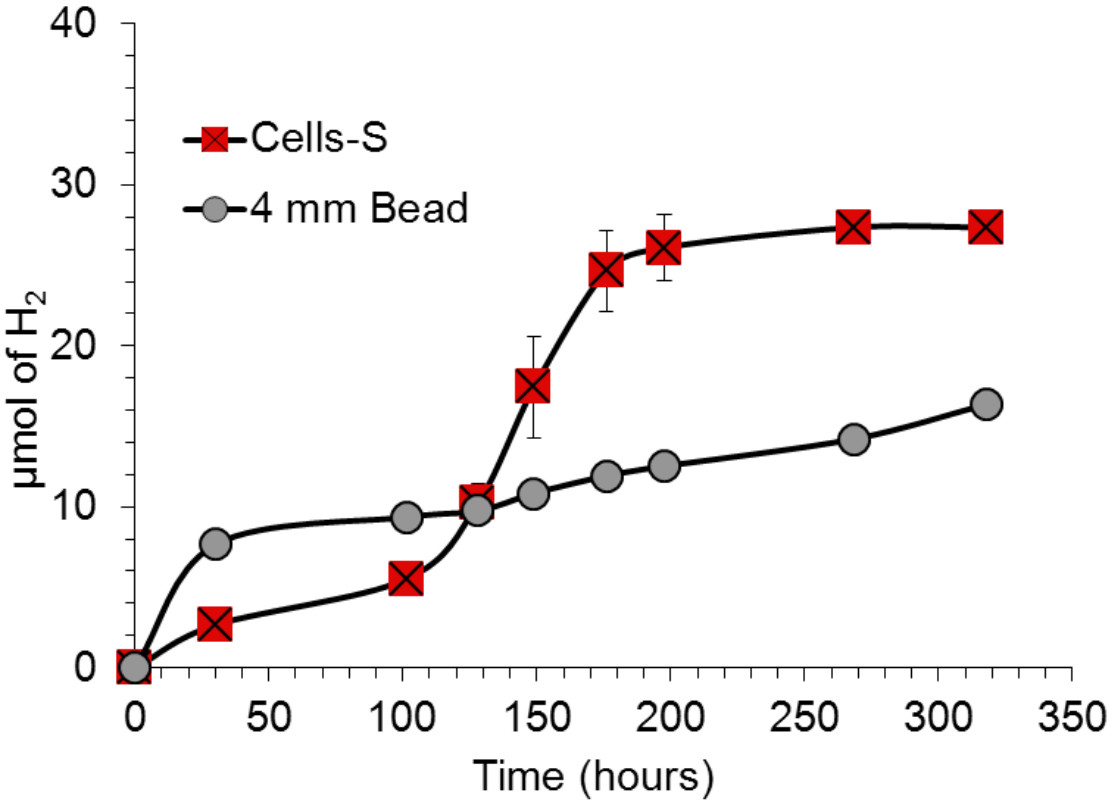

Figure 2.1. H_2 production by 4 mm alginate-encapsulated and freely suspended *C. reinhardtii* in TAP-S media purged with N_2 between sampling events.

Table 2.1
Rate of H_2 production (µmol H_2/hr) per vial.

	0-30 hrs	**30-101 hrs**	**101-176 hrs**	**198-318 hrs**
Freely suspended cells	0.089	0.040	0.256	0.011
Encapsulated cells	0.238	0.023	0.030	0.038

Cell Concentration

Cell density has been reported to be a crucial variable responsible for reduced cell viability (107) and/or productivity (105, 108) within immobilization matrices. We examined three cell densities, 1.5 x 10^6, 2.6 x 10^6, and 5.4 x 10^6 cells ml^{-1} (from here on out referred to as 0.5x, 1.0x and 2.0x respectively), and chose 4 mm diameter beads for

ease of fabrication. Beads with increased culture density were initially darker green in color and *in situ* chlorophyll assays indicated they contained 5.67, 6.39, and 17.6 µg chlorophyll ml^{-1} respectively.

After 22 hours, 2.0x beads produced twice as much H_2 when compared to 1.0x beads, and beads with fewer cells (0.5x) produced even less (Figure 2.2). As the experiment continued the difference in H_2 production between the three different initial cell densities within beads decreased. After 71 hours, 0.5x, 1.0x, and 2.0x yielded 17.4, 25.0, and 28.5 µmol of H_2 per vial respectively. After 71 hours, both *in situ* chlorophyll determination and H_2 production assays indicated the difference among 0.5x, 1.0x, and 2.0x beads decreased. The increase in chlorophyll content in lower cell density beads may reflect cell proliferation.

On an initial per cell basis, the more densely colonized beads produced less H_2 throughout the experiment. This is a likely results of higher cell densities permitting less light per cell and higher competition for nutrients and is consistent with the results of other immobilization studies (92, 96, 99, 105, 107, 108). As a result of these experiments we concluded that 2.6×10^6 cells ml^{-1} was the optimal cell concentration for H_2 production and used this concentration in subsequent experiments.

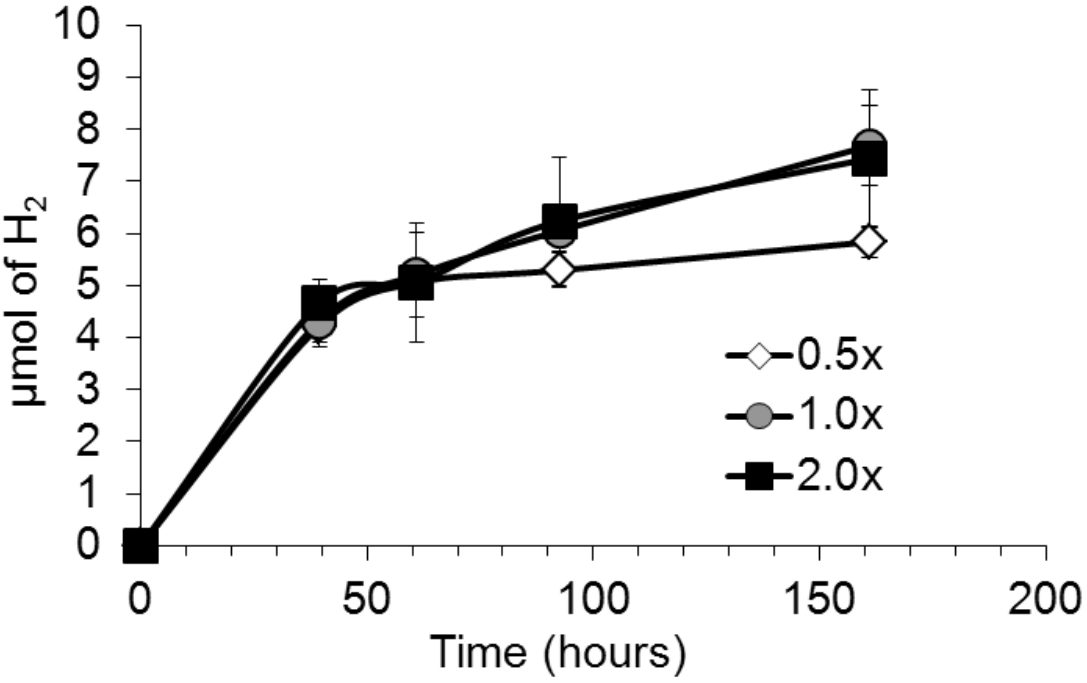

Figure 2.2. H_2 production by alginate-encapsulated *C. reinhardtii* of varying initial cell densities per bioreactor. 0.5x, 1.0x and 2.0x equate to 5 x 10^6, 2.6 x 10^6, and 5.4 x 10^6 cells ml^{-1} and 5.7, 6.4, and 17.6 mg chlorophyll ml^{-1} respectively.

Bead Diameter

In previous work it has been observed that diffusional limitations have been responsible for reduced metabolite production rates by alginate immobilized cells (99, 104, 105, 107, 108). To investigate if H_2 production could be optimized by modulating diffusion barriers in alginate, beads of 2, 3, and 4 mm diameter (Figure 2.3 inset) were synthesized and compared. A larger bead diameter would have more alginate per cell for substrates and products to diffuse through and presumably would produce H_2 more slowly. In previous studies however it has been shown that algae encapsulated in beads with diameters of 4 mm and 6 mm were slightly better than smaller 2.8 mm beads (108)

at removing ammonia, phosphate and nitrate from wastewater. Our observations indicate at least for the range between 2 and 4 mm for which beads can be easily fabricated that bead size does not impact H_2 production significantly (Figure 2.3). Since 4 mm beads are easiest to fabricate they were used exclusively in subsequent experiments.

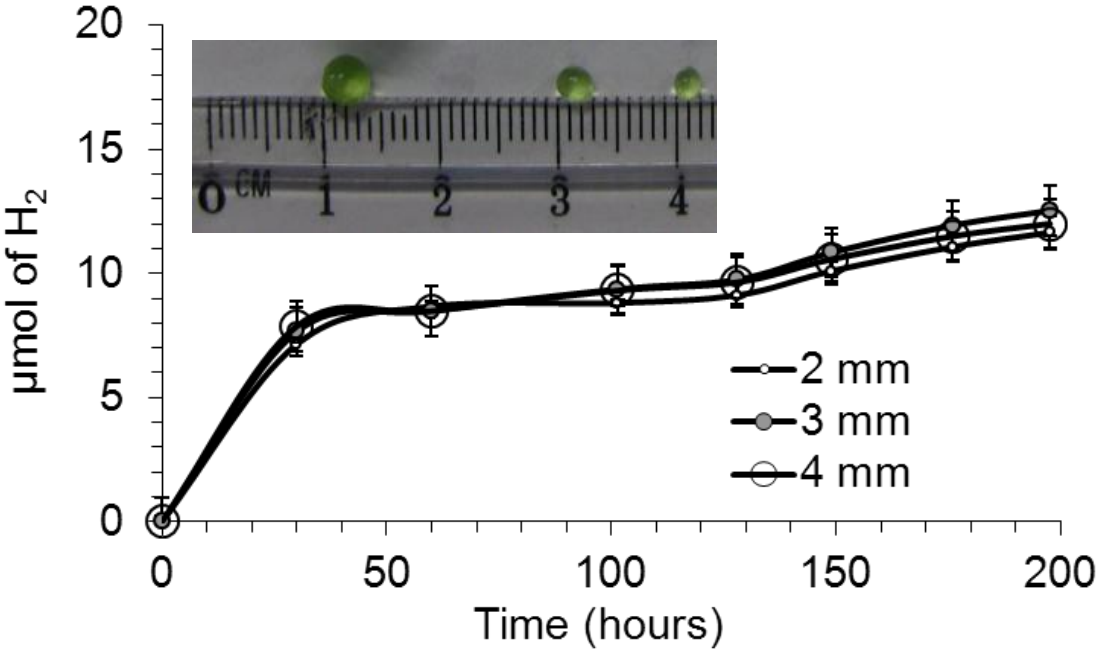

Figure 2.3. H_2 production by alginate-encapsulated *C. reinhardtii* from beads with diameters of 2, 3 and 4 mm. Inset shows actual beads next to 1 mm ruler markings.

N_2 Purging

It has been previously demonstrated that purging cultures of *C. reinhardtii* during photoproduction of H_2 in TAP-S with an inert gas such as Ar or N_2 can significantly increases H_2 yields (94). It has been suggested that sparging with an inert gas increases culture mixing and prevents heterogeneity of the culture which could lead to aerobic, O_2 producing, pockets (94). Purging with inert gases also removes any build-up of headspace gases including H_2 that would occur in a closed reactor including O_2 and H_2

that are both inhibitory toward H_2 production. Although continuous sparging with Ar has shown to provide the greatest yields of H_2 in *C. reinhardtii* (94), we examined the frequency at which headspace gases required sparging for sustained H_2 production. N_2 was used to sparge and replace headspace gases after each sampling event, while a duplicate set of vials were left to accumulate gases in the headspace. It was observed that headspace purging with N_2 increased H_2 production after just 4 hours. Reactors purged with N_2 continued to show increased H_2 production for the duration of the experiment. Interestingly, when headspaces were left unpurged and allowed to accumulate gases, these cultures eventually ceased production of H_2 after around 24 hours (Figure 2.4). These results suggest that headspaces should be purged somewhere around 24 hours to maximize H_2 production.

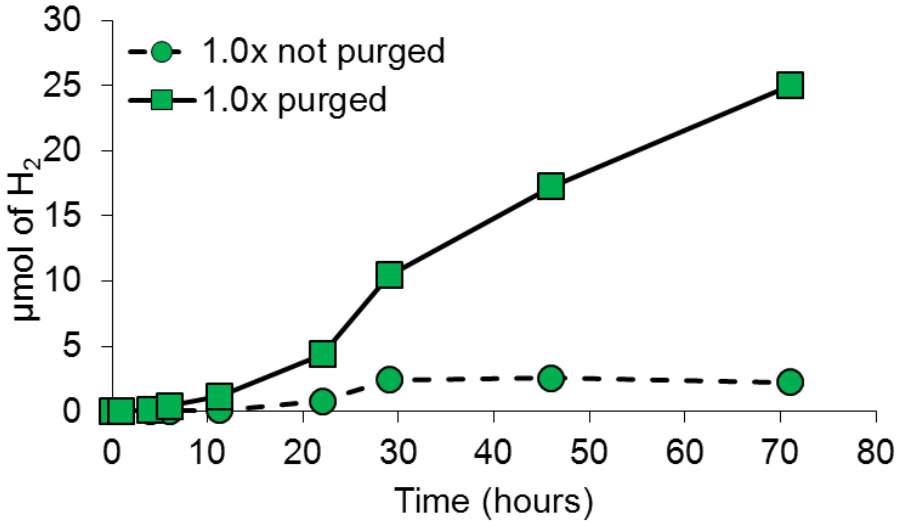

Figure 2.4. H_2 production by alginate-encapsulated *C. reinhardtii* of varying initial cell densities per bioreactor. Squares represent bioreactor purged with N_2 after each sampling point while circles represent unpurged bioreactors where gasses were allowed to accumulate. (Experiment repeated with varying cell concentrations yielding results with a standard deviation of ~3-6 µmol of H_2 in the last 40 hours when normalized to cell density [data not shown]).

Headspace Volume

Duplicate vials containing beads of *C. reinhardtii* with 3 different headspace volumes were periodically monitored for H_2 evolution over 160 hours. A total of 15 ml of culture (9 ml of beads and 6 ml of media) was added to the vials yielding headspace volumes of 10, 55, and 105 ml. It was observed that a threshold headspace H_2 concentration around 1-1.3% inhibited H_2 production (Table 2.2). Headspace volumes of 10, 55, and 105ml all reached this maximum H_2 concentration even though the volume of evolved H_2 increased as the headspace volume increased. Despite the large difference in headspace volumes tested, the maximum concentration of H_2 produced by encapsulated cells varied only slightly. As expected, gases built up quickest in vials with smaller headspace volumes. The concentration of H_2 within the headspace of the vials ranged from 0.7-2.4% during the first 16 hours, but leveled off at 1-1.3% after 135 hours. When half as many beads were used in the same total culture volume (3 ml of beads and 12 ml of media) a similar threshold was observed. The more rapid accumulation of H_2 in the vials with smaller headspaces, allowing the concentration to exceed the postulated inhibitory level for a short time, might be due to the momentum of the H_2 producing machinery and/or the delayed metabolic adaptation of the cells to the headspace H_2.

Table 2.2
H_2 produced as a percentage of total headspace volume

Headspace Volume	**16 hrs**	**39 hrs**	**93 hrs**	**112 hrs**	**135 hrs**
10 ml	2.37	2.39	1.70	1.29	1.25
55 ml	1.04	1.81	1.29	0.70 ±0.26[a]	1.01
105 ml	0.74	1.43	1.23	0.99	1.21 ±0.16[a]

[a]Values after the ± symbol represent standard deviations of triplicate samples and are < ±0.15% unless shown. Samples not purged with N_2 after sampling events.

Headspace Gas Composition

The relationship of headspace H_2 concentration and inhibition of H_2 production, was investigated by adding 0.5, 1.0, 4.8, 9.1 and 33.0% H_2 to vials and compared to a control that was purged daily with N_2 (Figure 2.5). Headspace H_2 concentrations of 0.5% decreased net H_2 production by almost an order of magnitude or more within the first 65 hours. Beyond 65 hours this sample showed little difference in H_2 evolution when compared to the control as did the sample with a concentration of 1.0% for the duration of the experiment. All H_2 concentrations above 1.0% resulted in net consumption of H_2 during the first 65 hours, while concentrations above 4.8% in the headspace yield a net consumption of gas throughout the experiment. It would appear that a headspace H_2 concentration above 1% but below 4.8% is the balancing point between H_2 production and H_2 consumption. This range is similar to what we saw when looking at the effect of headspace volume. The cessation of H_2 evolution is thought to be the result of product inhibition while its consumption may be due to either the oxyhydrogen or photoreduction reactions (109, 110).

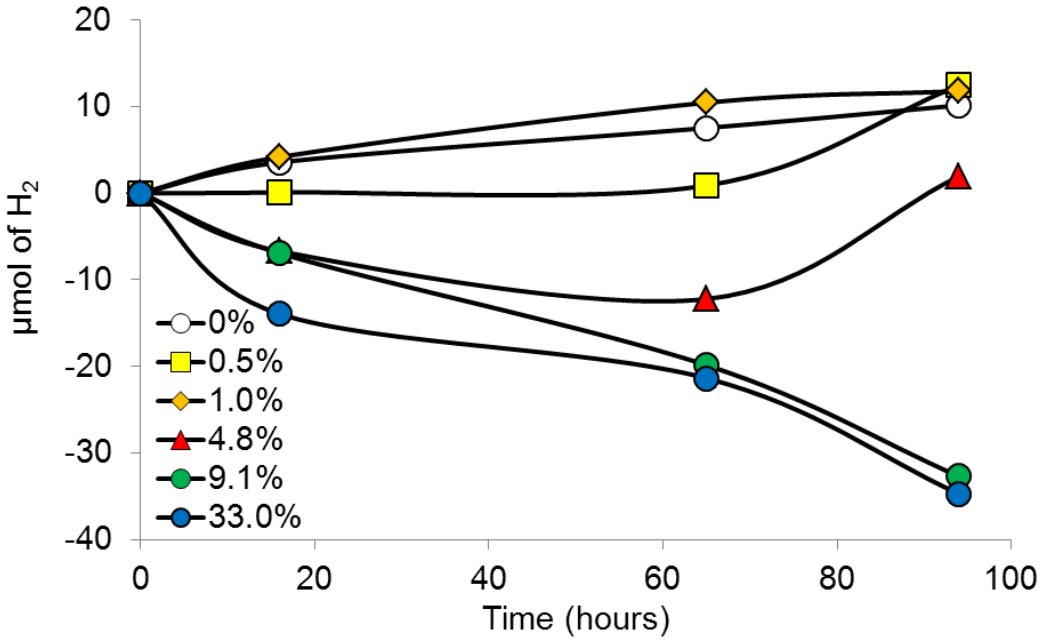

Figure 2.5. H_2 production by alginate-encapsulated *C. reinhardtii* in vials with headspaces containing added H_2. Legend shows percentage of H_2 added to headspace.

Hydrogenase activity is inhibited by O_2; an IC_{50} of just under 0.4% O_2 has been previously reported for freely suspended cells (111). We examined whether encapsulation of cells in alginate had any influence on the inhibitory effects of O_2 in culture. O_2 concentrations of 0.5% and 1.0% appeared to initially stimulate H_2 production and concentrations of 4.8%, 9.1%, and 33.3% immediately slowed H_2 production and eventually stopped its production after 65 hours (Figure 2.6). An IC_{50} at two time points, 16 and 64 hours (Figure 2.7), was determined to be 10.9% and 13.1% respectively, an increase of ~30 fold when compared to freely suspended cells of *C. reinhardtii* (IC_{50} of 0.394 +/- 0.068 % O_2) (111). These numbers may be hard to compare as the methods and sampling times are quite different, but suggest an increased O_2 tolerance for alginate encapsulated cells. Increased O_2 tolerance is likely afforded by the

calcium-alginate matrix which has been previously reported to limit the diffusion of substrates including O_2 (104, 112).

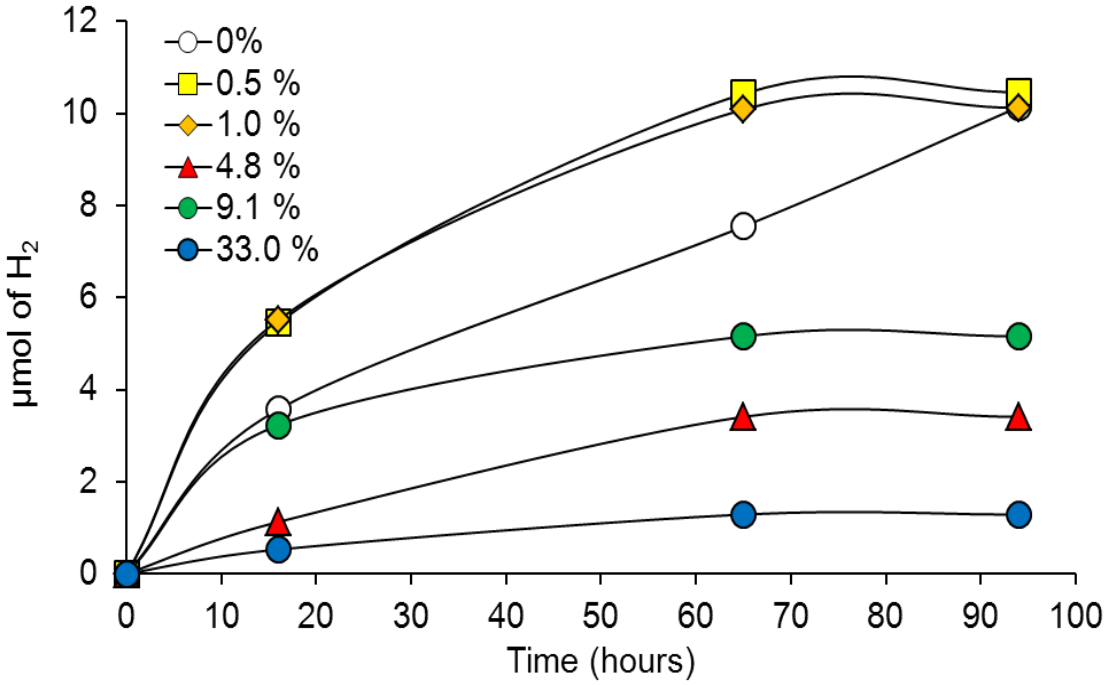

Figure 2.6. H_2 production by alginate-encapsulated *C. reinhardtii* in vials with headspaces containing added O_2. Legend shows percentage of O_2 added to headspace.

Results here suggest alginate encapsulation of *C. reinhardtii* provides prolonged protection against low concentrations of hydrogenase-inhibiting O_2 and temporary protection from much higher concentrations of O_2. The increased O_2 tolerance and prolongation of H_2 production by alginate encapsulation are promising qualities that have potential to be further exploited in bio-hydrogen production applications.

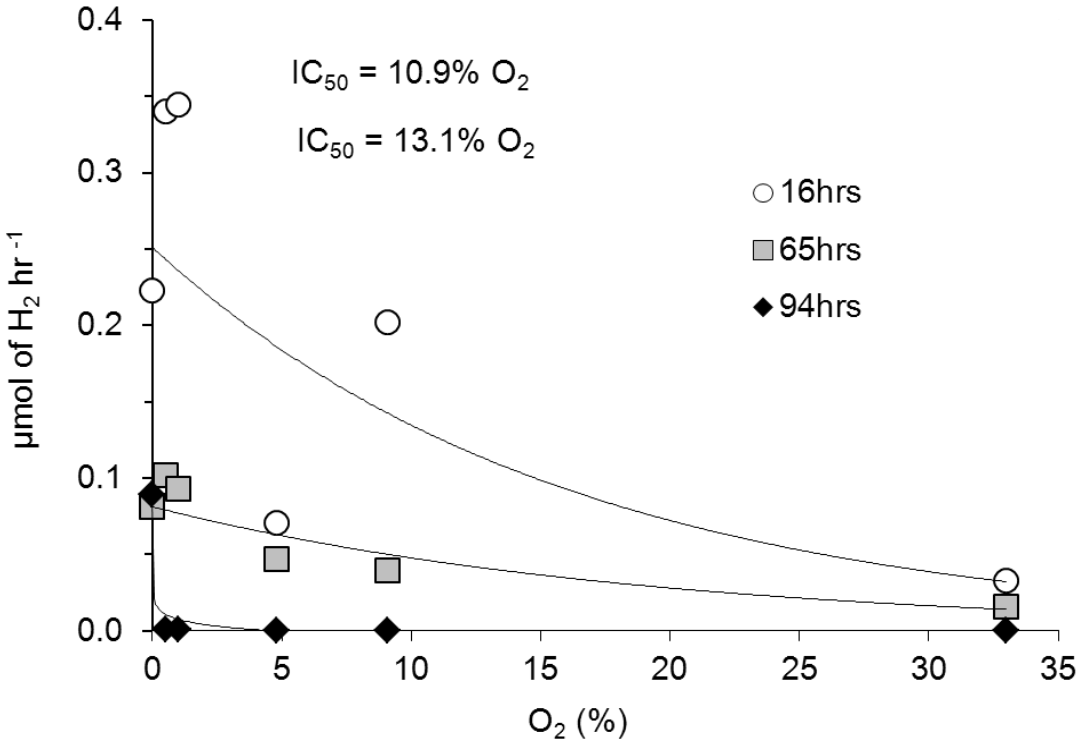

Figure 2.7. Effect of O_2 concentration on production of H_2 by encapsulated *C. reinhardtii* at 16, 65, and 94 hours. IC_{50} shown for 16 and 65 hour time points.

Summary and Conclusions

Rates of H_2 production reported here for sulfur-deprived, alginate-bead encapsulated *C. reinhardtii* are approximately an order of magnitude less than those reported for Al-borosilicate glass immobilized *C. reinhardtii* (94) and 60% of freely suspended cell controls. A major limitation of the study is the reactor design which was constrained by the need to do many replicates in parallel and required studies to be conducted in small sealed vials. The experimental design was sufficient to evaluate a number of important parameters regarding H_2 production by *C. reinhardtii* during immobilization in alginate beads and H_2 production should presumably be improved

through improved reactor engineering. Our results suggest H_2 production by alginate-encapsulated cells could extend beyond the 318 hour timeframe of this experiment which is much longer than freely suspended cells. Cells encapsulated in larger beads with diameters of 4 mm produced similar amounts of H_2 when compared to beads of 2 and 3 mm. Cell densities of 1.5×10^6 cells ml^{-1} yielded the greatest amount of H_2 on a per cell basis, while increases in cell density decreased the per cell H_2 production. Increases in headspace volume allowed for an increase in total volume of H_2 produced per cell but slightly decreased the concentration of H_2 produced in a given headspace. Headspace H_2 concentrations somewhere between 1 and 4.8 % are inhibitory to further bio-production of H_2 and, we think, cause a metabolism shift to oxyhydrogen or photoreduction reactions (109, 110). O_2 concentration of 1% or less in the headspace appear to stimulate H_2 production but levels of 4.8% or greater quickly inhibit bio-hydrogen production. As mentioned above the next generation of experimental design and reactor engineering could further optimize conditions to maximize H_2 production beyond what was reported here. Continuous or frequent purging is most likely the easiest and most effective way to increase hydrogen yields from alginate-encapsulated *C. reinhardtii* as previously suggested by others (94). Similarly, increasing headspace to a volume that prevents an accumulation of H_2 above 1% would allow for maximum production of bio-hydrogen in similar systems. Overall, immobilizing *C. reinhardtii* in alginate beads extends H_2 production beyond that of freely suspended cells at more consistent although slower rate. Alginate-encapsulation shows promise as an affordable and flexible method for immobilization of H_2 evolving algae.

CHAPTER 3

PHOTOTROPH CO-CULTURING FOR THE OPTIMAL PRODUCTION OF BIOFUELS

Contribution of Authors and Co-Authors

Manuscript in Chapter 3

Author: Jesse B. Therien
Contributions: Conceived and implemented the study design. Collected and analyzed data. Prepared the manuscript for submission to a peer-reviewed journal.

Co-Author: Oleg A. Zadvornyy
Contributions: Helped conceive and implemented the study design. Collected and analyzed
data. Helped write the results section of the draft manuscript.

Co-Author: John W. Peters
Contributions: Helped conceive and implement the study design, discussed results/implications, provided insight and edited the manuscript.

Manuscript Information Page

Jesse B. Therien, Oleg A. Zadvornyy, John W. Peters
Biotechnology for Biofuels
Status of Manuscript:
_X_ Prepared for submission to a peer-reviewed journal
____ Officially submitted to a peer-review journal
____ Accepted by a peer-reviewed journal
____ Published in a peer-reviewed journal

Publisher: BioMed Central

Background

With the ongoing increase in global energy demands, alternative energy has been at the forefront of modern research. Of the alternative energies, bioenergy has been of interest for its many benefits over currently used petroleum, natural gas and coal. These benefits include the carbon neutrality, renewability, low environmental toxicity, and reduction of dependence on foreign energy. The largest proportion of biofuels is produced from higher plants (20), providing mainly biodiesel and bio-ethanol. These fuels can replace diesel and gasoline, respectively, in today's conventional engines without modification. The infrastructure for many biofuels is lacking, but biodiesel and ethanol are able to use infrastructure already in place worldwide. Currently 5%-10% of gasoline sold in the US contains ethanol while biodiesel use is much less (113). Of these two biofuels, biodiesel has been considered the most viable long term solution in the US (114). Biodiesel can be produced from oil derived from plants that convert the sun's energy into chemical energy. Biodiesel from crops grown on arable land can compete with agricultural food production (20). An alternative to food crops as a biological source lipid biofuels is to use microalgae that grow in areas not suitable for crop growth like deserts. Microalgae are unicellular photosynthetic organisms that assimilate CO_2 and convert solar energy into multiple energy carriers such as, hydrogen (H_2), starch, and lipids (57). H_2 can be used directly as a clean fuel for hydrogen fuel cells, starch can be fermented to ethanol, while lipids can be converted to biodiesel. In addition to the production of multiple valuable metabolites, microalgae have higher efficiencies for converting solar energy into chemical energy than terrestrial biomass (114).

Co-culturing can be used as means to convert an otherwise unusable carbon source, using one organism, to a form that can be metabolized into something useful by another (115). In simpler terms, one organism can feed the other.

Some lipid-accumulating microalgae, such as *Chlamydomonas reinhardtii*, are mixotrophs and grow photosynthetically, chemotrophically on acetate, or a combination of the two (59). *C. reinhardtii* is a unicellular eukaryotic algae that grows well in Tris-Acetate-Phosphate (TAP) media between pH 6-8 at temperatures ranging from 15-35°C [Harris, 1989 #41], however pH 7 and 25-30 °C seem to be optimal conditions (63, 64, 116). Light and CO_2 are abundant and inexpensive, however, optimal growth of *C. reinhardtii* has been observed in mixotrophic conditions in the presence of acetate. Organic carbon sources, on which algae can grow, like acetate, are not cheap. A potential solution to mitigate the need to provide additional acetate exogenously for growth is to generate an optimized mixed culture in which *C. reinhardtii* is grown in concert with an organism that produces acetate as an end product. Some cyanobacteria, such as certain Synechococcus species, can produce acetate during photosynthesis and grow under conditions similar to the optimal growth conditions of *C. reinhardtii* (117)(118)(119). In addition, mutant strains of *C. reinhardtii*, and *Synechococcus* sp. 7002, have been developed to increase lipid and acetate accumulation respectively. The Sta6 mutant of *C. reinhardtii* has a defect in starch production and over accumulates lipids due to an inability to form starch (78), while the *Synechococcus* sp. 7002 mutant is called glgA-1 (119), and is unable to produce glycogen but over produces other metabolites including acetate. In this work we examine co-culturing wild-type (WT) and

mutant strains of *C. reinhardtii*, and *Synechococcus* sp. 7002 to examine if stable co cultures can be maintained that promote the growth of *C. reinhardtii* through the utilization of acetate produced by *Synechococcus* sp. 7002.

Results

Optimization of the Growth Conditions for Co-culturing *Synechococcus* sp. and *C. reinhartdii*.

Temperature Dependence of Growth. To determine the optimal growth temperature at which for a stable co-culture, both wild-type and mutant strains of *C. reinhartdii* and *Synechococcus* sp. PCC 7002 were grown on the optimized growth media for each organism (TAP media for *C. reinhartdii* and A^+ media for *Synechococcus* sp. PCC 7002. The results of our experiments show that the optimum temperature for the growth of *C. reinhartdii* is 30 °C and *Synechococcus* sp. 7002 is 38 °C which are the temperatures often used to grow these cultures. Increase in temperature from 30 °C to 34 °C and then to 38 °C increases the lag phase in *C. reinhartdii* cultures (Figure 3.1A). Decrease of the temperature from 38 °C to 34 °C and finally to 30 °C did not affect the growth of either wild type (Figure 3.1B) or mutant strains of *Synechococcus* sp. 7002 (data not shown). The results indicate that cultures can be maintained at the optimal growth temperature for *C. reinhartdii* without significant compromising the growth of *Synechococcus* sp. 7002.

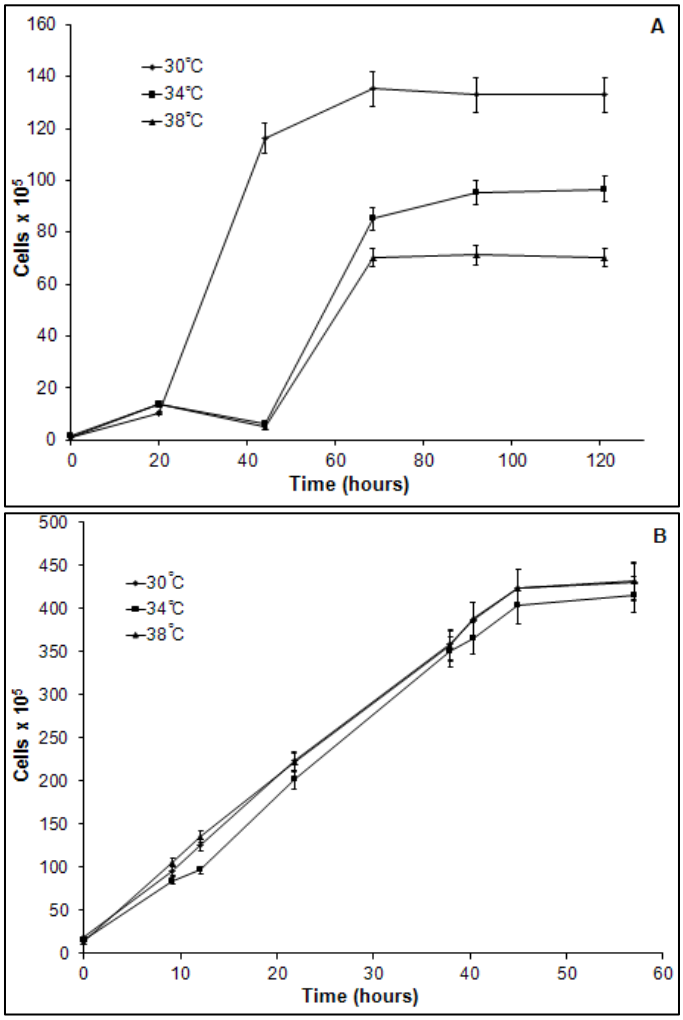

Figure 3.1. Growth of *C. reinhartdii* (A) and *Synechococcus* sp. (B) at 30 °C, 34 °C and 38 °C. Y-axis is in cells per ml.

Growth on Modified Media. As was discussed in the Methods section, the main differences between TAP medium (*C. reinhartdii*) and A^+ medium (*Synechococcus* sp.) is the source of nitrogen, found as ammonium chloride in TAP and sodium nitrate in A^+, and the presence vitamin B12 in A^+ and acetate in TAP (Appendix A). The results of these experiments have shown that *C. reinhartdii* cultures are unable to grow on A^+ and A^+ modified medium at 30 °C (Figure 3.2, and insert in Figure 3.2) and 38 °C (data not shown). However, cells of *Synechococcus* sp. were able to grow on TAP and TAP

modified media at 30 °C (Figure 3.2). Cell counts indicate that the cultures remain homogeneous and the number of cells correlates with optical cell density. The fact that we are able to generate a co-culture under the optimal conditions for *C. reinhartdii* is encouraging since *C. reinhartdii* is the target for biofuel production.

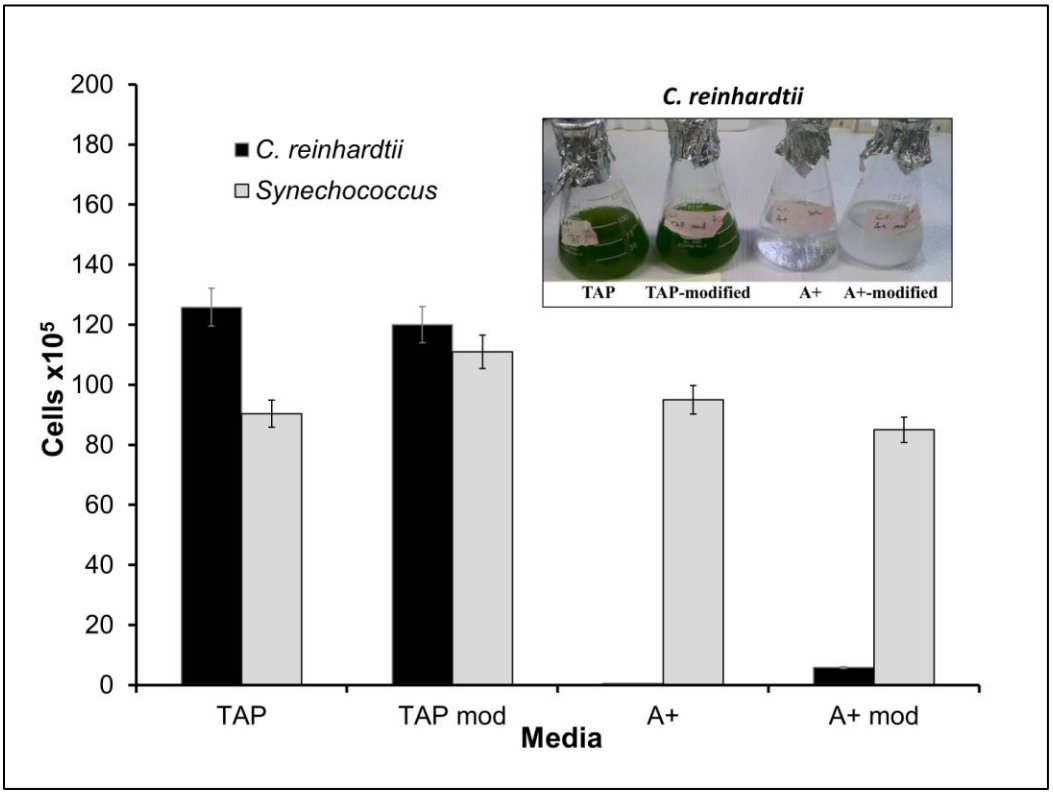

Figure 3.2. Growth of *C. reinhartdii* and *Synechococcus* sp. on TAP, TAP modified, A^+, A^+ modified media at 30°C after 124 hours. Y-axis is in cells per ml.

Exogenously Added Acetate.

Wild-type and mutant cultures of *C. reinhartdii* and *Synechococcus* sp. 7002 the experimental cultures have been grown in the presence and absence of acetate. Results of these experiments showed that the growth rates of the *C. reinhartdii* and *Synechococcus* sp. 7002 cultures were higher in the presence of acetate (Figure 3.3A and B). During the

growth of *C. reinhartdii* and *Synechococcus* sp. 7002 cultures, the amount of acetate consumed was monitored. As expected, the results indicated that, over time, the amount of acetate decreased in the wild-type and Sta6 mutant of *C. reinhartdii*. This correlated inversely to the increase in cell number (Figure 3.4A). Acetate production by wild-type and mutant *Synechococcus* sp. 7002 cultures growing on TAP modified media followed the growth curve (Figure 3.4B) indicating that accumulation of acetate increased with the increase culture cell density. Additionally, the production of acetate by the *Synechococcus* sp. 7002 glgA1 mutant on TAP modified media was higher when compared to wild-type cultures.

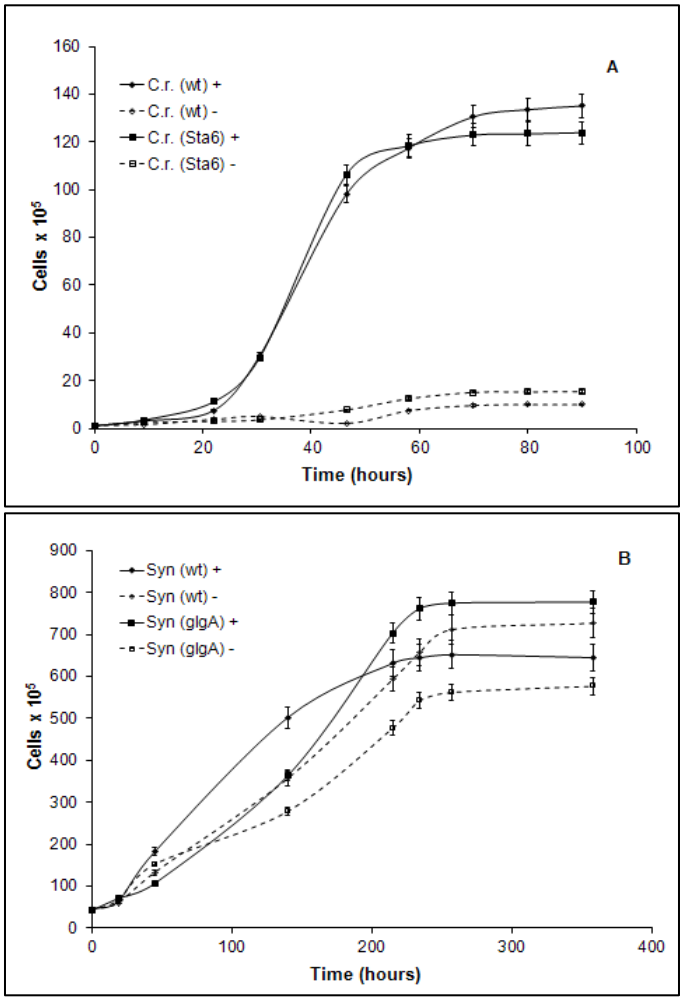

Figure 3.3. The effect of the presence (+) and absence (-) of acetate on the growth of both wild type and mutant *C. reinhartdii* (A) and *Synechococcus* (B) on TAP modified media at pH 7.0 and 30 ℃. Y-axis is in cells per ml.

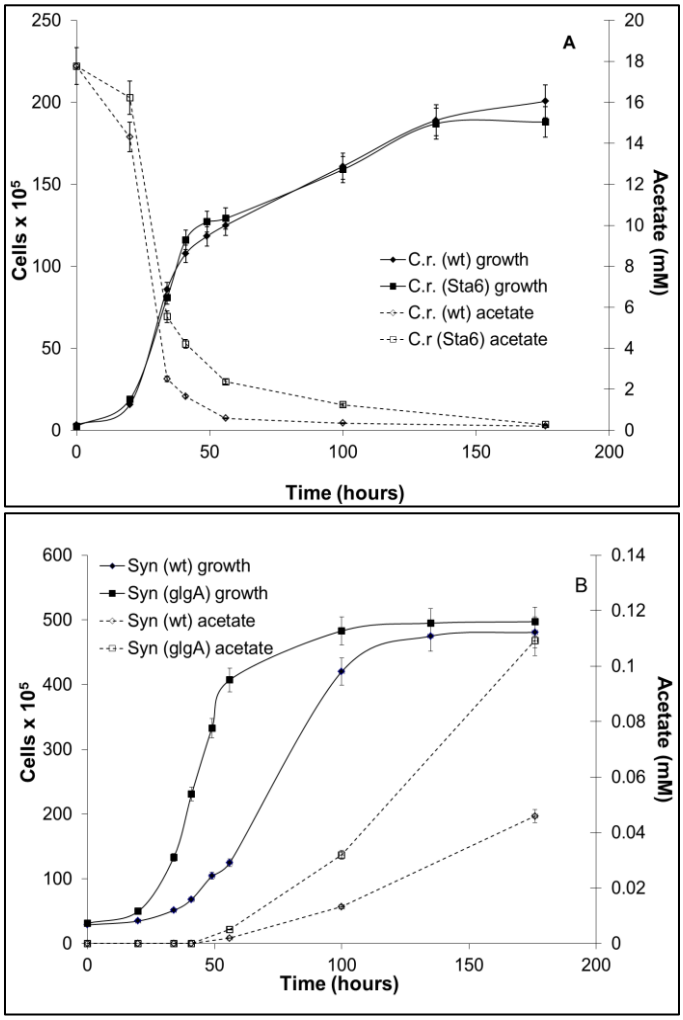

Figure 3.4. Growth and consumption of acetate by *C. reinhartdii* cultures (A), and growth and production of acetate by *Synechococcus sp.* cultures (B). All cultures grown on TAP modified media pH 7.0 at 30 ℃. Y-axis is in cells per ml.

Optimizing *Synechococcus* sp.
7002/*C. reinhardtii* co-cultures

Based on the previous experiments, co-culturing of the Sta6 mutant of *C. reinhartdii* with the glgA1 mutant of *Synechococcus* sp. 7002 was conducted on TAP modified media at pH 7.0 and 30 ℃. To investigate the effect of initial cell number in the inoculum during free cells co-culturing, different respective ratios of *C. reinhartdii* to *Synechococcus* sp. 7002 were used particularly 1:1 and 1:10. The ratio 1:10 was chosen

because *Synechococcus* sp. 7002 appeared to produce less acetate than required for the optimal growth of *C. reinhardtii* and so we would require a larger number of *Synechococcus* sp. 7002 in co-culture. Results of the co-culturing experiments with free cells revealed that *Synechococcus* sp. 7002 cells grew faster than *C. reinhardtii* for both ratios of 1:1 and 1:10 (data not shown) and eventually overwhelmed the co-culture. To avoid the problem of overgrowth by *Synechococcus* sp. 7002, these cells were immobilized in alginate beads (see Methods for details). The results of the experiments using immobilized *Synechococcus* sp. 7002 cells have shown that the growth rate of *C. reinhartdii* Sta6 mutants, in co-culture, improves when compared to free cells grown alone in the same medium with empty beads (Figure 3.5). Immobilization also controlled the growth of *Synechococcus* sp. 7002 and the cyanobacteria from overtaking the co-culture.

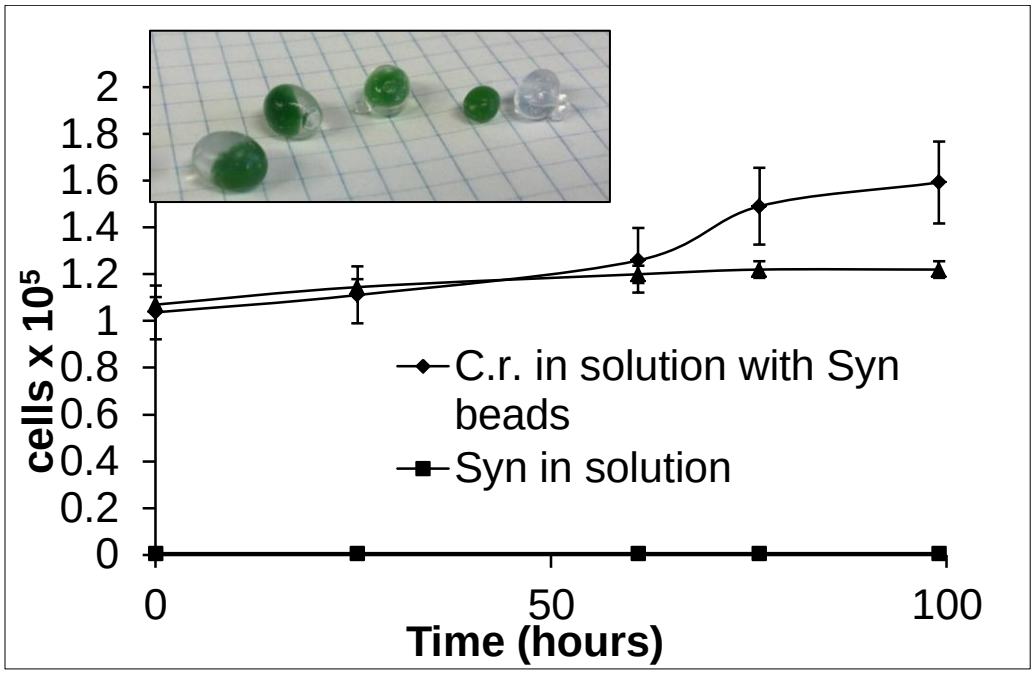

Figure 3.5. Growth of *C. reinhartdii* Sta6 mutant and bead-immobilized *Synechococcus* sp. glgA1 mutant cells, in TAP-modified media without acetate at pH 7.0. Inset shows the two layer coated alginate beads of *Synechococcus* sp. and a single coated (second from right) and empty bead (far right). Y-axis is in cells per ml.

Discussion

In the present work, we have demonstrated that an acetate over-producing mutant strain of *Synechococcus* PCC 7002 is able to support the improved growth of the eukaryotic algae, *C. reinhartdii* in a modified TAP medium. Optimal growth conditions able to support both organisms were determined by first investigating the temperature dependence of growth of each organisms in their respective media (Figure 3.1). Using A^+ media, *Synechococcus* PCC 7002 grew optimally at 38 °C, while in TAP media, *C. reinhartdii* grew best at 30 °C. Attempts to grow both organisms at a compromising temperature of 34 °C revealed a decrease in the growth of *C. reinhartdii* while growth of the cyanobacteria was unaffected. At 38°C, the growth of *C. reinhartdii* was further

reduced. Temperature tolerance of *Synechococcus* PCC7002 was superior and unaffected at all temperatures tested. For these reasons, 30 °C was chosen as a co-culturing temperature able to best support both organisms.

Growth of *C. reinhartdii* in A^+ media was negligible; however, *Synechococcus* PCC7002 grew nearly as well in TAP media as in A^+. To improve growth, small adjustments in each media were made by adding components to A^+ that were not present in A^+ but were found in TAP and vice versa (Appendix A). At 30 °C, it was observed that *C. reinhartdii* was still unable to grow well in A^+ after it was modified (Figure 3.2). This may have been due to a combination of high salt concentrations and slightly higher pH than normally used for growth of this microalgae. The cyanobacteria's growth, however, improved slightly after the TAP media was modified. This modified TAP media was made by adding $NaNO_3$ and vitamin B12 to regular TAP media and was considered to be optimal for co-culturing.

As previously shown (61), it was observed here that mixotrophic growth of *C. reinhartdii* surpassed autotrophic growth. Cultures grown in the absence of acetate, in both TAP and modified TAP media, grew extremely slowly (Figure 3.3A). Acetate analysis revealed the majority of acetate is consumed during the exponential phase of growth (around 50% is consumed in the first 24 hours) and the supply is nearly exhausted as the culture approaches stationary phase (Figure 3.4A). Similar trends were seen for both the wild type and mutant strains of *C. reinhartdii*. Acetate production in modified TAP media by both wild type and the mutant strain of *Synechococcus* sp. was monitored during a growth cycle. A lag of about forty hours, in acetate production, was observed for

both the wild type and mutant. However, as expected, the mutant strain produced over twice as much acetate as wild type cultures (Figure 3.4B). Here, a maximum acetate concentration of around 0.11 mM was achieved, a concentration shown to be sufficient to improve the growth of *C. reinhartdii* compared to monocultured cells in the same media.

Conclusions

An acetate over-producing mutant strain of *Synechococcus* sp. 7002 was shown to provide the acetate needed to sustain improved growth of a lipid-accumulating mutant strain of *C. reinhartdii* in co-culture at a temperature of 30 °C. It was demonstrated that wild type and glgA1 mutant strains of the cyanobacteria *Synechococcus* sp. 7002 were able to grow and produce acetate in a modified TAP medium. This same medium was also shown to support the growth of wild type and a lipid accumulating mutant strain of the eukaryotic algae *C. reinhartdii* if exogenous acetate was added. Alginate encapsulation of *Synechococcus* sp. 7002 was shown to prevent this organism from overtaking the co-culture which it was observed to do when freely suspended in co-culture. In the absence of exogenous acetate, improved growth of *C. reinhardtii* was provided by acetate produced by *Synechococcus* sp. 7002.. By increasing the ratio of encapsulated cyanobacteria to freely suspended algae, we feel a significant growth improvement can be attained for *C. reinhardtii* without the requirement for added acetate.

Methods

Growth of Microorganisms

Synechococcus sp. glgA1 knockout mutant was obtained on agar plates from the Donald Bryant lab at The Pennsylvania State University. Wild type and mutant cultures of *Synechococcus* were grown photoautotrophically in 50 ml Erlenmeyer flasks containing A^+ media (pH = 8.0) supplemented with B12 (117). Initial incubation was at 38°C in a water bath shaken at 100 rpm, and illuminated from the top with 100uE of fluorescent light. Flasks were sealed with tinfoil and sparged with 1% vol/vol CO_2 in air. Cultures were monitored at 600nm on a Thermo Spectronic Bio Mate 3 spectrophotometer.

Chlamydomonas reinhardtii sta6 mutant was obtained from the Matthew Posewitz lab at Colorado School of Mines. Wild type and mutant cells were grown photoautotrophically in 50 ml Erlenmeyer flasks sealed with tinfoil, containing TAP media (pH = 7.0). Cells were incubated at 30°C in a water bath shaken at 100 rpm, and illuminated from the top with 100uE of fluorescent light. Cultures were monitored at 750nm on a Thermo Spectronic Bio Mate 3 spectrophotometer.

Cells for all experiments were initially obtained from the above conditions. Cultures were prepared by centrifugation for 10 minutes at 8,000 x g, washed in media to be used, centrifuged again and finally resuspended in media to the required respective optical density. Individual cultures were grown at 30°C, 34°C and 38°C under the same conditions as above in A^+ and TAP media modified as later described. Optical densities of the co-cultures were monitored at both 600 and 750nm. Xenogenicity of the co-culture

was confirmed under a microscope and cell number was determined with a hemacytometer.

Media Modification

The composition of TAP and A^+ media can be found in the supplemental data. Modified TAP media was made by adding $NaNO_3$ and vitamin B12 to TAP media. A^+ media was modified by adding NH_4Cl and acetic acid, while concentrations of $NaNO_3$ and NaCl were cut in half.

Cell Immobilization

Alginate beads were made by dissolving 3g of sodium alginate directly in 100ml of prepared culture and adding it drop-wise with a syringe and needle into a 1% solution of $CaCl_2$ in growth media from a height of at least 30 cm. Bead size is controlled by needle gauge: 22 G yields 2 mm diameter beads, 18 G yields 3 mm beads while the 4 mm beads are made directly from a 10 ml syringe without a needle. Beads were formed immediately and were allowed to harden further in the $CaCl_2$ solution for 15 minutes. After hardening, beads were removed from the $CaCl_2$ solution and added to fresh growth media. To prevent cell leakage, double beads were made with an additional step; beads from above were dropped into a 3% alginate solution in media, removed, and dropped again into a 1% solution of $CaCl_2$ in media. Beads were allowed to harden as previously described.

Acetate Determination

Acetate concentration was determined by ^{H}NMR. Samples were centrifuged for 10 minutes at 14,000 x g and 500ul of supernatant was placed in a glass NMR tube to which 50ul of D_2O was added. Spectra were collected on a Bruker DRX500 NMR spectrometer operating at a frequency of 500.13MHz. A 1D NOESY pulse sequence with a 100ms mixing time was used. 32K data points were collected and the number of scans was 64 for each sample. The overall repetition was 4.28s and a presat pulse was used to suppress the water signal.

CHAPTER 4

GENOME OF CLOSTRIDIUM PASTEURIANUM, TRANSCRIPTIONAL ANALYSIS AND STRUCTURAL DETERMINANTS OF ITS HYDROGENASES

Contribution of Authors and Co-Authors

Manuscript in Chapter 3

Author: Jesse B. Therien

Contributions: Conceived and implemented the study design. Collected and analyzed data. Prepared the manuscript for submission to a peer-reviewed journal.

Co-Author: Trinity Hamilton

Contributions: Helped collect and analyze sequencing data. Provided insight into analysis of transcriptional data.

Co-Author: Donald Bryant

Contributions: Provided insight and discussed results of draft genome.

Co-Author: Zhenfeng Liu

Contributions: Collected and analyzed genome sequencing data. Provided insight and guidance to improve the quality of the draft genome.

Co-Author: Seth Noone

Contributions: Discussed the relevance of results he obtained from comparable experiments. Provided materials to improve analysis of transcriptomic data.

Co-Author: Paul King

Contributions: Discussed results and provided insight into their significance. Provided materials and helped design some experiments.

Co-Author: John W. Peters

Contributions: Helped conceive and implement the study design, discussed results/implications, provided insight and edited the manuscript.

Manuscript Information Page

Jesse B. Therien, Trinity L. Hamilton, Donald A. Bryant, Zhenfeng Liu, Seth M. Noone, Paul W. King, John W. Peters
Journal of Bacteriology
Status of Manuscript:
_X_ Prepared for submission to a peer-reviewed journal
____ Officially submitted to a peer-review journal
____ Accepted by a peer-reviewed journal
____ Published in a peer-reviewed journal

Publisher: American Society for Microbiology

Abstract

Clostridium pasteurianum (strain W5), the first free-living organism to be isolated nearly 120 years ago, has been the model organism for the study of nitrogen fixation and hydrogen metabolism for over a century. The first generation of biochemical characterization of complex iron-sulfur cluster containing [FeFe]-hydrogenases and Mo-nitrogenase were carried out from enzymes purified from *C. pasteurianum* and it was proposed that two [FeFe]-hydrogenases are expressed differentially under nitrogen-fixing and non-nitrogen-fixing conditions. It was suggested that the first characterized [FeFe]-hydrogenase (CpI) functioned in central metabolism in recycling reduced electron carriers that accumulated during fermentation under non nitrogen-fixing conditions via proton reduction. The second [FeFe]-hydrogenase, termed CpII, which was observed to be increased in abundance under nitrogen-fixing conditions, was proposed to have a role in capturing reducing equivalents lost as hydrogen during nitrogen reduction. In support of this, previous *in vitro* biochemical characterization of CpI and CpII indicate CpI has elevated proton reduction activity in comparison to CpII and CpII has elevated hydrogen oxidation in comparison to CpI. We have sequenced the genome of *C. pasteurianum* (strain W5) to gain further insight into the role of hydrogenases in metabolism. The genome sequence provides evidence for four hydrogenases including a unique third [FeFe]-hydrogenase and a [NiFe]-hydrogenase in addition to Mo-dependent and alternative (V-dependent and Fe-only) nitrogenases. The genome contains multiple copies of the nitrogenase Fe protein encoding *nifH* and gene context has also allowed us to infer roles for different *nifH* gene products in nitrogen fixation. Under nitrogen fixing

conditions we have shown that the transcription of an [FeFe]- and the [NiFe]-hydrogenase are increased along with the nitrogenase genes in concert with down regulation of the canonical [FeFe]-hydrogenase involved in central metabolism. Comparison of the primary sequences of CpI and CpII and their close homologues provides the basis for identifying key potential determinants of modulating hydrogen production and hydrogen oxidation activities.

Introduction

Clostridium pasteurianum (strain W5) is a gram-positive, spore-forming, obligately anaerobic bacteria found in soil and was the first free-living nitrogen-fixing organism to be isolated (120). For over 100 years, it has been a model for studying the biochemistry of nitrogen fixation and hydrogen metabolism. The first generation of biochemical characterization of complex iron-sulfur clusters from an [FeFe]-hydrogenase and Mo-nitrogenase were carried out from enzymes purified from *C. pasteurianum*. Following the discovery of hydrogenase in *C. pasteurianum* (121) the first preparations of a soluble hydrogenase were obtained from this organism (122, 123). Subsequently, the presence of a second [FeFe] hydrogenase (CpII) was revealed (30) and its physical and catalytic properties studied along with the first (CpI) (124). Decades later the first structure of an [FeFe] hydrogenase (CpI) was determined from *C. pasteurianum* (39). Along a parallel track, the first cell-free N_2-fixation was observed using extracts of *C. pasteurianum* (125). Genetic studies have since elucidated the molybdenum nitrogenase

operon (126) and structures of the iron and MoFe proteins from *C. pasteurianum* have been determined (127, 128).

The *Clostridia* are a diverse group of anaerobes that produce many fermentative metabolites. These metabolites include important solvents like acetone and many alcohols such as butanol, isopropanol, and ethanol (129). Clostridia are able to ferment a variety of carbohydrates: starch, glucose, fructose, mannose, sucrose, lactose, xylose, arabinose, melezitoze, inulin, mannitol, and other carbohydrates from dairy and wood wastes (129). The high demand for acetone during World War I and for butanol in the 1920's and 1930's, led to the construction of massive fermentation plants (129). For example, one plant in Peoria, Illinois, had the capacity to culture 2.5 million gallons at a time and, in combination with a secondary plant, was producing over one hundred tons of solvents a day (130). In general, clostridia gain their energy from the conversion of a hexose to butyrate, acetate, CO_2 and H_2 (Figure 4.1).

Fermentation typically consists of the conversion of glucose to pyruvate through the glycolytic pathway. Reduced NADH produced during glycolysis can subsequently reduce ferredoxin via NADH:ferredoxin oxidoreductase which then can reduce protons to H_2 via hydrogenase. At this point, pyruvate can be drained away through the action of lactate dehydrogenase, but otherwise is converted to acetyl-CoA via pyruvate:ferredoxin oxidoreductase with the concomitant production of CO_2. During this step, reduced ferredoxin can again be used to supply hydrogenase with ability to reduce protons to H_2. Acetyl-CoA, is then converted to either acetate or butyrate, in the case of one of *C. pasteurianum*.

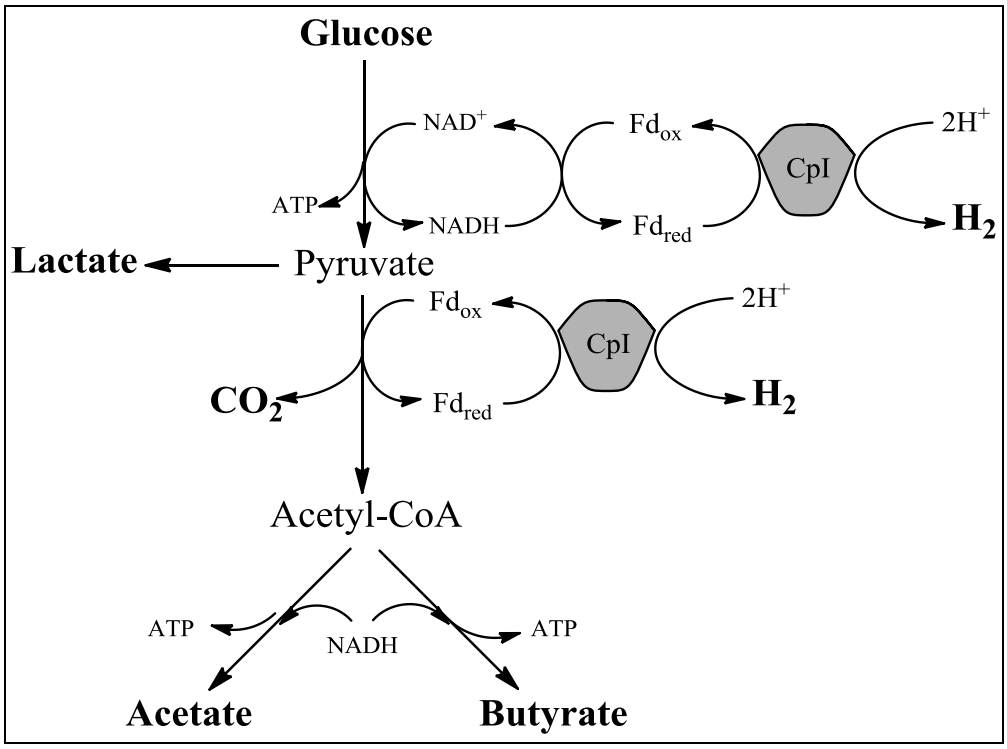

Figure 4.1. Fermentation of glucose by *C. pasteurianum* producing H_2, CO_2, acetate, and butyrate. CpI indicates an [FeFe]-hydrogenase.

This sort of metabolism yields either three moles of ATP/glucose if the final product is butyrate, or four moles of ATP/glucose if the final product is acetate (131). Since products are usually a mix of acetate and butyrate, in the case of *C. pasteurianum*, the actual amount of hydrogen produced per mole of glucose depends on acetate/butyrate ratio (132).

As mentioned, the enzyme responsible for maintaining the proper redox state of Clostridia during fermentation is hydrogenase. Hydrogenases do this by coupling electrons with protons to form hydrogen. Even though this catalysis is reversible many hydrogenases preferentially catalyze this reaction in one direction. Therefore, if an organism needed to efficiently both reduced protons and oxidize H_2, it would be

beneficial to possess two hydrogenases tuned for each reaction. In fact, a large number of clostridal species have been shown to have multiple hydrogenases (132, 133) the first of which was *C. pasteurianum*. Years after the first hydrogenase of *C. pasteurianum* (CpI) was purified (122, 123) a second hydrogenase (CpII) was isolated and purified (30, 31). As purified, molecular weights were shown to be 60.5 kDa and 53 kDa for CpI and CpII respectively. After its initial characterization(122), CpI was observed to produce H_2 in vitro using methyl viologen as an electron carrier (123), while CpII was first thought to be a unidirectional H_2-oxidizing hydrogenase (30). It was later shown that CpI and CpII are bidirectional and catalyzed both the production and uptake of H_2 (31). A comparison of the rates of H_2 evolution and oxidation revealed that CpI produces H_2 550 times faster than CpII (5,500 vs. 10 μmol of H_2/min respectively) while it oxidizes H_2 about 30% slower than CpII (24,000 vs. 34,000 μmol of H_2/min respectively) (28). With the ability to purify CpI and CpII, it was shown colorimetrically that CpI contained 20.1 ± 0.7 moles of iron per mole of protein while CpII contained 13.8 ± 0.4 (134). In both CpI and CpII, fourteen of these iron atoms were attributed to a six-iron hydrogenase cluster (H-cluster (135)), thought to be where catalysis takes place, and two [4Fe4S] accessory "ferredoxin" clusters (F-clusters (135)) suspected of facilitating electron transfer to the H-cluster (134, 136). The remaining iron atoms in CpI were suspected to comprise two [4Fe4S] clusters, but would require a total of 22 iron atoms per protein, which was inconsistent with previous results. Using Resonance Raman spectroscopy, an additional [2Fe2S] cluster was detected in CpI, but not CpII (137). CpI was now thought to contain a six-iron H-

cluster and four F-clusters (three [4Fe4S] clusters and a [2Fe2S] cluster) consistent with the 20.1 ± 0.7 irons/molecule.

CpII was shown to be relatively inactive at both H_2 production and H_2 uptake when using methyl viologen as the electron carrier, but when using methylene blue as the electron carrier, H_2 uptake activity was much higher than CpI (124). The midpoint potentials for methyl viologen (-440 mV) and methylene blue (+11 mV) suggesting that CpII might be catalytically limited by high potential F-clusters (135). Redox potentiometry indicated that oxidized CpI and CpII had similar midpoint potentials with E_m values of - 400 and - 410 mV respectively. However, reduction of the enzymes yielded E_m values of - 420 mV for CpI and -180 mV for CpII.

In other words, CpII would likely have a hard time reducing the H-cluster (- 410 mV), for proton reduction, via the F-clusters (-180 mV). On the other hand, the midpoint potential of the F- and H-clusters of CpI are fairly close (-420 and -400 mV respectively) to each other, and to the reduction potential of the H_2/H^+ electrode , allowing the enzyme to readily catalyze the reversible reaction in both directions, as demonstrated in previous *in vitro* assays (124).

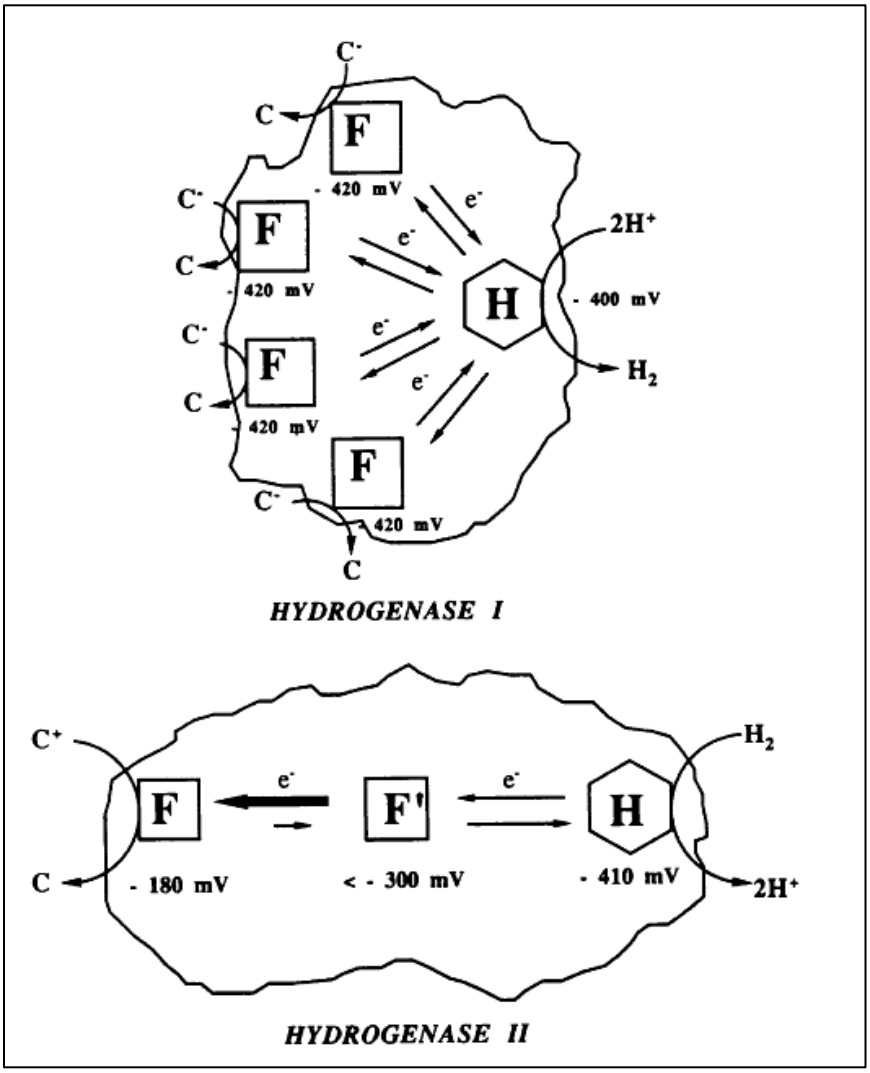

Figure 4.2. Proposed electron flow for hydrogenase I (CpI) and hydrogenase II (CpII). Midpoint potentials are given for the H- and F-clusters and suggest preferred direction of flow. Diagram taken from (135).

Hydrogen producing hydrogenases in anaerobes, as mentioned, are used as a way to dispose of accumulated reducing equivalents that build up during fermentation. Hydrogen uptake hydrogenases are typically coupled to energy yielding/conserving reactions. A very energy intensive reaction is that of nitrogen fixation. Here, for every mole of

dinitrogen reduced, 8 electrons and 16 ATP are used to produce 2 moles of ammonia and 1 mole of dihydrogen; the reaction is seen below.

$$\mathbf{N_2 + 8H^+ + 8e^- + 16MgATP \longrightarrow 2NH_3 + H_2 + 16MgADP + 16Pi}$$

The high ATP/electron demand of nitrogen fixation can stress an organism energetically; therefore the presence of an uptake hydrogenase would be valuable. As a fermenting anaerobe, it is essential that *C. pasteurianum* possess a hydrogenase to rid itself of accumulated reducing potential. This explains the role of CpI, but leaves us wondering about the biological function of CpII. Fittingly, *C. pasteurianum* is a nitrogen fixer and would greatly benefit from an uptake hydrogenase during nitrogen fixation. Preferential H_2 oxidation by CpII would suggest it may function during nitrogen fixation. In some nitrogen fixing organisms such as *Azotobacter vinelandii* (138), *Rhodopseudomonas palustris* (139), and others (140, 141), uptake hydrogenases have been shown to be co-transcribed with the nitrogen fixing machinery. However without the gene sequence of CpII, similar transcriptional studies are not possible.

To determine if CpII is indeed used during nitrogen fixation to recycle H_2 and conserve energy, we planned to conduct transcriptional analysis of the hydrogenases from cells of *C. pasteurianum* grown under nitrogen-fixing conditions. With the increasingly affordable cost of genome sequencing and the useful data we could obtain, we assembled a draft genome. The draft genome would allow us to identify the gene context of the two hydrogenases and the previously sequenced (126) nitrogenase (*nif*) gene cluster possibly offering insight into their relationships. From the draft genome, we also planned to design

targeted gene expression studies aimed at the expression of CpI and CpII under nitrogen-fixing conditions when compared to non-nitrogen-fixing conditions.

Materials and Methods

Growth Conditions

Freeze-dried *C. pasteurianum* W5 (ATCC® 6013™) was obtained from ATCC and rehydrated with Difco™ Reinforced Clostridial Medium following the ATCC protocol. Sealed 25 ml glass serum vials (Weaton) containing 10 ml of Difco™ Reinforced Clostridial Medium under a headspace of 10% H_2-10% CO_2-80% N_2 were then inoculated with the rehydrated culture and incubated at 37°C following ATCC propagation procedures for this organism. Agar plates of the above medium were used to store *C. pasteurianum* W5 for further use; initially grown at 37°C for 24-48 hours before being stored at room temperature in an anaerobic chamber.

For genome sequencing, cultures began from a single colony from a plate of Difco™ Reinforced Clostridial Medium that was inoculated into a sealed 25ml serum vials containing 10ml of the same media, under a headspace of 10% H_2-10% CO_2-80% N_2 and then incubated overnight at 37°C. 1 ml of culture was then spun down at 14,000 x g at room temperature before extracting DNA.

For qRT-PCR, cultures began in a similar manner as above, then 1-5 ml of overnight culture were used to inoculate 50 ml of both DM-11 (142) (N+; containing NH_4Cl and $(NH_4)_3SO_4$) and DM-11-N (N-; fixed nitrogen free) media to an OD_{650} = ~0.020 and was then sparged with 10% H_2-10% CO_2-80% N_2 for 10 minutes and incubated overnight. This was repeated once more after which point a C_2H_2 reduction

assay (143) was performed to ensure N_2 fixation was taking place in the N- culture. Then 1 ml (N+) and 6ml (N-) of this culture was added to 50 ml of either N+ or N- media in a 123ml sealed serum vial to make a starting OD_{650} = ~0.020. Again, the vials were sparged with the gas mix and incubated overnight at 37°C. The following day, a C_2H_2 reduction assay was done again to ensure the N- culture was indeed fixing N_2 and 500 µl samples were mixed with 1 ml of QIAGEN RNAprotect Bacterial Reagent® following the kit's included procedure, and either used for RNA extraction immediately or frozen at -20 °C until later RNA extraction.

Genome Sequencing

Total genomic DNA of *C. pasteurianum* W5 was extracted using a Promega Wizard® Plus SV minipreps DNA purification system and its concentration determined by Nano Drop to be 220 ng/ul ($Abs_{260/280}$ = 2.04). Genomic DNA was then submitted to the Genomics Core Facility at The Pennsylvania State University for SOLiD sequencing. With the help of the Genomics Core Facility, contigs were assembled onto six scaffolds leaving thirty standalone contigs that did not initially fit anywhere.

Gaps were closed by PCR using primers designed around 200 bases in from the end of each contig. GoTaq® 2x Master Mix reagent by Promega was used for the PCR on a Techne Touchgene Gradient thermal Cycler. Amplicons were then purified either directly using QIAquick PCR Purification Kit or from agarose gels using the same Qiaex II Gel Extraction Kit both from QIAGEN. Purified PCR products were then sent for sequencing to Davis Sequencing in Davis, CA. Sequence data was then assembled using BioEdit.

Annotation analysis was completed using the RAST (Rapid Annotation using Subsystem Technology) prokaryotic genome annotation server.

Preparation of Total RNA

RNA of *C. pasteurianum* W5 was extracted using QIAGEN RNeasy® Mini Kit followed by a DNase treatment step using RQ1 RNase-Free DNase by Promega and a repurification using the QIAGEN RNeasy® Mini Kit. RNA concentration was then determined using Qubit® RNA Assay Kit and was then frozen at -20 °C until further analysis.

Quantitative RT-PCR (qRT-PCR)

Primers were designed for the 4 hydrogenases (CpI, CpII, CpIII and the large subunit of [NiFe]), 3 nitrogenase α-subunits (*nifD, vnfD*, and *anfD*) and the 16S rRNA small subunit using the Integrated DNA Technologies SciTools qPCR online primer designing software. qRT-PCR was performed on a Rotor-Gene-Q real-time PCR detection system from Qiagen using the *Power* SYBR® green RNA-to-C_T™ *1-Step* Kit from Applied Biosystems according to the included protocol. Reactions were done in triplicate with control reaction mixtures containing no reverse transcriptase.

Results and Discussion

Genome

Initial sequencing resulted in 145 contigs ranging from 511 to 251,858 bases yielding an estimated genome size of 4,206,741 bp. The average contig length was

29,012 bases and the average number of reads per contig was 1,618. As with most other *Clostridial* species, the GC content was very low at 30%.

After closing 90% (131 of 145) of the gaps, annotation analysis predicted 4347 protein coding sequences (CDSs), which accounted for 83% of the genome coverage. The Tandem Repeats Database v2.30 (142) indicated the presence of 216 tandem repeats; the highest copy number was 17.5 for the two base repeat of TA and the longest repeat was 408 bases with two copies. There were 69 RNA genes. Annotation identified 41 transposases and nine mobile elements, 28 of which appeared on contig4, eleven on contig2, three on contig3 and five on contig1. Interestingly, between *anfH* and *anfDGK*, a transposase and mobile element protein are found. A *nifH* and *nifD* homologue appear adjacent to a transposase and mobile element at the end of contig4. CpII is between a copy of *vnfE/vnfN* (< 6000 bases) and a transposase (15,000 bases). The CpIII gene is just over 10,000 bases from an ISPsy14 transposase. As previously shown for *nifH1* and *nifH2* genes (144), codon usage over the entire genome coding region, determined using Mobyle (http://mobyle.pasteur.fr/cgi-bin/portal.py?#forms::codonw), is very biased toward A+T in the wobble position. When possible, all 3rd codon positions are preferentially A. In *C. perfringens* and *C. acetobutylicum*, GC content of 31% and 29% respectively, this same A+T bias is observed (145).

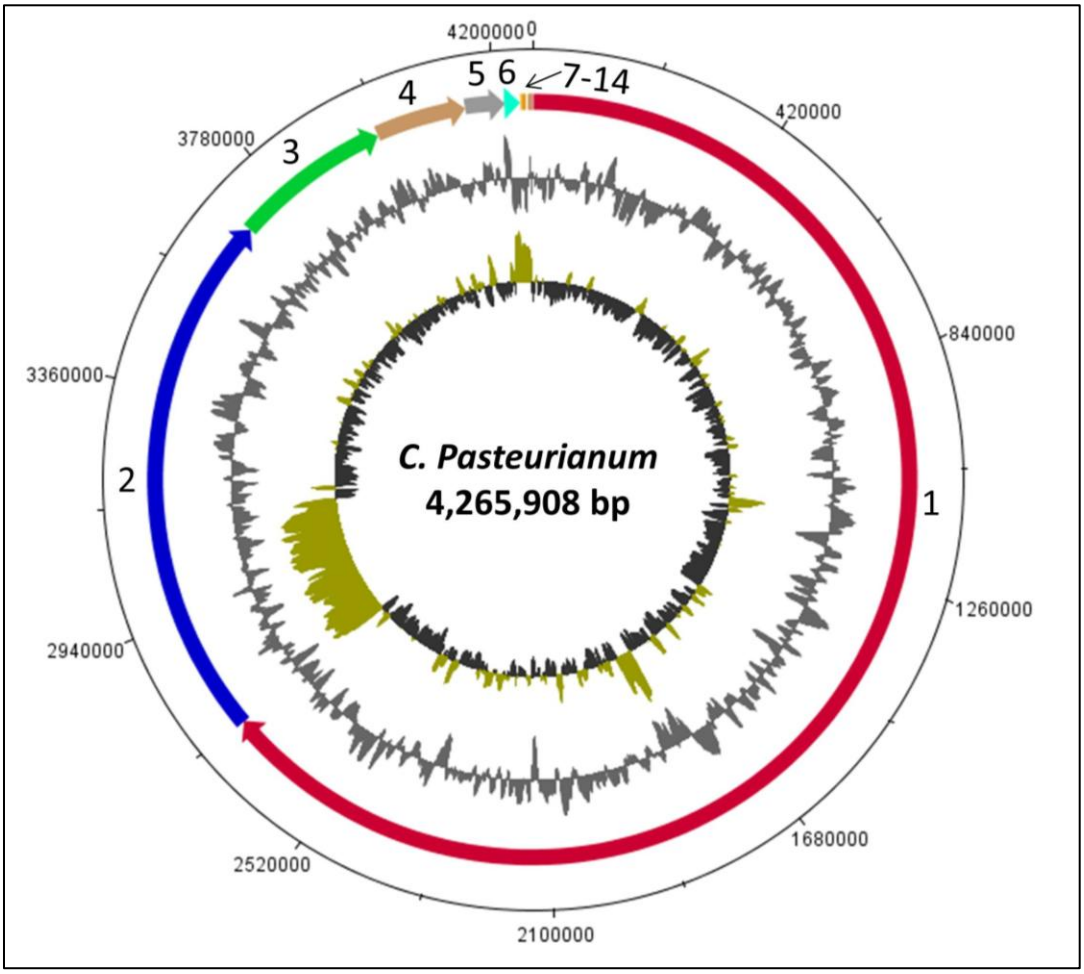

Figure 4.3. Draft genome of *C. pasteurianum*. Outer circle shows the scale in number of bases. Ring 1 shows current draft contigs; ring 2 shows GC-content; ring 3 (inner ring) shows GC-skew.

According to RAST, the closest neighbors with a completed genome were shown to be numerous (twelve) strains of *Clostridium botulinum*, *Clostridium novyi* NT, and *Clostridium sporogenes* ATCC 15579. *C. botulinum* strains are quite numerous and represent the largest species of clostridia with complete genomes; according to National Center for Biotechnology Information, 13 complete genomes and 11 partial genomes currently exist in the database.

The genome of *C. pasteurianum* has revealed a total of three [FeFe]- and one [NiFe]-hydrogenase in addition to three forms of nitrogenases. All four hydrogenases are distributed throughout the largest contig (2,726,463 bp) (figure 4.5). The nitrogenase gene clusters are found on two different contigs; the Fe-only nitrogenase gene cluster is upstream of CpII while both the Mo- and V-dependent nitrogenases gene clusters are found on a smaller contig (72,322 bp) adjacent to one another (figure 4.5).

Hydrogenases

The genome confirms all three [FeFe]-hydrogenases, CpI, CpII, and what we are calling CpIII in addition to a [NiFe]-hydrogenase. While most [FeFe]-hydrogenase containing genomes possess multiple copies of structural genes, as seen in *C. pasteurianum* and other clostridia (133) (132), most often there is only one copy of the maturase genes *hydE*, *hydF*, and *hydG* (39). Both HydE and HydG belong to the radical S-adensosylmethionine superfamily of proteins while HydF is a GTPase. The genes encoding the maturases can be found together as a cluster (*hydEFG*), as two sets (*hydEF, hydG* or *hydE, hydFG*), or alone (39) as was observed in *C. pasteurianum*. Figure 4.5 shows the delocalization of the maturase genes on the genome. The encoded protein sequence of CpII (458 residues) is slightly shorter than that of CpI (574 residues) while CpIII is shorter still (450 residues). As illustrated in figure 3, all versions of [FeFe] hydrogenase contain the conserved [FeFe]-hydrogenase H-cluster signature motifs (25). These motifs encompass the H-cluster binding cysteines. Phylogenetic clustering of the [FeFe] hydrogenases' H-cluster domains of *C. pasteurianum* has previously shown them to fall into groups A2 (CpI), A4 (CpII), and B2 (CpIII) (133). Group A2 is comprised of

soluble, monomeric, hydrogen producing enzymes. Enzymes of group A4 contain a long C-terminal domain that ligates two small rubredoxins and one rubrerythrin center (133). Members of group B2 have an average size of 450 amino acids and an additional characteristic cysteine residue in the P1 motif (TS**C**CCPxW) of the H-cluster (132). Interestingly, the ferredoxin-binding motif closest to the N-terminus of clostridial B2 members is $Cx_2Cx_2Cx_3C$; this is similar to that of the *nif*-associated ferredoxin in *Rhizobium meliloti* which is $Cx_2Cx_8Cx_3C$ (132).

	P1	P2	P3
CpI	…FTS**C**C**P**GW…	…VM**PC**TS**K**KFE…	…EKQYHFI**E**VMA**C**HG**GC**VN**G**G…
CpII	…FTS**C**C**P**AW…	…VT**PC**TA**K**KAE…	…EKKYDFV**E**VMT**C**RG**GC**IG**G**G…
CpIII	…TSC**C**C**P**MW…	…VG**PC**IA**K**KAE…	…EVAANFI**E**GMG**C**VG**GC**VG**G**P…

*P1-^{296}[FILT][ST][SCM]**C**[CS]**P**[AGSMIV][FWY]^{303}

*P2-^{352}[FILV][MGTV]**PC**xx**K**[DKQRS]x[EV]^{361}

*P3-^{495}**E**xM**x**C**C**xx**GC**xx**G**[AGP]^{507}

Figure 4.4. Conserved residues of the three signature H-clusters motifs (P1, P2, and P3) found in CpI, CpII, and CpIII. *Modified from Vignais and Billoud (25). An "x" indicates any amino acid while bold letters represent strictly conserved residues.

The [NiFe] hydrogenase gene cluster contains the required accessory genes (*HypABCEFD* and *HoxN)* downstream of the structural genes, *HyaAB*, encoding the large and small subunits respectively (Figure 4.5). The protein sequence of the large subunit contains previously described (25) L1 and L2 signatures characteristic of membrane-bound H_2 uptake hydrogenases. The L1 and L2 motifs encompass the highly conserved cysteine pairs (CxxC) near each terminus that ligate the NiFe center. Unlike [FeFe]-hydrogenases, maturases for the [NiFe]-hydrogenase are often found with the structural genes within a single gene cluster. In *C. pasteurianum*, this gene cluster is not in close

proximity to any other hydrogenase or nitrogenase genes. The large subunit (*HyaB*) clusters phylogenetically with other *Clostridia* in group 1 (132) (data not shown) which are membrane-associated uptake hydrogenases (25).

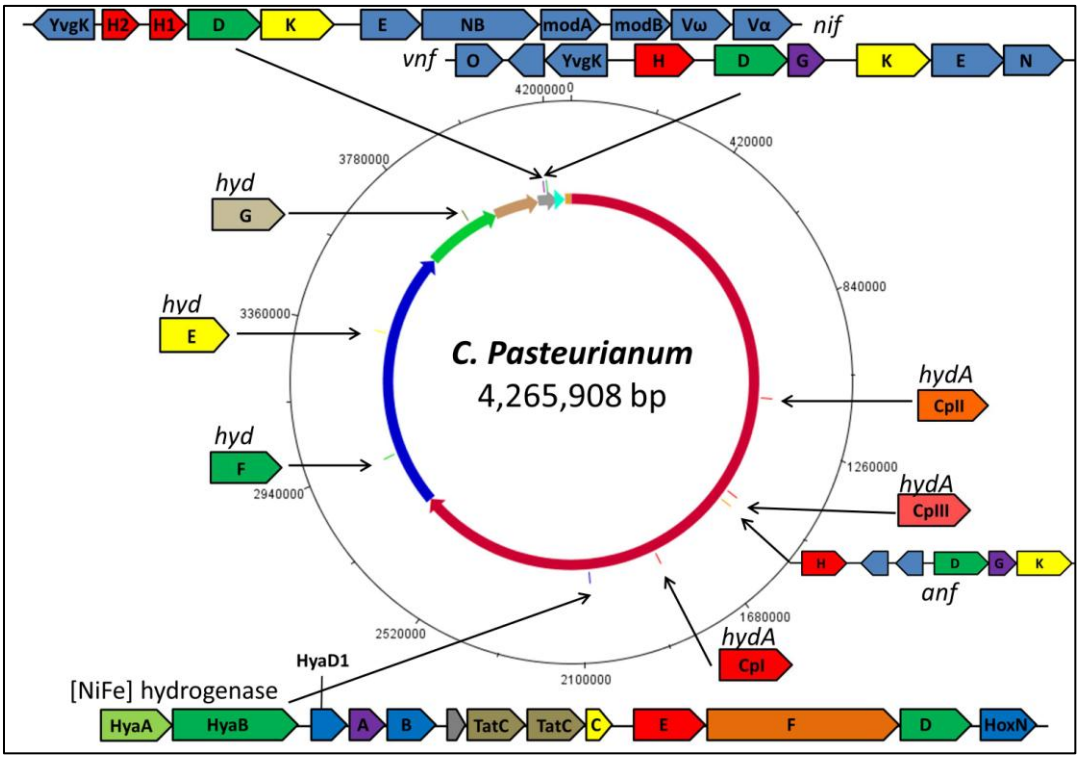

Figure 4.5. Hydrogenase and nitrogenase gene clusters of *C. pasteurianum* and their location on the draft genome.

Nitrogenases

In addition to the operon of the Mo-dependent nitrogenase, *nif*$H_2H_1DKENBCV_\omega V_\alpha$, the two alternative nitrogenase gene clusters are also found in *C. pasteurianum* (V-dependent and Fe-only) (Figure 4.5). Each of the 3 versions of the nitrogenase α-subunit, namely *nifD*, *vnfD* and *anfD*, contain conserved amino acid sequences flanking a histidine residue near the C-terminus of the nitrogenase (Figure 4.6) (146).

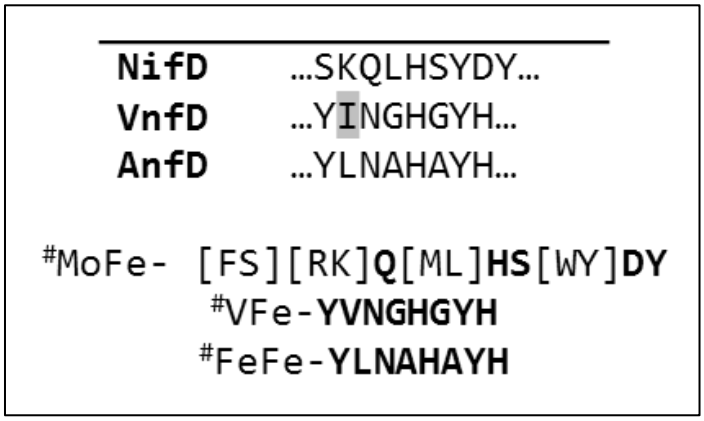

Figure 4.6. Conserved regions of the three nitrogenases of *C. pasteurianum* flanking a conserved His near the C-terminus of the three nitrogenase MoFe proteins. #Modified from Eady (146)

The V-dependent nitrogenase gene cluster consists of *vnfHDGKEN* and is just upstream of the Mo-dependent nitrogenase gene cluster. This varies slightly from the V-nitrogenase gene clusters of two other model organisms containing both alternative nitrogenases; *R. palustris*, where *vnfDGK* and *vnfH* are separated by a gene of unknown function (139), and *A. vinelandii*, where *vnfDGK* are separated from *vnfH* by four genes (138). What was once called *nifH5* (147) appears to be *vnfH*, the gene encoding for the iron-protein of the V-nitrogenase. As proposed by Chen *et al.* (148), the most divergent of the *nifH*-like genes identified, *nifH3* (126, 147), appears to be *anfH*, encoding for the iron protein of the Fe-only nitrogenase. Gene context shows that this gene is located in the Fe-nitrogenase gene cluster just under 2 kb up-stream of *anfDGK* as previously thought (148). This differs from *R. palustris* (139) and *A. vinelandii* (149) where *anfH* immediately precedes *anfDGK*. However, as with *R. palustris* and *A. vinelandii*, the Fe-only nitrogenase gene cluster contains only structural genes *anfHDGK* and no accessory genes. As has been proposed for other diazotrophs, it is likely that the accessory genes

from the V- and Mo-nitrogenases are used to encode for the maturases required to form active Fe-nitrogenase. Finally, the gene context of *nifH*4 doesn't propose a function, although transcription of this gene was previously observed in N_2-fixing cells (147).

Transcriptional Analysis

Transcripts of the three [FeFe]-hydrogenase genes of *C. pasteurianum* all changed under N_2-fixing conditions. The transcription of CpI and CpIII from cells grown in media devoid of fixed nitrogen (DM-11 N-) contained fewer transcripts (4.8 and 1.5 fold respectively) when compared to cells grown in nitrogen-replete media (DM-11). The reduction of dinitrogen to ammonia and the reduction of protons to dihydrogen both depends on reducing equivalents. However, the assimilation of nitrogen is much more important and the electron requirement of nitrogenase (16 electrons) far exceeds that of hydrogenase (2 electrons). Therefore, it would be in the cell's interest shut down any competing metabolism.

Along the same line, production of reducing equivalents would be beneficial to the nitrogen fixing operation. Hydrogen oxidizing enzymes would produce reducing equivalents and contribute to nitrogenase's needs. Under N_2-fixing conditions transcripts of CpII were observed to increase 16.0 fold (Figure 4.7). It has been reported that N_2 fixing cultures of *C. pasteurianum* oxidized twice as much H_2 as cultures growing on media containing NH_3, that the ratio of CpII/CpI expressed in cultures fixing N_2 was 50% higher than in cultures not fixing N_2 (30), and that CpII had low H_2 producing rates (compared to CpI) and high H_2 oxidizing rates *in vitro* (28). These observations suggest that the increase in transcription of CpII likely leads to an increase in CpII enzyme which

in turn increases rates of H_2 oxidation and production of reducing equivalents which would be in demand during N_2-fixation.

Once again, when compared to cultures grown in media containing NH_3, qRT-PCR indicated a 5.4 fold increase in the number of transcripts for large subunit of the [NiFe]-hydrogenase in cultures fixing nitrogen. This increase is similar to what was found in *A. vinelandii* (138). In a similar study with *R. palustris* (139), an increase in *hupL* (encoding for the large subunit of the [NiFe]-hydrogenase (59)) transcription was observed. A frame shift in the *hupV* gene (encoding for part of the [NiFe]-hydrogenase system (59)) rendered the organism unable to oxidized H_2. Likely because of this, during diazotrophic growth, an increase in H_2 production was observed as cultures went from using Mo- to V- to Fe-only nitrogenases; these nitrogenases theoretically produce 1, 3 and 9 moles of hydrogen respectively for every 2 moles of NH_3 produced (150). In the former two experiments, it was suggested that the [NiFe]-hydrogenases functioned to recycle H_2 during N_2-fixation.

To determine if the alternative nitrogenase systems were expressed constitutively with the Mo-nitrogenase under N_2 fixing conditions, like *Rhodopseudomonas palustris* (139), or if the expression of the alternatives are possibly controlled by the presence of molybdenum or vanadium as is seen in *Azotobacter vinelandii* (138, 151-153), primers were designed for α-subunits *nifD*, *vnfD*, and *anfD* for use in qRT-PCR experiments. When compared to control cultures, transcription of the α-subunit of each nitrogenase form increased with the greatest increase seen by *nifD* at 276.9 fold, followed by *vnfD* at 3.7 fold and *anfD* at 2.2 fold when grown under N_2-fixing conditions in the presence of

Mo (Figure 4.7). For *nifD*, these result are in agreement with studies that have shown transcription of the neighboring *nifH*1 gene (147) and expression of this protein under similar conditions (154).

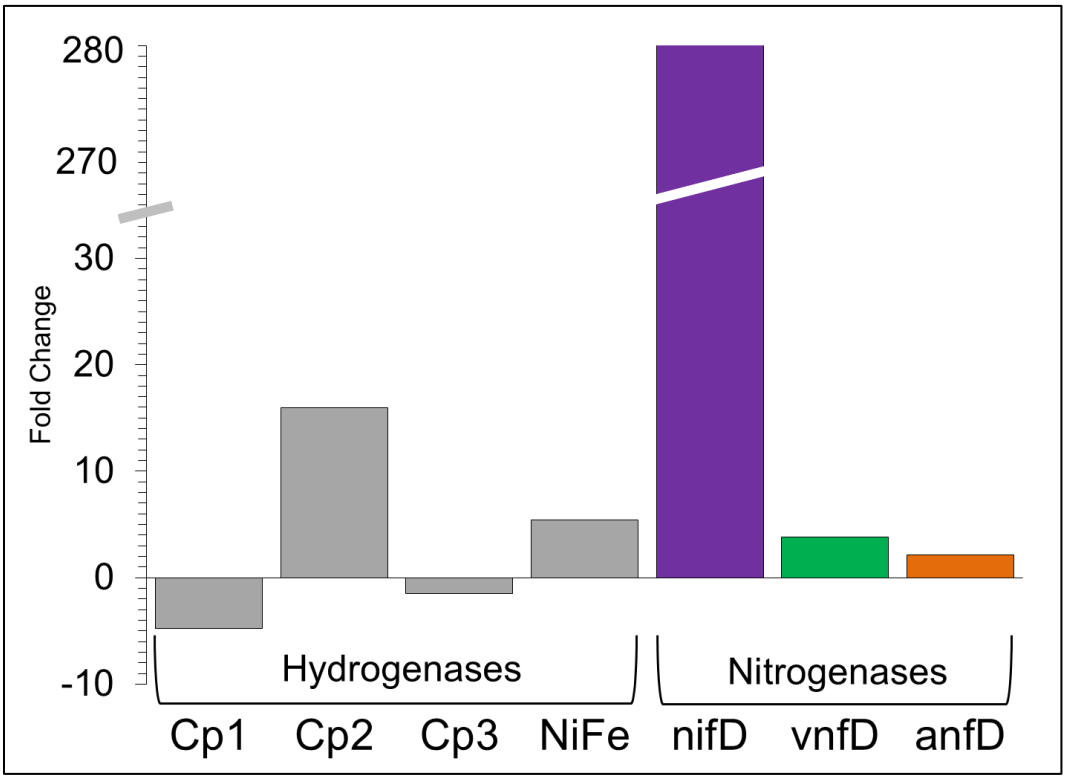

Figure 4.7. Fold change in transcription of hydrogenase and nitrogenase genes under N_2-fixing conditions as determined by qRT-PCR.

The observed increase in transcription of *vnfD* (3.7 fold) suggests that it is constitutively expressed, although at a much lower rate than *nifD*, during N_2-fixation even in presence of molybdenum. This would be similar to *R. palustris* (139) but different from *A. vinelandii* (153). Transcripts for *nifH*5 (now shown to be *vnfH*), encoding for the Fe-protein of the V-dependent nitrogenase, were previously observed in N_2-fixing cultures but were not quantified (147). Wang *et. al.* mentioned that it was

unclear if these transcripts were translated or not because NifH5 (VnfH) was not co-purified with NifH1. Our observed lower level of transcription, compared to *nifD*, might explain why it was not observed in their purifications. It may be possible that *vnfD* is transcribed, but not translated into an active nitrogenase or that not all the required structural/accessory genes are transcribed. Further qRT-PCR of RNA from cultures grown under N_2-fixing, metal limited conditions lacking Mo, and Mo/V are currently underway. Preliminary results indicate that the expression of all three nitrogenase genes encoding for the α-subunits increase regardless of metal (Mo and/or V) availability.

Transcription of *anfD* increased just over 2.2 fold under N_2-fixing conditions, again alluding to its expression being constitutive under these conditions, albeit at a lower level than both *nifD* and *vnfD*. As with *vnfD*, this increase in transcription would be similar to *R. palustris* (139) but different from *A. vinelandii* (151). Unlike *vnfH*, transcripts of *anfH* were not observed under N_2-fixing conditions in a previous study by Wang *et. al*. (147).

Homology models of CpII and CpIII can be seen in Figure 4.8 and show the absence of accessory domains seen in CpI. All [FeFe]-hydrogenases contain an active site termed the H-cluster (Figure 1.4). Here, a [4Fe-4S] cluster and a covalently bound [2Fe] subcluster are found ligated by conserved residues characteristic of [FeFe]-hydrogenases (Figure 4.4). However, a variable feature that can be used to differentiate between [FeFe]-hydrogenases is the presence/absence of accessory cluster binding domains. In CpI, accessory (41) clusters named FS4A, FS4B, FS4C (all [4Fe4S] clusters) and FS2 (a [2Fe2S] cluster) can be found in these domains (Figure 1.4) (39). Starting at the N-

terminus of the 574 amino acid sequence of CpI, there are conserved cysteine residues for each cluster sequentially binding clusters FS2, FS4C, FS4B and FS4A. At the N-terminus of CpII, the amino acid sequence is over 100 amino acids shorter (458 amino acids) than that of CpI and therefore lacks residues responsible for binding accessory clusters FS2 and FS4C (cyan and violet domains in Figure 4.8). However, conserved regions binding the remaining [4Fe4S] and [2Fe] clusters of the H-cluster (blue domains) and two [4Fe4S] accessory clusters (green domain) can be found. The number of iron atoms per mole of purified CpII has been published as 13.8 ± 0.4 (28) which corresponds to 6 irons in the H-cluster plus 8 irons from FS4A and FS4B shown in the homology model below. In CpIII, the shortest of the three *C. pasteurianum* [FeFe]-hydrogenases at 450 amino acids in length, the N-terminal arrangement of cyteines is unique. Sequence alignment reveals that the FS4A binding motif is conserved, while the FS4B motif lacks two of the four cysteines typically seen ligating this cluster. Our homology model shows a loop region surrounding the location of the FS4C cluster, but only one cysteine in the vicinity at 5.5 angstroms from the cluster. Further biochemical characterization would be needed to say whether or not there is an (41) cluster where FS4B resides in CpI.

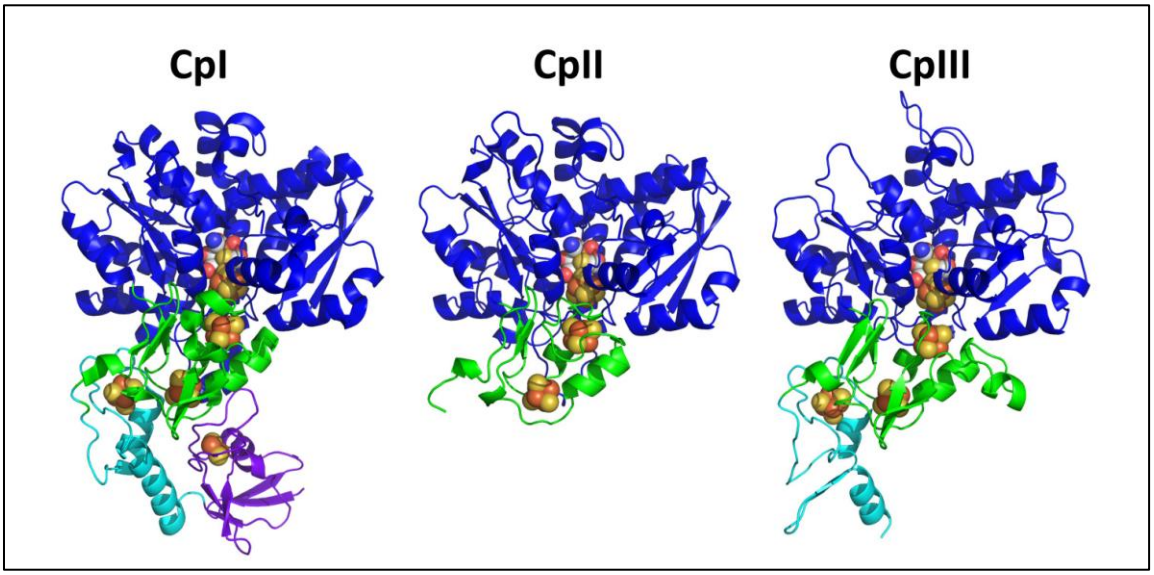

Figure 4.8. Crystal structure of CpI and homology models of CpII an d CpIII. Homology models based on structure of CpI. H-cluster domain colored in blue, accessory clusters colored in green, cyan, and violet.

The presence or absence of accessory (41) clusters and the ligand environment likely play a role in tuning the active site H-cluster to either preferentially produce or consume H_2. However, examples of hydrogenases that favorably reduce protons to H_2 and contain only the H-cluster domain exist. And the best studied H_2-producing hydrogenase, CpI, contains four accessory (41) clusters and is one of the most active H_2-producing enzymes known. So, without a more in depth study of the ligands surrounding and binding the clusters, the fact that a cluster is bound or not does not, in itself, define the type of catalysis the hydrogenase might undergo. For this, we must investigate the ligands in close proximity to the (41) clusters. The most important (41) clusters are those of the H-cluster. To explore the properties and effects of residue modifications that may modify the reduction potential of the H-cluster, residues within a 5 angstrom radius around the H-cluster were determined from the structure of CpI and homology model of

CpII. Of the residues within 5 angstroms of the H-cluster, two residues nearest the 2Fe subcluster have, what we propose to be, significant changes. Residues A230 and M353 in CpI correspond to 99S and T223 in CpII respectively. The alanine (A230) in CpI is 3.7 Å from the CN^- ligand while the serine (99S) of CpII is 2.4 Å. The close proximity of the hydroxyl group of serine to the CN^- of the 2-Fe subcluster allows for hydrogen bonding in CpII but not CpI. Hydrogen bonding might contibute to the preferential hydrogen oxidation exibited by CpII.

The second set of residues are M353 in CpI and T223 in CpII. This methionine residue of CpI likely stabilizes the bridging CO by S-O electrostatic interaction (117). The crystal stucture of CpI shows the sulfur of M353 to be 3.2 Å from the bridging CO ligand while our homology model shows the oxygen and carbon of the CpII threonine side chain to be 6.7 Å and 4.9 Å away respectively. Interestingly, Knörzer *et al.* showed that the most frequent substitution for M353 in 409 CpI homologues was T353. They then, in *C. pasteurianum*, mutagenically substituded M353 for L353 which is said to have no effect on the overall protein structure. A significant decrease in H_2 production (15% of WT) and a slight decrease in H_2 oxidation (74% of WT) was observed and was attributed to lowered turnover rate. EPR suggested slight differences in the electronic structure and it was suggested this might impeded the the transition between different redox states. Cyclic voltametry of the mutated enzyme showed slightly lowered K_m, but similar catalytic bias (for the forward and reverse reactions). This may help explain the reduced production of H_2 by CpII when compared to CpI (28) where CpII was nearly 500 time less active.

Conclusion

Despite years of in-depth studies of *C. pasteurianum* W5 and specifically its hydrogenases, our initial analysis of the genome has revealed a new [NiFe]-hydrogenase and confirmed the presence of a third [FeFe]-hydrogenase. In addition to the known Mo-nitrogenase gene cluster, we have revealed both the V-dependent and Fe-only alternative nitrogenase gene clusters. The alternative nitrogenase gene clusters have allowed us to re-assign two of the four *nifH*-like genes previously identified. Specifically, *nifH*3 has turned out to be *anfH* while *nifH*5 is actually *vnfH*. Transcriptomic analysis using qRT-PCR has revealed that transcription of CpII and the [NiFe]-hydrogenase is increased under N_2-fixing conditions suggesting their role in recycling/uptake of H_2 produced as a byproduct during the nitrogenase-catalyzed reduction of atmospheric N_2 to NH_4. Although not definitive, the increase in transcripts of all three nitrogenase α-subunits suggests their constitutive expression under N_2-fixing conditions. A more detailed analysis of metal limited (Mo and Mo/V deficient) cultures under the same condition is currently being planned to better understand the roles of the alternative nitrogenase systems. The presence of all three nitrogenase systems is somewhat rare and, along with our draft genome, makes *C. pasteurianum* a great anaerobic model organism for future comparative N_2-fixation studies.

Transcriptional analysis of the hydrogenases of *C. pasteurianum* under nitrogen-fixing conditions has helped in the comparison of CpI and CpII, effective hydrogen producing and oxidizing enzymes respectively. CpII has been known to be a poor hydrogen producing hydrogenase and our hypothesis that it may play a role in hydrogen

uptake during nitrogen-fixation seems to be correct according to our gene expression studies. In addition, homology modeling has afforded us the opportunity to compare CpI and CpII at a structural level and investigate key residues within the enzyme that may play important roles in tuning the enzyme for one reaction or the other. Around the H-cluster, two interesting differences were observed; residues A230 and M353 in CpI correspond to 99S and T223. These variations provide altered H-cluster environments and may contribute to the observed differences in catalytic activities.

CHAPTER 5

CONCLUDING REMARKS

With increasing global population come increases in global energy consumption, primarily in the form of fossil fuels; a finite resource that is continually depleted and will eventually run out. Currently, the U.S. is dependent primarily on fossil fuels, the majority of which are imported. Dependence on foreign energy has had great impact on countries around the world and can put national security at risk. For many countries, becoming energy independent is of paramount importance and will require the implementation of renewable energies. Renewable energy resources are very diverse and can be used to supplement and eventually replace many current energy needs. Additionally, from an environmental standpoint, renewable energies have the benefit of reducing greenhouse gas emissions and conserving our planet. Work presented here contributes in different ways to the diverse field of bio-energy. In the second chapter the benefits of algal encapsulation to increase the duration and oxygen tolerance of hydrogen production were discussed. This immobilization technique was then implemented in co-culturing studies described in chapter three. There, co-culturing two organisms for the eventual production of lipids for biodiesel were described. Using alginate immobilization, we were able to limit the growth of one organism and increase the growth of the other. Alginate-bead immobilization has been shown to be a flexible technique with multiple beneficial applications for bio-energy production; from facilitating culture handling to controlling growth in co-culture. Finally, in the fourth chapter the genome of a model hydrogen

producing bacteria revealed additional genes encoding uncharacterized hydrogenase. Gene sequences allowed us to build homology models for two of the three [FeFe]-hydrogenases and compare them to the third. These models revealed differences in the overall structure, but also differences in the environment surrounding the H-cluster. Some of these differences are hypothesized to play a role in the tuning of [FeFe]-hydrogenase and its catalytic efficiency. Moreover, the transcription of hydrogenases was monitored under conditions of nitrogen fixation providing a metabolic backdrop on which structural differences can be placed. In addition to the studies of chapter four, the sequenced genome of *C. pasteurianum* paves the way for many hydrogenase studies to come and increases our overall understanding of the enzyme responsible for biological hydrogen production. Barriers remain for the wide-spread integration of renewable energy, but optimization and new discovery of technologies used for bio-energy continue. With each new discovery, including those described here, our understanding of alternative energies improves. The insights provided here can be used as stepping stones to energy independence.

REFERENCE CITED

1. **Hedberg D, Kullander S, Frank H.** 2010. The world needs a new energy paradigm. Ambio **39 Suppl 1:**1-10.

2. **D.O.E.** 2011. International Energy Outlook 2011 (IEO2011).

3. **Administration USEI.** 2013. U.S. Imports of Crude Oil and Petroleum Products.

4. **Administration USEI.** 2012. Annual Energy Review 2011.

5. 2012. FY 2013 Budget Request.

6. **Antoni D, Zverlov VV, Schwarz WH.** 2007. Biofuels from microbes. Applied microbiology and biotechnology **77:**23-35.

7. **Galbe M, Zacchi G.** 2002. A review of the production of ethanol from softwood. Applied microbiology and biotechnology **59:**618-628.

8. **Dias MOS, Cunha MP, Jesus CDF, Rocha GJM, Pradella JGC, Rossell CEV, Maciel Filho R, Bonomi A.** 2011. Second generation ethanol in Brazil: Can it compete with electricity production? Bioresource technology **102:**8964-8971.

9. **Magazine EP.** 2012. Raizen to begin cellulosic ethanol production in 2014.

10. **Nallathambi Gunaseelan V.** 1997. Anaerobic digestion of biomass for methane production: A review. Biomass and Bioenergy **13:**83-114.

11. **Ahring BK, Westermann P.** 2007. Coproduction of bioethanol with other biofuels. Advances in biochemical engineering/biotechnology **108:**289-302.
12. 2013. Biogas Data.

13. **Agency USEP.** 2013. Energy Projects and Candidate Landfills.

14. **E.P.A.** 2011. U.S. Anaerobic Digester Status: A 2011 Snapshot.

15. **E.P.A.** 2012. AgSTAR: Operating Anaerobic Digester Projects.

16. **Bolan NS, Thangarajan R, Seshadri B, Jena U, Das KC, Wang H, Naidu R.** 2012. Landfills as a biorefinery to produce biomass and capture biogas. Bioresource technology.

17. **Beylot A, Villeneuve J, Bellenfant G.** 2013. Life Cycle Assessment of landfill biogas management: Sensitivity to diffuse and combustion air emissions. Waste Management **33:**401-411.

18. **Ersahin ME, Gomec CY, Dereli RK, Arikan O, Ozturk I.** 2011. Biomethane production as an alternative bioenergy source from codigesters treating municipal sludge and organic fraction of municipal solid wastes. Journal of biomedicine & biotechnology **2011:**953065.

19. **Solazyme** 2011, posting date. Solazyme Announces First U.S. Commercial Passenger Flight on Advanced Biofuel. [Online.]

20. **Schenk PM, Thomas-Hall SR, Stephens E, Marx UC, Mussgnug JH, Posten C, Kruse O, Hankamer B.** 2008. Second generation biofuels: high-efficiency microalgae for biodiesel production. Bioenergy Research **1:**20-43.

21. **Peters J, Boyd E, D'Adamo S, Mulder D, Therien J, Posewitz M.** 2013. Hydrogenases, Nitrogenases, Anoxia, and H2 Production in Water-Oxidizing Phototrophs, p. 37-75. *In* Borowitzka MA, Moheimani NR (ed.), Algae for Biofuels and Energy, vol. 5. Springer Netherlands.

22. **Logan BE.** 2009. Exoelectrogenic bacteria that power microbial fuel cells. Nat Rev Micro **7:**375-381.

23. **Hallenbeck PC, Ghosh D, Skonieczny MT, Yargeau V.** 2009. Microbiological and engineering aspects of biohydrogen production. Indian journal of microbiology **49:**48-59.

24. **Züttel A, Remhof A, Borgschulte A, Friedrichs O.** 2010. Hydrogen: the future energy carrier. Philosophical Transactions of the Royal Society A: Mathematical, Physical and Engineering Sciences **368:**3329-3342.

25. **Vignais PM, Billoud B.** 2007. Occurrence, classification, and biological function of hydrogenases: an overview. Chemical reviews **107:**4206-4272.

26. **Vignais PM, Billoud B, Meyer J.** 2001. Classification and phylogeny of hydrogenases. FEMS microbiology reviews **25:**455-501.

27. **Richard Cammack MF, Robert Robson, Barbel Friedrich, Paulette M. Vignais, Oliver Lenz, Annette Colbeau.** 2001. Hydrogen as a Fuel: Learning from Nature, 1st ed. Taylor & Francis Inc., London & New York.

28. **Adams MW.** 1990. The structure and mechanism of iron-hydrogenases. Biochimica et biophysica acta **1020:**115-145.

29. **Nicolet Y, Piras C, Legrand P, Hatchikian CE, Fontecilla-Camps JC.** 1999. Desulfovibrio desulfuricans iron hydrogenase: the structure shows unusual coordination to an active site Fe binuclear center. Structure (London, England : 1993) **7:**13-23.

30. **Chen J-S, Blanchard DK.** 1978. Isolation and properties of a unidirectional H2-oxidizing hydrogenase from the strictly anaerobic N2-fixing bacterium Clostridium pasteurianum W5. Biochemical and biophysical research communications **84:**1144-1150.

31. **Adams MWW, Mortenson LE.** 1984. The purification of hydrogenase II (uptake hydrogenase) from the anaerobic N2-fixing bacterium Clostridium pasteurianum. Biochimica et Biophysica Acta (BBA) - Bioenergetics **766:**51-61.

32. **Meyer J.** 2007. [FeFe] hydrogenases and their evolution: a genomic perspective. Cellular and molecular life sciences : CMLS **64:**1063-1084.

33. **Ludwig M, Schulz-Friedrich R, Appel J.** 2006. Occurrence of hydrogenases in cyanobacteria and anoxygenic photosynthetic bacteria: implications for the phylogenetic origin of cyanobacterial and algal hydrogenases. Journal of molecular evolution **63:**758-768.

34. **Appel J, Schulz R.** 1998. Hydrogen metabolism in organisms with oxygenic photosynthesis: hydrogenases as important regulatory devices for a proper redox poising? Journal of Photochemistry and Photobiology B: Biology **47:**1-11.

35. **Bothe H, Schmitz O, Yates MG, Newton WE.** 2010. Nitrogen fixation and hydrogen metabolism in cyanobacteria. Microbiology and molecular biology reviews : MMBR **74:**529-551.

36. **Buhrke T, Lenz O, Porthun A, Friedrich B.** 2004. The H2-sensing complex of Ralstonia eutropha: interaction between a regulatory [NiFe] hydrogenase and a histidine protein kinase. Molecular Microbiology **51:**1677-1689.

37. **Thauer RK, Klein AR, Hartmann GC.** 1996. Reactions with Molecular Hydrogen in Microorganisms: Evidence for a Purely Organic Hydrogenation Catalyst. Chemical reviews **96:**3031-3042.

38. **Pilak O, Mamat B, Vogt S, Hagemeier CH, Thauer RK, Shima S, Vonrhein C, Warkentin E, Ermler U.** 2006. The crystal structure of the apoenzyme of the iron-sulphur cluster-free hydrogenase. J Mol Biol **358:**798-809.

39. **Peters JW, Lanzilotta WN, Lemon BJ, Seefeldt LC.** 1998. X-ray Crystal Structure of the Fe-Only Hydrogenase (Cpl) from Clostridium pasteurianum to 1.8 Angstrom Resolution. Science (New York, N.Y.) **282:**1853-1858.

40. **Nicolet Y, Piras C, Legrand P, Hatchikian CE, Fontecilla-Camps JC.** 1999. Desulfovibrio desulfuricans iron hydrogenase: the structure shows unusual coordination to an active site Fe binuclear center. Structure (London, England : 1993) **7:**13-23.

41. **Siaut M, Cuine S, Cagnon C, Fessler B, Nguyen M, Carrier P, Beyly A, Beisson F, Triantaphylides C, Li-Beisson Y, Peltier G.** 2011. Oil accumulation in the model green alga Chlamydomonas reinhardtii: characterization, variability between common laboratory strains and relationship with starch reserves. BMC Biotechnology **11:**7.

42. **Volbeda A, Charon MH, Piras C, Hatchikian EC, Frey M, Fontecilla-Camps JC.** 1995. Crystal structure of the nickel-iron hydrogenase from Desulfovibrio gigas. Nature **373:**580-587.

43. **Ogata H, Mizoguchi Y, Mizuno N, Miki K, Adachi S-i, Yasuoka N, Yagi T, Yamauchi O, Hirota S, Higuchi Y.** 2002. Structural Studies of the Carbon Monoxide Complex of [NiFe]hydrogenase from Desulfovibrio vulgaris Miyazaki F: Suggestion for the Initial Activation Site for Dihydrogen. Journal of the American Chemical Society **124:**11628-11635.

44. **Rousset M, Montet Y, Guigliarelli B, Forget N, Asso M, Bertrand P, Fontecilla-Camps JC, Hatchikian EC.** 1998. [3Fe-4S] to [4Fe-4S] cluster conversion in Desulfovibrio fructosovorans [NiFe] hydrogenase by site-directed mutagenesis. Proceedings of the National Academy of Sciences of the United States of America **95:**11625-11630.

45. **Ogata H, Kellers P, Lubitz W.** 2010. The crystal structure of the [NiFe] hydrogenase from the photosynthetic bacterium Allochromatium vinosum: characterization of the oxidized enzyme (Ni-A state). Journal of molecular biology **402:**428-444.

46. **Shomura Y, Yoon KS, Nishihara H, Higuchi Y.** 2011. Structural basis for a [4Fe-3S] cluster in the oxygen-tolerant membrane-bound [NiFe]-hydrogenase. Nature **479:**253-256.

47. **Shima S, Ataka K.** 2011. Isocyanides inhibit [Fe]-hydrogenase with very high affinity. FEBS letters **585:**353-356.

48. **Matsumoto T, Kabe R, Nonaka K, Ando T, Yoon K-S, Nakai H, Ogo S.** 2011. Model Study of CO Inhibition of [NiFe]hydrogenase. Inorganic Chemistry **50:**8902-8906.

49. **Nicolet Y, Fontecilla-Camps JC, Fontecave M.** 2010. Maturation of [FeFe]-hydrogenases: Structures and mechanisms. International Journal of Hydrogen Energy **35:**10750-10760.

50. **Pilet E, Nicolet Y, Mathevon C, Douki T, Fontecilla-Camps JC, Fontecave M.** 2009. The role of the maturase HydG in [FeFe]-hydrogenase active site synthesis and assembly. FEBS letters **583:**506-511.

51. **Casalot L, Rousset M.** 2001. Maturation of the [NiFe] hydrogenases. Trends in microbiology **9:**228-237.

52. **Fontecilla-Camps JC, Volbeda A, Cavazza C, Nicolet Y.** 2007. Structure/function relationships of [NiFe]- and [FeFe]-hydrogenases. Chem Rev **107:**4273-4303.

53. **Paschos A, Glass RS, Böck A.** 2001. Carbamoylphosphate requirement for synthesis of the active center of [NiFe]-hydrogenases. FEBS letters **488:**9-12.

54. **Reissmann S, Hochleitner E, Wang H, Paschos A, Lottspeich F, Glass RS, Böck A.** 2003. Taming of a Poison: Biosynthesis of the NiFe-Hydrogenase Cyanide Ligands. Science **299:**1067-1070.

55. **Fouchard S, Hemschemeier A, Caruana A, Pruvost J, Legrand J, Happe T, Peltier G, Cournac L.** 2005. Autotrophic and mixotrophic hydrogen photoproduction in sulfur-deprived chlamydomonas cells. Applied and environmental microbiology **71:**6199-6205.

56. **Harris EH.** 2001. CHLAMYDOMONAS AS A MODEL ORGANISM. Annu Rev Plant Physiol Plant Mol Biol **52:**363-406.

57. **Beer LL, Boyd ES, Peters JW, Posewitz MC.** 2009. Engineering algae for biohydrogen and biofuel production. Current Opinion in Biotechnology **20:**264-271.

58. **Hu Q, Sommerfeld M, Jarvis E, Ghirardi M, Posewitz M, Seibert M, Darzins A.** 2008. Microalgal triacylglycerols as feedstocks for biofuel production: perspectives and advances. The Plant Journal **54:**621-639.

59. **Harris EH.** 1989. The Chlamydomonas Sourcebook: Introduction to Chlamydomonas and Its Laboratory Use. **1**.

60. **Heifetz PB, Förster B, Osmond CB, Giles LJ, Boynton JE.** 2000. Effects of Acetate on Facultative Autotrophy inChlamydomonas reinhardtii Assessed by Photosynthetic Measurements and Stable Isotope Analyses. Plant Physiology **122:**1439-1446.

61. **Sager R, Granick S.** 1953. NUTRITIONAL STUDIES WITH CHLAMYDOMONAS REINHARDI. Annals of the New York Academy of Sciences **56:**831-838.

62. **Johnson X, Alric J.** 2012. Interaction between Starch Breakdown, Acetate Assimilation, and Photosynthetic Cyclic Electron Flow in Chlamydomonas reinhardtii. Journal of Biological Chemistry **287:**26445-26452.

63. **Tsygankov AA, Kosourov SN, Tolstygina IV, Ghirardi ML, Seibert M.** 2006. Hydrogen production by sulfur-deprived Chlamydomonas reinhardtii under photoautotrophic conditions. International Journal of Hydrogen Energy **31:**1574-1584.

64. **Laurinavichene TV, Fedorov AS, Ghirardi ML, Seibert M, Tsygankov AA.** 2006. Demonstration of sustained hydrogen photoproduction by immobilized, sulfur-deprived Chlamydomonas reinhardtii cells. International Journal of Hydrogen Energy **31:**659-667.

65. **Ghirardi ML, Zhang L, Lee JW, Flynn T, Seibert M, Greenbaum E, Melis A.** 2000. Microalgae: a green source of renewable H(2). Trends in biotechnology **18:**506-511.

66. **Zhang L, Happe T, Melis A.** 2002. Biochemical and morphological characterization of sulfur-deprived and H2-producing Chlamydomonas reinhardtii (green alga). Planta **214:**552-561.

67. **Kosourov S, Seibert M, Ghirardi ML.** 2003. Effects of extracellular pH on the metabolic pathways in sulfur-deprived, H2-producing Chlamydomonas reinhardtii cultures. Plant & cell physiology **44:**146-155.

68. **Melis A, Zhang L, Forestier M, Ghirardi ML, Seibert M.** 2000. Sustained photobiological hydrogen gas production upon reversible inactivation of oxygen evolution in the green alga Chlamydomonas reinhardtii. Plant Physiol **122:**127-136.

69. **Tsygankov AA, Hirata Y, Miyake M, Asada Y, Miyake J.** 1994. Photobioreactor with photosynthetic bacteria immobilized on porous glass for hydrogen photoproduction. Journal of Fermentation and Bioengineering **77:**575-578.

70. **Cohen J, Kim K, King P, Seibert M, Schulten K.** 2005. Finding gas diffusion pathways in proteins: application to O2 and H2 transport in CpI [FeFe]-hydrogenase and the role of packing defects. Structure (London, England : 1993) **13:**1321-1329.

71. **Lautier T, Ezanno P, Baffert C, Fourmond V, Cournac L, Fontecilla-Camps JC, Soucaille P, Bertrand P, Meynial-Salles I, Leger C.** 2011. The quest for a functional substrate access tunnel in FeFe hydrogenase. Faraday Discussions **148:**385-407.

72. **Stapleton JA, Swartz JR.** 2010. A cell-free microtiter plate screen for improved [FeFe] hydrogenases. PloS one **5:**e10554.

73. **Bingham AS, Smith PR, Swartz JR.** 2012. Evolution of an [FeFe] hydrogenase with decreased oxygen sensitivity. International Journal of Hydrogen Energy **37:**2965-2976.

74. **Wahlen BD, Willis RM, Seefeldt LC.** 2011. Biodiesel production by simultaneous extraction and conversion of total lipids from microalgae, cyanobacteria, and wild mixed-cultures. Bioresource technology **102:**2724-2730.

75. **Yoo G, Park WK, Kim CW, Choi YE, Yang JW.** 2012. Direct lipid extraction from wet Chlamydomonas reinhardtii biomass using osmotic shock. Bioresource technology **123:**717-722.

76. **Fan J, Yan C, Andre C, Shanklin J, Schwender J, Xu C.** 2012. Oil accumulation is controlled by carbon precursor supply for fatty acid synthesis in Chlamydomonas reinhardtii. Plant and Cell Physiology **53:**1380-1390.

77. **Merchant SS, Kropat J, Liu B, Shaw J, Warakanont J.** 2012. TAG, You're it! Chlamydomonas as a reference organism for understanding algal triacylglycerol accumulation. Current Opinion in Biotechnology **23:**352-363.

78. **Zabawinski C, Van Den Koornhuyse N, #039, Hulst C, Schlichting R, Giersch C, Delrue B, Lacroix JM, Preiss J, Ball S.** 2001. Starchless mutants of Chlamydomonas reinhardtii lack the small subunit of a heterotetrameric ADP-glucose pyrophosphorylase, vol. 183.

79. **Work VH, Radakovits R, Jinkerson RE, Meuser JE, Elliott LG, Vinyard DJ, Laurens LML, Dismukes GC, Posewitz MC.** 2010. Increased Lipid Accumulation in the Chlamydomonas reinhardtii sta7-10 Starchless

Isoamylase Mutant and Increased Carbohydrate Synthesis in Complemented Strains. Eukaryotic Cell **9:**1251-1261.

80. **Li Y, Han D, Hu G, Dauvillee D, Sommerfeld M, Ball S, Hu Q.** 2010. Chlamydomonas starchless mutant defective in ADP-glucose pyrophosphorylase hyper-accumulates triacylglycerol. Metabolic engineering **12:**387-391.

81. **Kruse O, Rupprecht J, Bader K-P, Thomas-Hall S, Schenk PM, Finazzi G, Hankamer B.** 2005. Improved Photobiological H2 Production in Engineered Green Algal Cells. Journal of Biological Chemistry **280:**34170-34177.

82. **Doebbe A, Rupprecht J, Beckmann J, Mussgnug JH, Hallmann A, Hankamer B, Kruse O.** 2007. Functional integration of the HUP1 hexose symporter gene into the genome of C. reinhardtii: Impacts on biological H(2) production. J Biotechnol **131:**27-33.

83. **Mata TM, Martins AA, Caetano NS.** 2010. Microalgae for biodiesel production and other applications: A review. Renewable and Sustainable Energy Reviews **14:**217-232.

84. **Robinson PK, Mak AL, Trevan MD.** 1986. Immobilized algae; a review. Process biochemistry. **21:**122-127.

85. **Robinson PK, Goulding KH, Mak AL, Trevan MD.** 1986. Factors affecting the growth characteristics of alginate-entrapped Chlorella. Enzyme and Microbial Technology **8:**729-733.

86. **Santos-Rosa F, Galvan, F. .** 1989. Ammonium photoproduction by free and immobilized cells of Chlamydomonas reinhardtii. Applied microbiology and biotechnology. **31**.

87. **Vilchez C, Galvan, F., Vega, J.M. .** 1991. Glycolate photoproduction by free and algniate-entrapped cells of Chlamydomonas reinhardtii. . Applied microbiology and biotechnology. **35**.

88. **Moreno-Garrido I.** 2008. Microalgae immobilization: Current techniques and uses. Bioresource technology **99:**3949-3964.

89. **Brouers M, Hall DO.** 1986. Ammonia and hydrogen production by immobilized cyanobacteria. Journal of Biotechnology **3:**307-321.

90. **Benemann JR.** 1997. Feasibility analysis of photobiological hydrogen production. International association for hydrogen energy **22:**979-987.

91. **Wykoff DD, Davies JP, Melis A, Grossman AR.** 1998. The regulation of photosynthetic electron transport during nutrient deprivation in Chlamydomonas reinhardtii. Plant Physiol **117:**129-139.

92. **Robinson PK, Mak AL, Trevan MD.** 1986. Immobilized algae: a review. Process Biochemistry**:**122-127.

93. **Kosourov S, Tsygankov A, Seibert M, Ghirardi ML.** 2002. Sustained hydrogen photoproduction by Chlamydomonas reinhardtii: Effects of culture parameters. Biotechnol Bioeng **78:**731-740.

94. **Laurinavichene TV, Fedorova AS, Ghirardib ML, Seibertb M, Tsygankova AA.** 2006. Demonstration of sustained hydrogen photoproduction by immobilized, sulfur-deprived Chlamydomonas reinhardtii cells. international journal of hydrogen energy **31:**659-667.

95. **Brouers M, Hall DO.** 1986. Ammonia and hydrogen production by immobilized cyanobacteria. Journal of Biotechnology **3:**307-321.

96. **Moreno-Garrido I.** 2008. Microalgae immobilization: current techniques and uses. Bioresour Technol **99:**3949-3964.

97. **Francisco Santos-Rosa FG, Jose M. Vega.** 1989. Photoproduction of ammonium by Chlamydomonas reinhardtii cells immobilized in barium alginate: a reactor feaibility study. Applied Microbiology and Biotechnology **32:**285-290.

98. **Carlos Vilchez FG, Jose M. Vega.** 1991. Glycolate photoproduction by free and alginate-entrapped cells of Chlamydomonas reinhardtii. Applied Microbiology and Biotechnology **35:**716-719.

99. **Robinson PK, Goulding KH, Simpkins I, Mak AL, Trevan MD.** 1986. Factors affecting the growth characteristics of alginate-entrapped Chlorella. Enzyme and microbial technology **8:**729-733.

100. **Mallick N.** 2006. Methods in Biotechnology: Immobilization of enzymes and cells, second ed. Humana Press: Totowa, New Jersey, Madrid, Spain.

101. **Harris EH.** 1989. The Chlamydomonas Sourcebook: A Comprehensive Guide to Biology and Laboratory Use

102. **Gisby PE, Hall DO.** 1980. Biophotolytic H2 production using alginate-immobilized chloroplasts, enzymes and synthetic catalysts. Nature **287:**251-253.

103. **Rao KK, Muallem A, Bruce DL, Smith GD, Hall DO.** 1982. Immobilization of chloroplasts, algae and hydrogenases in various solid supports for the photoproduction of hydrogen. Biochemical Society Transactions **10:**527-528.

104. **Robinson PK, Dainty AL, Goulding KH, Simpkins I, Trevan MD.** 1985. Physiology of alginate-immobilized Chlorella. Enzyme Microbial Technology **7:**212-216.

105. **Adlercreutz P, Mattiasson B.** 1982. Oxygen supply to immobilized cells: 1. Oxygen prodution by immobilized Chlorella pyrenoidosa. Enzyme Microbial Technology **4:**332-336.

106. **Martinsen A, Storrø I, Skjårk-Bræk G.** 1992. Alginate as immobilization material: III. Diffusional properties. Biotechnology and Bioengineering **39:**186-194.

107. **Tam NF, Wong YS.** 2000. Effect of immobilized microalgal bead concentrations on wastewater nutrient removal. Environ Pollut **107:**145-151.

108. **Hameed MSA.** 2007. Effect of algal density in bead, bead size and bead concentrations on wastewater nutrient removal. African Journal of biotechnology **6:**1185-1191.

109. **Chen C, Gibbs M.** 1992. Coupling of Carbon Dioxide Fixation to the Oxyhydrogen Reaction in the Isolated Chloroplast of Chlamydomonas reinhardtii. Plant Physiol **100:**1361-1365.

110. **Maione TE, Gibbs M.** 1986. Association of the Chloroplastic Respiratory and Photosynthetic Electron Transport Chains of Chlamydomonas reinhardii with Photoreduction and the Oxyhydrogen Reaction. Plant Physiology **80:**364-368.

111. **Ghirardi M, Togasaki R, Seibert M.** 1997. Oxygen sensitivity of algal H₂- production. Applied Biochemistry and Biotechnology **63-65:**141-151.

112. **Kierstan M, Bucke C.** 1977. The immobilization of microbial cells, subcellular organelles, and enzymes in calcium alginate gels. Biotechnology and Bioengineering **19:**387-397.

113. **Energy USDsooEeaR** 2013, posting date. Energy Basics. [Online.]

114. **Posten C, Schaub G.** 2009. Microalgae and terrestrial biomass as source for fuels—A process view. Journal of Biotechnology **142:**64-69.

115. **Dwidar M, Kim S, Jeon BS, Um Y, Mitchell RJ, Sang BI.** 2013. Co-culturing a novel Bacillus strain with Clostridium tyrobutyricum ATCC 25755 to produce butyric acid from sucrose. Biotechnology for biofuels **6:**35.

116. **Heifetz PB, Forster B, Osmond CB, Giles LJ, Boynton JE.** 2000. Effects of acetate on facultative autotrophy in Chlamydomonas reinhardtii assessed by photosynthetic measurements and stable isotope analyses. Plant Physiol **122:**1439-1445.

117. **Stevens SE, Patterson COP, Myers J.** 1973. THE PRODUCTION OF HYDROGEN PEROXIDE BY BLUE-GREEN ALGAE: A SURVEY1. Journal of Phycology **9:**427-430.

118. **Ludwig M, Bryant DA.** 2012. Synechococcus sp. Strain PCC 7002 Transcriptome: Acclimation to Temperature, Salinity, Oxidative Stress, and Mixotrophic Growth Conditions. Frontiers in microbiology **3:**354.

119. **Xu Y, Tiago Guerra L, Li Z, Ludwig M, Charles Dismukes G, Bryant DA.** 2013. Altered carbohydrate metabolism in glycogen synthase mutants of Synechococcus sp. strain PCC 7002: Cell factories for soluble sugars. Metabolic engineering **16:**56-67.

120. **Winogradsky S.** 1895. Recherches sure l'assimilation de l'azote libre de l'atmosphere par les microbes. Archives des science biologique **3:**297-352.

121. **Valentine RC, Mortenson LE, Carnahan JE.** 1963. The Hydrogenase System of Clostridium pasteurianum. Journal of Biological Chemistry **238:**1141-1144.

122. **Nakos G, Mortenson L.** 1971. Purification and properties of hydrogenase, an iron sulfur protein, from Clostridium pasteurianum W5. Biochimica et Biophysica Acta (BBA) - Enzymology **227:**576-583.

123. **Chen J-S, Mortenson LE.** 1974. Purification and properties of hydrogenase from Clostridium pasteurianum W5. Biochimica et Biophysica Acta (BBA) - Protein Structure **371:**283-298.

124. **Adams MW, Mortenson LE.** 1984. The physical and catalytic properties of hydrogenase II of Clostridium pasteurianum. A comparison with hydrogenase I. The Journal of biological chemistry **259:**7045-7055.

125. **Carnahan JE, Mortenson LE, Mower HF, Castle JE.** 1960. Nitrogen fixation in cell-free extracts of Clostridium pasteurianum. Biochimica et Biophysica Acta **44:**520-535.

126. **Chen JS, Johnson JL.** 1993. Molecular biology of nitrogen fixation in the clostridia. Biotechnology (Reading, Mass.) **25:**371-392.

127. **Kim J, Woo D, Rees DC.** 1993. X-ray crystal structure of the nitrogenase molybdenum-iron protein from Clostridium pasteurianum at 3.0-A resolution. Biochemistry **32:**7104-7115.

128. **Schlessman JL, Woo D, Joshua-Tor L, Howard JB, Rees DC.** 1998. Conformational variability in structures of the nitrogenase iron proteins from Azotobacter vinelandii and Clostridium pasteurianum. Journal of molecular biology **280:**669-685.

129. **Jones DT, Woods DR.** 1986. Acetone-butanol fermentation revisited. Microbiological reviews **50:**484-524.

130. **Gabriel CL.** 1928. Butanol Fermentation Process1. Industrial & Engineering Chemistry **20:**1063-1067.

131. **Thauer RK, Jungermann K, Decker K.** 1977. Energy conservation in chemotrophic anaerobic bacteria. Bacteriological reviews **41:**100-180.

132. **Calusinska M, Happe T, Joris B, Wilmotte A.** 2010. The surprising diversity of clostridial hydrogenases: a comparative genomic perspective. Microbiology (Reading, England) **156:**1575-1588.

133. **Calusinska M, Joris B, Wilmotte A.** 2011. Genetic diversity and amplification of different clostridial [FeFe] hydrogenases by group-specific degenerate primers. Letters in applied microbiology **53:**473-480.

134. **Adams MW, Eccleston E, Howard JB.** 1989. Iron-sulfur clusters of hydrogenase I and hydrogenase II of Clostridium pasteurianum. Proceedings of the National Academy of Sciences **86:**4932-4936.

135. **Adams MW.** 1987. The mechanisms of H2 activation and CO binding by hydrogenase I and hydrogenase II of Clostridium pasteurianum. Journal of Biological Chemistry **262:**15054-15061.

136. **Rusnak FM, Adams MW, Mortenson LE, Munck E.** 1987. Mossbauer study of Clostridium pasteurianum hydrogenase II. Evidence for a novel three-iron cluster. The Journal of biological chemistry **262:**38-41.

137. **Macor KA, Czernuszewicz RS, Adams MW, Spiro TG.** 1987. An investigation of hydrogenase I and hydrogenase II from Clostridium pasteurianum by resonance Raman spectroscopy. Evidence for a [2Fe-2S] cluster in hydrogenase I. The Journal of biological chemistry **262:**9945-9947.

138. **Hamilton TL, Ludwig M, Dixon R, Boyd ES, Dos Santos PC, Setubal JC, Bryant DA, Dean DR, Peters JW.** 2011. Transcriptional profiling of nitrogen fixation in Azotobacter vinelandii. Journal of bacteriology **193:**4477-4486.

139. **Oda Y, Samanta SK, Rey FE, Wu L, Liu X, Yan T, Zhou J, Harwood CS.** 2005. Functional genomic analysis of three nitrogenase isozymes in the photosynthetic bacterium Rhodopseudomonas palustris. Journal of bacteriology **187:**7784-7794.

140. **Brito B, Martinez M, Fernandez D, Rey L, Cabrera E, Palacios JM, Imperial J, Ruiz-Argueso T.** 1997. Hydrogenase genes from Rhizobium leguminosarum bv. viciae are controlled by the nitrogen fixation regulatory protein nifA. Proceedings of the National Academy of Sciences of the United States of America **94:**6019-6024.

141. **Lindberg P, Hansel A, Lindblad P.** 2000. hupS and hupL constitute a transcription unit in the cyanobacterium Nostoc sp. PCC 73102. Arch Microbiol **174:**129-133.

142. **Mallette MF, Reece P, Dawes EA.** 1974. Culture of Clostridium pasteurianum in Defined Medium and Growth as a Function of Sulfate Concentration. Applied Microbiology **28:**999-1003.

143. **Hardy RWF, Holsten RD, Jackson EK, Burns RC.** 1968. The Acetylene-Ethylene Assay for N2 Fixation: Laboratory and Field Evaluation. Plant Physiology **43:**1185-1207.

144. **Chen KC, Chen JS, Johnson JL.** 1986. Structural features of multiple nifH-like sequences and very biased codon usage in nitrogenase genes of Clostridium pasteurianum. Journal of bacteriology **166:**162-172.

145. **Musto H, Romero H, Zavala A.** 2003. Translational selection is operative for synonymous codon usage in Clostridium perfringens and Clostridium acetobutylicum. Microbiology (Reading, England) **149:**855-863.

146. **Eady RR.** 1996. Structure–Function Relationships of Alternative Nitrogenases. Chemical Reviews **96:**3013-3030.

147. **Wang SZ, Chen JS, Johnson JL.** 1988. The presence of five nifH-like sequences in Clostridium pasteurianum: sequence divergence and transcription properties. Nucleic acids research **16:**439-454.

148. **Zinoni F, Robson RM, Robson RL.** 1993. Organization of potential alternative nitrogenase genes from Clostridium pasteurianum. Biochimica et Biophysica Acta (BBA) - Gene Structure and Expression **1174:**83-86.

149. **Joerger RD, Jacobson MR, Premakumar R, Wolfinger ED, Bishop PE.** 1989. Nucleotide sequence and mutational analysis of the structural genes (anfHDGK) for the second alternative nitrogenase from Azotobacter vinelandii. Journal of bacteriology **171:**1075-1086.

150. 2002. Nitrogen Fixation at the Millennium, 1st ed. Elsevier Science.

151. **Premakumar R, Jacobson MR, Loveless TM, Bishop PE.** 1992. Characterization of transcripts expressed from nitrogenase-3 structural genes of Azotobacter vinelandii. Canadian journal of microbiology **38:**929-936.

152. **Jacobson MR, Premakumar R, Bishop PE.** 1986. Transcriptional regulation of nitrogen fixation by molybdenum in Azotobacter vinelandii. Journal of bacteriology **167:**480-486.

153. **Jacobitz S, Bishop PE.** 1992. Regulation of nitrogenase-2 in Azotobacter vinelandii by ammonium, molybdenum, and vanadium. Journal of bacteriology **174:**3884-3888.

154. **Kasap M, Chen JS.** 2005. Clostridium pasteurianum W5 synthesizes two NifH-related polypeptides under nitrogen-fixing conditions. Microbiology (Reading, England) **151:**2353-2362.

APPENDIX A

TABLE OF MEDIA COMPOSITION USED FOR CO-CULTURING IN CHAPTER 3. DASHES INDICATE THE ABSENCE OF A COMPONENT

	TAP	A^+	TAP mod	A^+ mod
TRIS Base	2.42g	1g	2.42g	1g
$NaNO_3$	-	1	1	0.5
NH_4Cl	15	-	15	7.5
$MgSO_4(7H_2O)$	4	5	4	5
$CaCl_2(2H_2O)$	2	2.7	2	2.7
NaCl	-	18	-	9
KCl	-	0.6	-	0.6
K_2HPO_4	0.29	-	0.29	-
KH_2PO_4	0.14	0.05	0.14	0.05
$Na_2EDTA(2H_2O)$	Y	Y	Y	Y
$ZnSO_4$[1]/$ZnCl$[2]	Y[1]	Y[2]	Y[1]	Y[2]
H_3BO_3	Y	Y	Y	Y
$MnCl_2$	Y	Y	Y	Y
$FeSO_4$[1]/$FeCl_3$[2]	Y[1]	Y[2]	Y[1]	Y[2]
CoCl	Y	Y	Y	Y
$CuSO_4$	Y	Y	Y	Y
MoO_3	Y	Y	Y	Y
Glacial Acetic Acid	1ml	-	1ml	1ml
B12	-	Y	Y	Y
pH	7	8	7 and 8	7 and 8